



U.S. Department  
of Transportation

Federal Railroad  
Administration

# Locomotive Crashworthiness Research: Modeling, Simulation, and Validation

---

Office of Research  
and Development  
Washington, DC 20590

NOTICE

This document is disseminated under the sponsorship of the Department of Transportation in the interest of information exchange. The United States Government assumes no liability for its contents or use thereof.

NOTICE

The United States Government does not endorse products or manufacturers. Trade or manufacturers' names appear herein solely because they are considered essential to the objective of this report.

**Technical Report Documentation Page**

1. Report No.		2. Government Accession No.		3. Recipient's Catalog No.	
4. Title and Subtitle  Locomotive Crashworthiness Research: Modeling, Simulation, and Validation				5. Report Date  July 2001	
				6. Performing Organization Code	
7. Author(s)  Stephen Kokkins, Wayne Kong, Kash Kasturi				8. Performing Organization Report No.  DOT/FRA/ORD-01/23	
9. Performing Organization Name and Address  Foster-Miller, Inc. 350 Second Avenue Waltham, MA 02154-1196				10. Work Unit No. (TRAIS)	
				11. Contract or Grant No. DTFR53-95-C-00049	
12. Sponsoring Agency Name and Address  U.S. Department of Transportation Federal Railroad Administration Office of Research and Development 1120 Vermont Ave, NW MS20 Washington, DC 20590				13. Type of Report and Period Covered  Final Report 10/07/97 – 12/31/00	
				14. Sponsoring Agency Code	
15. Supplementary Notes					
16. Abstract  A technique was developed to realistically simulate the dynamic, nonlinear structural behavior of moving rail vehicles and objects struck during a collision. A new approach considered the interdependence of the many vehicles connected in typical rail consists. This was accomplished by combining the dynamic modeling of the consist as a whole with "embedded" detailed models of the lead locomotive and the objects with which it collides, including standing car consists and ISO-type shipping containers.  This method used the LS-DYNA program which simulated the three-dimensional effects of non-linear, elasto-plastic material behavior plus the effects of large deflections, buckling, energy absorption, and fracture. It was possible to generate and visualize the collision process and view the most significant locomotive structural deformations, movements, and decelerations. These insights into the structural performance and interactions of the various areas of the locomotive, including the cab and interior areas, relate directly to crew survivability in collisions. Several types of locomotive design improvements were also assessed with this method. Validation studies using a historical accident were also successfully performed. This system can be run on personal desktop computers, increasing access to the method by workers in the railroad community.					
17. Key Words  locomotive, crashworthiness, analysis, simulation, safety, dynamic				18. Distribution Statement Document is available to the U.S. public through the National Technical Information Service, Springfield, VA 22161	
19. Security Classif. (of this report) Unclassified		20. Security Classif. (of this page) Unclassified		21. No. of Pages 102	
				22. Price	



## **PREFACE**

---

This report presents a summary of the work done to date by Foster-Miller on the Locomotive Crashworthiness Research program, Tasks 1 and 2. These addressed development of the collision simulation methodology, parametric and design studies, and verification comparisons. Additional test and test support tasks are now underway, and will be the subject of future reports.

This work was performed under the contract DTFR53-95-C-00049, Task Order No. 8 from the Federal Railroad Administration (FRA). Mr. John Punwani of the FRA was the Technical Monitor. Foster-Miller wishes to acknowledge the strong technical guidance provided by Mr. John Punwani throughout the program.

The project was performed in consultation with various organizations and Foster-Miller wishes to acknowledge the continued support given by the locomotive and car manufacturers in the conduct of this research. These included: Mark Huang, Mike Lorenzen and Tom Scott, of the Electro-Motive Division of General Motors; Al Bieber of the Transportation Systems Division of the General Electric Co.; Greg Saxton at Gunderson, Inc., Johnstown America Corporation, and Shaun Richmond at Thrall, Inc. They provided generic data enabling creation of realistic locomotive and carbody models, and kindly provided review and comment during their formulation.

Thanks are also due to Ms. Claire Orth, Chief of the Equipment and Operating Practices Research Division, and Mr. Steven Ditmeyer, Director of the Office of Research and Development, both at the Federal Railroad Administration, for their valuable comments on the earlier version of this report.

The authors wish to thank Foster-Miller's technical writers for their help in the revised version of the report.



# SI\* (MODERN METRIC) CONVERSION FACTORS

## APPROXIMATE CONVERSIONS TO SI UNITS

Symbol	When You Know	Multiply By	To Find	Symbol	When You Know	Multiply By	To Find	Symbol
<b>LENGTH</b>								
in	inches	25.4	millimeters	mm	millimeters	0.039	inches	in
ft	feet	0.305	meters	m	meters	3.28	feet	ft
yd	yards	0.914	kilometers	km	kilometers	1.09	yards	yd
mi	miles	1.61				0.621	miles	mi
<b>AREA</b>								
in <sup>2</sup>	square inches	645.2	millimeters squared	mm <sup>2</sup>	millimeters squared	0.0016	square inches	in <sup>2</sup>
ft <sup>2</sup>	square feet	0.093	meters squared	m <sup>2</sup>	meters squared	10.764	square feet	ft <sup>2</sup>
yd <sup>2</sup>	square yards	0.836	meters squared	m <sup>2</sup>	meters squared	1.195	square yards	ac
ac	acres	0.405	hectares	ha	hectares	2.47	acres	mi <sup>2</sup>
mi <sup>2</sup>	square miles	2.59	kilometers squared	km <sup>2</sup>	kilometers squared	0.386	square miles	
<b>VOLUME</b>								
fl oz	fluid ounces	29.57	milliliters	ml	milliliters	0.034	fluid ounces	fl oz
gal	gallons	3.785	liters	l	liters	0.264	gallons	gal
ft <sup>3</sup>	cubic feet	0.028	meters cubed	m <sup>3</sup>	meters cubed	35.71	cubic feet	ft <sup>3</sup>
yd <sup>3</sup>	cubic yards	0.765	meters cubed	m <sup>3</sup>	meters cubed	1.307	cubic yards	yd <sup>3</sup>
NOTE: Volumes greater than 1000 l shall be shown in m <sup>3</sup> .								
<b>MASS</b>								
oz	ounces	28.35	grams	g	grams	0.035	ounces	oz
lb	pounds	0.454	kilograms	kg	kilograms	2.202	pounds	lb
T	short tons (2000 lb)	0.907	megagrams	Mg	megagrams	1.103	short tons (2000 lb)	T
<b>TEMPERATURE (exact)</b>								
°F	Fahrenheit temperature	5(F-32)/9 or (F-32)/1.8	Celsius temperature	°C	Celsius temperature	1.8C + 32	Fahrenheit temperature	°F
<b>ILLUMINATION</b>								
fc	foot-candles	10.76	lux	lx	lux	0.0929	foot-candles	fc
fl	foot-Lamberts	3.426	candela/m <sup>2</sup>	cd/m <sup>2</sup>	candela/m <sup>2</sup>	0.2919	foot-Lamberts	fl
<b>FORCE and PRESSURE or STRESS</b>								
lbf	poundforce	4.45	newtons	N	newtons	0.225	poundforce	lbf
psi	poundforce per square inch	6.89	kilopascals	kPa	kilopascals	0.145	poundforce per square inch	psi

\* SI is the symbol for the International System of Units

(Revised January 1992)





# CONTENTS

---

Section	Page
<b>EXECUTIVE SUMMARY .....</b>	<b>xvii</b>
<b>1. INTRODUCTION .....</b>	<b>1</b>
1.1 Background.....	1
1.2 Objectives .....	1
<b>2. MODELING AND SIMULATION METHOD DEVELOPMENT .....</b>	<b>3</b>
2.1 Overview .....	3
2.2 Technical Approach .....	3
2.2.1 Collision Scenarios .....	4
2.2.2 Analytical Models .....	5
2.3 Development of Finite Element Models .....	10
2.3.1 Finite Element Model of Loco1 .....	12
2.3.2 FE Model of Loco2 .....	18
2.3.3 Models of Cars and Objects in Collision with Locomotive .....	20
2.3.4 Modeling of Materials and Other Features .....	23
2.4 Results of Test Collisions for Development of Simulation Methods .....	25
2.4.1 Baseline Simulation with Loco1 .....	25
2.4.2 Baseline Simulation with Loco2 .....	30
2.5 Summary of Test Collision Studies .....	35
2.5.1 Simulation Method Developed for Rail Vehicle Collisions .....	37
2.5.2 Guide to Modeling Characteristics for Simulations .....	37
2.5.3 Summary .....	39
<b>3. PARAMETRIC STUDIES OF LOCOMOTIVE CRASHWORTHINESS .....</b>	<b>41</b>
3.1 Collisions with Standing Hopper/Box Car Consist .....	41
3.1.1 Effects of Collision Speed .....	41
3.1.2 Effects of Car End Consist: Box Car versus Hopper Car .....	42
3.2 Collisions with ISO-Type Containers .....	45
3.2.1 Effects of Collision Speed .....	45
3.2.2 Effects of Container Strength .....	45
3.2.3 Effects of Container Weight .....	47
3.3 Locomotive-to-Locomotive Collisions in Consists .....	48

<b>Section</b>	<b>Page</b>
3.3.1	Two-Thirds Lateral Offset ..... 49
3.3.2	One-Third Lateral Offset ..... 49
3.3.3	Head-On Collision ..... 51
3.3.4	Cab Deceleration During Locomotive-to-Locomotive Collisions ..... 51
3.4	Discussions on Parametric Studies ..... 51
<b>4.</b>	<b>MODEL VALIDATION STUDIES ..... 53</b>
4.1	Objectives ..... 53
4.2	Historical Accident Candidates for Validation Simulations ..... 54
4.3	Accident Selection for Validation ..... 54
4.3.1	Assessment of Coupled-Locomotive Override (Scenario 1) ..... 54
4.3.2	Assessment of Locomotive Collision with Standing Spine Car (Scenario 2) ..... 56
4.4	Simulation of the Spine Car Accident (Scenario 2) ..... 56
4.4.1	Modeling of Spine Car and Consist ..... 56
4.4.2	Comparison of Simulation and Accident Outcomes ..... 58
4.5	Supplemental Validation Studies: Coupled Locomotive Override (Scenario 1) ..... 62
4.5.1	Modeling Approach ..... 62
4.5.2	Observations ..... 65
4.6	Summary ..... 69
<b>5.</b>	<b>POTENTIAL LOCOMOTIVE STRUCTURAL IMPROVEMENTS ..... 71</b>
5.1	Strengthening Studies of Large Freight Locomotive 1 (Loco1) ..... 71
5.1.1	Strengthening of Windshield/Cab Corner Post Area ..... 72
5.1.2	Strengthening of Short Hood ..... 72
5.1.3	Interconnection of Collision Posts ..... 73
5.1.4	Adding Stiffening Flanges to Collision Posts ..... 74
5.2	Strengthening Study of Second Large Freight Locomotive (Loco2) ..... 78
5.2.1	Strengthening of Windshield and Corner Post Area ..... 78
5.2.2	Strengthening of Short Hood ..... 79
5.2.3	Upward Extension of the Collision Posts ..... 80
5.3	Summary of Strengthening Studies ..... 80
<b>6.</b>	<b>CONCLUSIONS AND RECOMMENDATIONS ..... 83</b>
6.1	Conclusions ..... 83
6.2	Recommendations ..... 85
<b>7.</b>	<b>REFERENCES ..... 87</b>

## ILLUSTRATIONS

---

Figure	Page
1. Collision scenario between the locomotive consist and hopper/box car consist fouling ROW at a turnout .....	6
2. Collision scenario between the locomotive consist and ISO type container .....	6
3. Typical U.S. heavy freight locomotive .....	7
4. Schematic of the front areas of a typical locomotive .....	8
5. Collision scenario between primary locomotive consist and hopper car consist .....	10
6. Top view of locomotive front end in collision with ISO type container .....	11
7. End view of locomotive front end in collision with ISO container .....	11
8. FE model of the Loco1 locomotive .....	13
9. Close-up of the front portion of Loco1 model .....	14
10. FE model of the Loco1 anticlimber .....	14
11. Draft gear spring stiffness .....	15
12. FE model of Loco1 draft gear and draft gear pocket .....	16
13. FE model of Loco1 endplate and snow plow .....	16
14. FE model of the Loco1 truck (bogie) .....	17
15. The FE model of the Loco2 locomotive with detailed rear end .....	19
16. FE model of the Loco2 locomotive with simplified rear end .....	20
17. FE model of the lead hopper car .....	21
18. FE model of the ISO container .....	22
19. FE model of the primary Loco1 consist .....	23
20. Elasto-plastic properties of metals .....	24
21. Collision configuration between Loco1 and hopper car consists .....	26
22. Top view of the 50 mph collision between Loco1 and hopper car consists at 1 second .....	26
23. Close-up view of the 50 mph collision between Loco1 and hopper car consists at 1 second .....	27
24. Velocity profiles of locomotive and hopper cars of the Loco1 consist .....	28
25. Cab floor deceleration for the 50 mph collision between Loco1 and offset, standing hopper car consists .....	28
26. Total collision force between Loco1 and offset, standing hopper car consists .....	29
27. Collision configuration between Loco1 consist and suspended ISO container .....	29
28. Close-up view of the 50 mph collision between Loco1 consist and container at 0.4 seconds .....	30
29. Cab floor deceleration for the 50 mph collision between Loco1 consist and container .....	31

<b>Figure</b>	<b>Page</b>
30. Collision force for the 50 mph collision between Loco1 consist and container .....	31
31. Close-up view of the deformations of locomotive and box car at the end of simulation (1 second) for the 30 mph case .....	32
32. Deformed locomotive at the end of simulation (1 second) for the 30 mph case .....	32
33. Deformed locomotive at the end of simulation (1 second) for the 50 mph case .....	33
34. Deformations of the locomotive and container at the end of simulation (0.5 second) for the 50 mph collision .....	34
35. Lateral view of the deformed locomotive at the end of simulation (0.5 second) for the 50 mph collision .....	34
36. Side view of the two locomotive consists at the end of simulation (1 second) for the 50 mph collision .....	35
37. Close-up of the deformations of both locomotives at the end of simulation (1 second) for the 50 mph collision .....	36
38. Time history of deceleration at the Loco2 cab floor for the 50 mph collision .....	36
39. Top view of the locomotive and hopper consists at t = 1 second for the 30 mph case .....	42
40. The deformed locomotive for the 30 mph collision with the standing hopper consist .....	43
41. The deformed locomotive for the 50 mph collision with the standing hopper consist .....	43
42. The deformed locomotive for the 50 mph collision with the standing box car consist .....	44
43. The deformed locomotive for the 30 mph collision with the 30,000 pound aluminum container .....	46
44. The deformed locomotive for the 50 mph collision with the 30,000 pound aluminum container .....	46
45. The deformed locomotive for the 50 mph collision with the 30,000 pound all-steel container .....	47
46. The deformed locomotive for the 50 mph collision with the 60,000 pounds aluminum container .....	48
47. The deformed locomotives at the end of simulation for the 50 mph two-thirds offset collision .....	49
48. Lateral view of the deformed two locomotive consists at the end of simulation for the 50 mph one-third offset collision .....	50
49. The deformed locomotives at the end of simulation for the 50 mph one-third offset collision .....	50
50. Lateral view of the deformed locomotives for the 50 mph head-on collision .....	51
51. Example of cab floor decelerations for collision between locomotive consist at 50 mph with stationary hopper and box car consists .....	52
52. Accident Scenario 1 .....	55
53. Accident Scenario 2 .....	55
54. FE model of the intermodal spine car .....	57

<b>Figure</b>	<b>Page</b>
55. Collision configuration between the moving Loco1 and stationary spine car consists .....	57
56. Lateral view of collision zone .....	58
57. Isometric view of collision showing spine car buckling upward (t = 0.5 seconds) midway in collision .....	59
58. Lateral view showing buckled spine car and early contact with short hood (t = 0.5 seconds) .....	59
59. Lateral view showing the movement of the spine car up and over the locomotive hood and cab (t = 1.0 second) .....	60
60. Later view showing the damage to the locomotive windshield and roof area (t = 1.5 seconds). Spine carbody is rolling off away from the viewer .....	61
61. Top view showing spine car rolling off to the left of locomotive (t = 1.5 seconds) before it falls inverted on the wayside .....	61
62. Leading Loco1 locomotive with detailed rear end .....	63
63. Close-up of rear end of the lead locomotive .....	63
64. Lateral view of the lead and trailing locomotives .....	64
65. Locomotive consist for override analysis .....	64
66. Deformed shape showing rear end of lead locomotive and front end of trailing locomotive at 0.2 seconds for 30 mph collision with 6 in height offset .....	66
67. Deformed shape showing rear end of lead locomotive and front end of trailing locomotive at 0.5 seconds for 30 mph collision with 6 in height offset .....	66
68. Deformed shape showing rear end of lead locomotive and front end of trailing locomotive at 0.18 seconds for 50 mph collision with 6 in height offset .....	67
69. Deformed shape showing rear end of lead locomotive and front end of trailing locomotive at 0.5 seconds for 50 mph collision with 6 in height offset .....	67
70. Deformed shape showing rear end of lead locomotive and front end of trailing locomotive at 0.5 seconds for 30 mph collision with 10 in height offset .....	68
71. Deformed shape showing rear end of lead locomotive and front end of overriding coupled locomotive at 1.5 seconds for 30 mph collision with 10 in height offset .....	68
72. Locomotive with strengthened windshield/corner post in 50 mph collision with 60,000 pound all-aluminum container (t = 0.4 seconds) .....	73
73. Locomotive with strengthened short hood in 50 mph collision with 60,000 pound all-aluminum container (t = 0.4 seconds) .....	74
74. Baseline collision posts for 50 mph one-third offset (40 in) collision between Loco1 consist and standing locomotive-headed consist (t = 1 second) .....	75
75. Interconnected collision posts for 50 mph one-third offset (40 in) collision between Loco1 consist and standing locomotive-headed consist (t = 1 second) .....	75
76. Total collision force between two loco consists and force borne by collision posts (CP) of the stationary locomotive for a 50 mph collision .....	76
77. Deformed collision posts with 5 in flanges at t = 1 second for the 2/3 offset 50 mph between the moving Loco1 consist and stationary box car consist .....	77

<b>Figure</b>	<b>Page</b>
78. Deformed collision posts with 10 in flanges at t = 1 second for the 2/3 offset 50 mph between the moving Loco1 consist and stationary box car consist .....	77
79. Lateral view of the deformed Loco2 with strengthened windshield and corner post area at t = 0.5 seconds for the 50 mph collision .....	79
80. Lateral view of the deformed Loco2 with strengthened short hood at t = 0.5 seconds for the 50 mph collision .....	80
81. Deformed Loco2 with strengthened collision posts at t = 1 s for the 30 mph case .....	81

## ACRONYMS

---

AAR	Association of American Railroads
CG	Center of gravity
CP	Collision posts
FE	Finite element
FRA	Federal Railroad Administration
NTSB	National Transportation Safety Board
ROW	Right of way
RSERA	Railroad Safety Enforcement and Review Act





## EXECUTIVE SUMMARY

---

Evaluation of locomotive crashworthiness is vitally important for assessing the safety of current rail operations and determining future requirements for design improvements. The current program investigated the behavior of locomotives and consists in various collision scenarios, with the overall objective of improving both the crashworthiness of the structures and the survivability of train crews.

The primary objective of this effort was to develop and demonstrate an advanced computerized simulation technique that makes it possible to realistically visualize the locomotive collision process. This technique enables investigators to predict the structural and dynamic behavior of locomotives and consists in various collision scenarios, and can aid in the efforts to improve both the crashworthiness of the structures and the survivability of train crews. Also, cost-effectiveness of design changes can now be explored when their effect could be seen using these visualizations. Comparison of model results with actual accident scenarios provided validation of the simulation models.

The simulation technique was developed utilizing the LS-DYNA finite element (FE) code, with the innovation of combining the dynamic modeling of the consist as a whole with “embedded” detailed models of the lead locomotive, other railcars in the consist, and the objects with which it collides. The three-dimensional interaction between all participating structures in collisions is inherently considered in one process, rather than “decoupling” the analysis of overall consist responses from the local structures on the detail level. Large freight locomotives from both U.S. manufacturers were used as a baseline type, but the approach has application to other types of rail vehicles and consists using the guidelines developed.

With the cooperation of locomotive and car manufacturers, several detailed finite element models were developed, including two heavy freight locomotives, a covered and uncovered hopper car, a boxcar variation, and an intermodal/spine car. Also, techniques for modeling the draft gear and suspensions, including stops and other nonlinearities were developed to assemble the consists.

Successful simulations were conducted with full locomotive-headed consists in many offset/oblique collision scenarios. These included collisions with other standing car consists, other locomotives, and objects such as ISO-type shipping containers. The behavior of both the locomotive structures and the objects in collision could be seen in animated form, and followed during various stages of the collisions. This system was developed to run on high-end personal desktop computers, so that a wide range of workers in government and industry could conveniently utilize the procedures.

Parametric studies evaluated the effects of various basic factors on the overall collision process and local structure behavior. These factors included variation of: collision speed, strength and weight of struck objects, type of struck car end structures, and lateral offset at the collision zone. These parametric studies used the various collision scenarios, each appropriate for the locomotive area involved.

Simulation of an actual historical collision served as an initial verification of the technique. An accident that occurred in Phoenixville, PA in 1996, involving a locomotive-headed consist “rear-ending” a standing intermodal flat (“spine”) car consist, was the focus of the verification. Both the collision process and locomotive damage predicted in the simulation were consistent with the National Transportation Safety Board (NTSB) report and photographic records of the aftermath of the accident. Other verification-oriented studies of locomotive-to-locomotive override were also conducted, further demonstrating the potential of the approach.

Several types of generic structural improvements to the locomotive were evaluated. The strengthening of the corner post, windshield top and the corner post-to-roof connection were valuable in reducing cab intrusions. In offset collisions, results showed how the lateral stiffening of collision posts via flanges was a better approach than interconnection of the collision posts. The studies demonstrated the ability for designers to investigate preliminary designs via collision simulations.

This method can be applied to not only locomotives, but also other rail vehicles involved in collisions—as an aid to designers, and to industry, government and labor involved in advancing the safety of our rail system. Simulations can be conducted in advance of dynamic and static tests used by designers, enabling evaluation of many more trial designs or configurations before expensive actual tests are conducted. This parallels practices used in the auto and aircraft industries.

With more experience, the method could be used in accident reconstruction and to better understand the possible sequence of events in complex collisions, in conjunction with the on-site accident investigations. The method can also incorporate computerized human “dummies” to investigate interior crashworthiness and evolve safety improvements for the crewmembers.

# 1. INTRODUCTION

---

Evaluation of locomotive crashworthiness is vitally important for assessing the safety of current rail vehicle operations, and determining future requirements for design improvements. The current program investigated the behavior of locomotives and consists in various collision scenarios, with the objective of improving both the crashworthiness of the structures and the survivability of train crews. Research in this area has been prompted by Public Law 102-365, the Railroad Safety Enforcement and Review Act (RSERA), dealing with the cost benefit analysis of crashworthiness improvements.

## 1.1 Background

The initial stages of a rail collision can involve crushing and deformation of the contacting vehicles with other vehicles or objects. The dynamic interactions between these can be complex, depending on the crush behavior of the contacting structures plus the overall motions and inertial effects of the consist elements. One of the main purposes of this program is to develop new and realistic techniques for crash simulations, and to learn how to use these effectively to improve the crashworthiness of locomotives and cab cars.

Recent rail collisions involving locomotives and cab cars involved not only the direct head-on type of collisions between locomotives and other consists or track obstructions, but also oblique, sideswipe, and shifted load types of collisions. This is especially important since off-center locomotive collisions can directly affect the side cab areas containing the operator's station; also, depending on their lateral offset, they may circumvent the protection of the traditional crashworthiness improvements such as central collision posts, anticlimbers, or short-hood structural strength requirements, as found in the 1990 Association of American Railroads (AAR) S-580 standard. These types of collisions can present great risk to the locomotive operators by allowing crushing or damage directly to the lateral and upper cab areas.

Design improvements addressing these conditions need guidance and insight into the structural behavior during such collisions. The simulation methods should be capable of reflecting the behavior of locomotives and cab cars under these conditions with adequate fidelity to be useful in design investigations and subsequent improvements.

## 1.2 Objectives

The purpose of this project was to develop the methodology for locomotive and cab car crash simulations, with the objective of realistically predicting the response and interactions of the rail vehicles and objects involved. These would be suitable for both offset/oblique and in-line

scenarios. The simulation methodology can also evaluate design alternatives, which will improve the crashworthiness of the locomotives and cab cars.

The program was structured with the following objectives:

- Develop appropriate structural models of locomotives and other rail vehicles for the simulation of generic collision scenarios.
- Conduct parametric studies with locomotives to evaluate the crashworthiness of structural improvements.

This report describes the work completed in support of the development of the analytical methods, with application to selected collision scenarios for evaluation, validation and refinement of the analytical approach. These scenarios were also used to study the effectiveness of some selected structural improvements. They are intended to represent realistic and possible conditions, and include offset or oblique situations that could threaten train crews in accidents.

## **2. MODELING AND SIMULATION METHOD DEVELOPMENT**

---

### **2.1 Overview**

The use of dynamic simulations that can adequately represent the nonlinear, elasto-plastic crushing behavior of the actual structures during contact and collision can greatly improve understanding of the initial crash process and performance of crashworthiness improvements (countermeasures). Large deflections can occur during the collision process. These deflections alter the contact and resistance of the structures during the short time of collision engagement. Analytical methods can predict buckling, yield and fracture of the various elements, materials and connections making up the vehicle structure involved in the collision process. These techniques already exist in a high state of refinement in the auto industry. This task focused on their application to the specific needs with regard to locomotive crashworthiness.

The primary purpose of this effort was to generate and visualize the early stages of the collision process in which the most significant locomotive structural deformations, movements, and decelerations would occur. These give insight into the structural performance and interactions of the various components of the locomotive in three dimensions, including the cab and interior areas, which relate directly to crew survivability in the initial collision. This was accomplished by combining the dynamic modeling of the consist as a whole with “embedded” detailed models of the lead locomotive and the objects with which it collides, including standing car consists and ISO-type shipping containers. This approach synthesizes the complex interaction process between all participating structures in the collision into one process. The development of the detailed locomotive, car and consist models, and their response in such collisions comprise the activity in Task 1 and are described fully in this section.

### **2.2 Technical Approach**

Current techniques are now available which can adequately represent the dynamic, nonlinear structural behavior of the moving rail vehicles and objects struck during a collision. This approach is adapted from that already used in the automobile industry for evaluation of crash responses, not only for the structures themselves, but also for the human occupants and interior elements. One new aspect developed here for use in rail collisions considers the interdependence of the many vehicles connected in typical rail consists, including the important effects that trailing vehicles have on the dynamic interactions in the zones of direct collision. This is an important aspect in the overall analysis of rail vehicle behavior, including more severe collisions which involve large structural deformations, failure, and crushing.

The method utilizes dynamic finite element (FE) analysis tools, one of which is the LS-DYNA (1) program, selected for use in this project. Fully coupled dynamic modeling with the capabilities of the LS-DYNA program can simulate the three-dimensional (3-D) structures in collisions with the combined effects of nonlinear, elasto-plastic material behavior plus the effects of large deflections, buckling and energy absorption. These capabilities are required to adequately represent the deformation and crushing behavior of rail vehicles in serious collisions that threaten train crews.

This approach has been effectively applied to crashworthiness-related problems. Compatible preprocessors were used for the efficient generation of structural models from various data sources, and post-processors were also used to furnish graphic and animated direct viewing of the dynamic collision process. This greatly aided the interpretation of results. Also, this system can run on personal desktop computers, so that the procedures developed here can be conveniently utilized later by a wide range of workers in government and industry. All computational work was conducted on desktops, to ensure practicality for further applications.

The overall technical approach and the analyses used are summarized in this section, while the details of the model development and description of all constituents are described in the subsection 2.3. The exploration and development of this analytical strategy was the objective of Task 1 in the program.

### **2.2.1 Collision Scenarios**

Two general types of LS-DYNA models were developed to meet the needs of the locomotive collision simulation. The basic concept incorporates relatively detailed structural FE models of a typical lead vehicle and the objects struck, “embedded” within a larger-scale model of the consist as a whole. This is referred to as the "model-in-model" concept. This locomotive-headed consist is referred to as the “primary” consist. Evaluation of the lead vehicle behavior and its crew occupant environment is required for assessing safety and effectiveness of design features. The object or other consist struck by the primary consist was included in the same overall model, again with the contacting areas modeled in adequate detail so as to attempt to provide representation of the local crushing, load transfer, and large-scale deformations. The work in this task showed that this analytical approach works successfully.

This approach has the advantage that the dynamic interaction effects between the various constituents of the colliding consists and contacting, deforming structures would be coherently represented in the analytical process, rather than uncoupled into separate analyses.

The objective of this modeling approach was to simulate primarily the earlier stages of the collision process, in which the most significant structural deformations and decelerations tend to occur. The procedures also show later parts of the consist response (such as the familiar “accordion” pattern for consists in collisions), but this late-stage behavior is subject to many variables such as the wayside environment, etc., and is less useful for locomotive crashworthiness improvement work than the primary collision event.

Development and refinement of the simulation approach used a limited selection of generalized rail collision scenarios, which reflect two different and common situations. The aim was to exercise the technique over a representative range of conditions. This was done to ensure that its simulation capabilities could be expected to handle a reasonable number of real accident types. These types include the two broad classes of in-line and offset/oblique collisions. The general locomotive collision scenarios that were therefore incorporated in this Task included: 1) in-line collisions of locomotive-headed consists with the head or tail of other consists; 2) oblique/offset collisions of the locomotive-headed consists with car(s) fouling the Right Of Way (ROW) (such as at a turnout); and 3) offset collisions of the locomotive-headed consists with “shifted loads” such as ISO-type or trailer-type containers loose from cars on an adjacent track. Priority was given to the oblique/offset situations, since these represent potentially more dangerous situations.

## **2.2.2 Analytical Models**

For both the crushing and overall consist behavior, the ability to represent the 3-D response is extremely useful in the case of offset/oblique situations. Therefore, detailed LS-DYNA dynamic-structural models of the lead locomotive and the objects with which it collides, were developed, as well as LS-DYNA models for the overall consists containing these vehicles.

The two generalized offset/oblique collision scenarios used for developing and refining the simulation technique represented the types (2) and (3) above. These are shown in Figures 1 and 2. In the first type, a standing consist of loaded cars is shown fouling the right of way (ROW) at a turnout, projecting approximately 3 feet into the path of the four-vehicle locomotive-headed consist, traveling over a range of moderate speeds (30 to 50 mph). In the second type, a loaded 8 x 8 x 20 foot ISO-type container is shown “suspended” as if it were shifted off the upper level of a flat car container stack. (This represents only one of many such loads that could and have been involved in such collisions.) The locomotive was assumed to strike it with the short hood/cab area, just outside the collision posts and above the locomotive sill level.

These scenarios represented a somewhat more threatening situation for collision effects in the short hood and cab area, relative to comparable in-line collisions in which the S-580-type features (main collision posts, etc.) would be fully mobilized. They would therefore serve to fully exercise the methodology, and highlight structural areas of the locomotive that might fail earlier in a collision, which could then guide design improvements most effectively. Finally, these general scenarios could be modified later to simulate actual accidents, which would serve to progressively verify and refine the methods.

### **2.2.2.1 Modeling of Lead Locomotive**

Two locomotives manufactured by two leading U.S. freight locomotive companies were selected as typical designs. One of the modern locomotives is shown in Figure 3. This is a wide-nose design that includes the structural features described in the S-580 standard (comprising front collision post, anticlimber, and short hood strength). Since the front hood is the full width of the locomotive (approximately 10 ft), the cab area is protected to a greater extent than in earlier

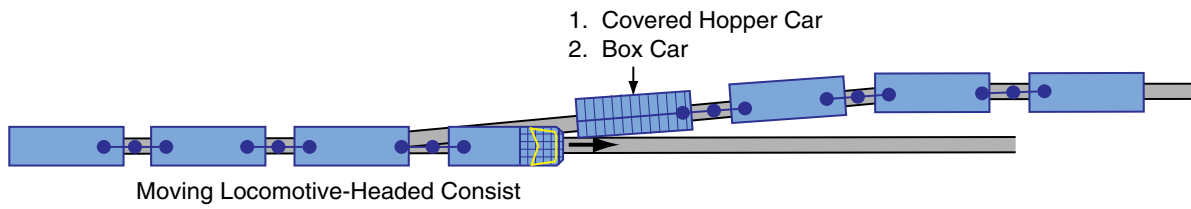


*Figure 1. Collision scenario between the locomotive consist and hopper/box car consist fouling the main track at a turnout*

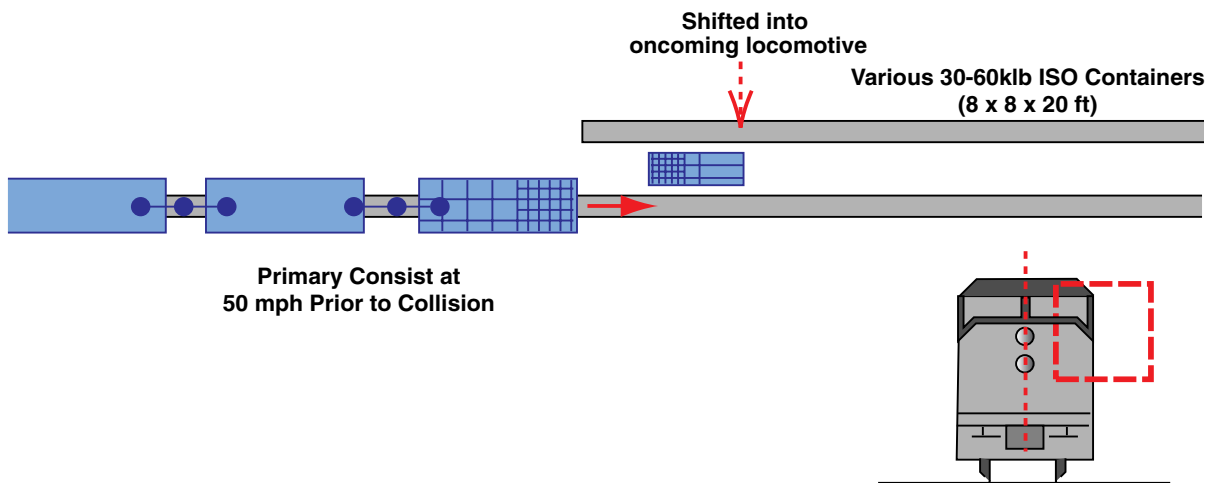


*Figure 2. Collision scenario between the locomotive consist and ISO type container*





*Figure 3. Typical U.S. heavy freight locomotive*

designs with a narrower hood section. For this reason, wide-nose designs are reported to represent virtually all main line locomotives ordered today.

The manufacturers provided extensive cooperative support for this effort, by providing appropriate drawings and local FE data files. Their technical design personnel also provided review at several points in the modeling process, to assure that correct and consistent modeling assumptions were made for their family of locomotives.

A locomotive model included all the basic structural and mechanical components, including all structure, major equipment, powerplant, separate bogies and suspension, and draft gear, all with appropriate masses and inertias. This used progressively finer element meshes proceeding to forward areas of the locomotive, with special attention to all potential contact surfaces. All the previously cited nonlinear geometric and material characteristics were included. The trailing end of the locomotives had a coarser FE mesh consisting of rectangular elements with the masses/ inertias distributed at their respective center-of-gravity (CG) locations in the structure. An outline of the lead locomotive model is shown in Figure 4, with a full description of the modeling process found in subsection 2.3 of this report. This type of model was used in all the “developmental” crash scenarios.

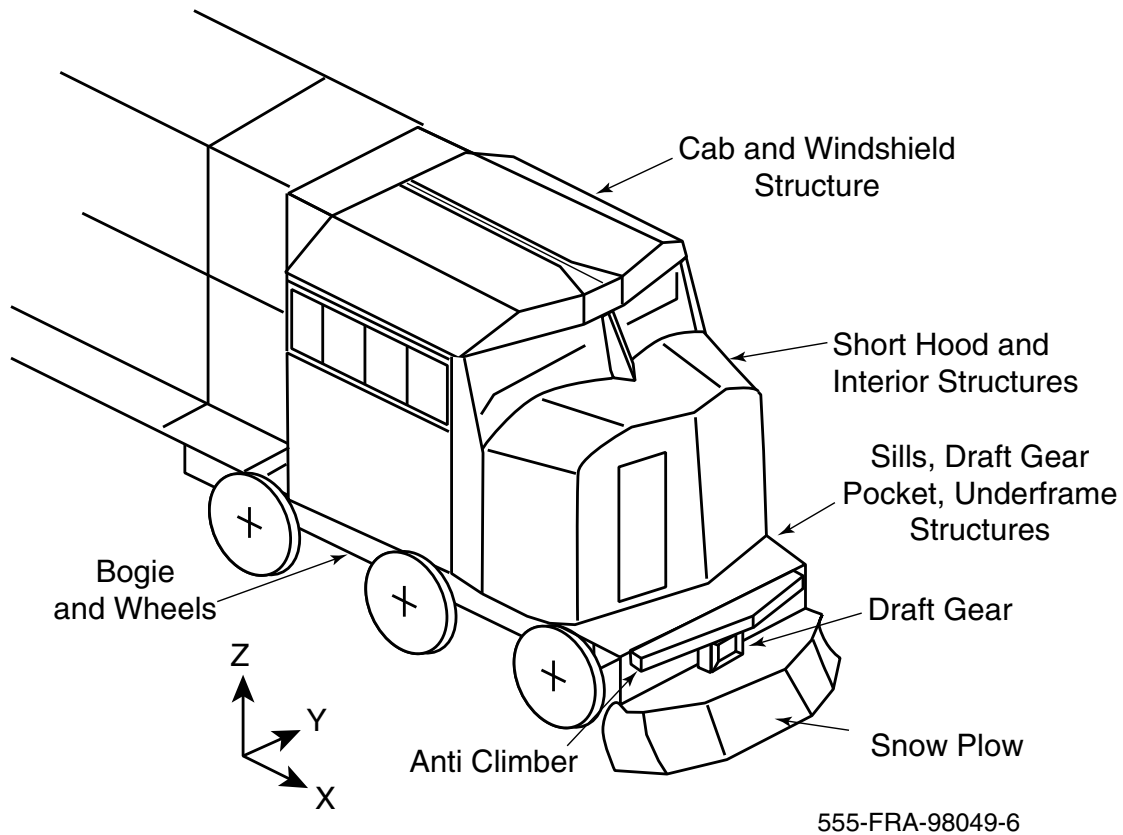


*Figure 4. Schematic of the front areas of a typical locomotive*

#### **2.2.2.2 Locomotive-Headed Consist**

A detailed locomotive model was integrated into an overall consist model using HyperMesh (2). This served as a representative situation in which an adequate number of vehicles would contribute to the loading effects at the zone of impact on the lead locomotive of interest. It was decided to construct a four-vehicle consist comprising the lead locomotive, plus three coupled cars. Total car weights were assumed to be 200,000 pounds representing an average of 80 percent maximum loaded weight. The locomotive weighs 415,000 pounds. (These weights can easily be revised.) While the specifics of these are fully described in subsection 2.3, the principal characteristics of this consist model included:

- Contacting vehicle (lead locomotive) is a full deformable model, with finer detail for all forward structures.
- Draft gear represented by articulating elements (end pin and coupler), with nonlinear spring rates including travel restrictions.

- Carbody as simplified plate structures on suspension, plus separate bogies. All have correct mass/inertias for 200,000 pound cars based on a general hopper car layout.
- Ground interaction represented by “orthogonal” friction (0.3 in in the travel direction and 0.8 in in the transverse direction proved to give reasonable results after experimentation with ranges of values).

### **2.2.2.3 Colliding Objects and Consists**

The colliding objects used in the development of the overall analysis technique included standing car consists and ISO-type shipping containers, both in oblique/offset situations.

#### *Standing Cars in Consist Fouling Right of Way (ROW)*

For the standing cars, two types were considered: a “standard” hopper car and a related box car. The intent is to provide a representative carbody (as part of a consist) to be impacted in an offset/oblique scenario, to assess the safety implications of such collisions on locomotive design features. For this oblique collision scenario, this secondary consist was assumed to be standing in a turnout, partially overlapping the path of the moving locomotive-headed consist in the “through” direction.

A candidate hopper car was selected from industry reference data, and a detailed LS-DYNA model developed. As in the locomotive model, this model has progressively finer detail elements moving toward the impact (contact) end, with the same type of modeling characteristics as the locomotive. Much work was performed in collision trials using this model, but some of the unique characteristics of the hopper car body (such as the “open” vertical corner structure having no midspan support) led to the later use of a simplified boxcar model as well. This determined if there were any differences in the way these two different car ends “engaged” the locomotive end corner structure in the oblique collision, since the car sill height above the rail is well below that of the locomotive. The coupler for the leading hopper car was modeled to take into account the initial surface contacts between the secondary consist (standing cars) and the primary (moving locomotive-headed) consist.

These were joined into a four car consist (“secondary consist”) using similar methods as described for the locomotive-lead consist: all vehicles contained deformable draft gears, suspensions, bogies, correct mass/inertias, and simplified carbody model. The standing consist was aligned at an 8 to 9 degree angle, with an overlap of approximately 40 in on the locomotive width, representing a typical “fouled” turnout orientation. This reflected a situation in which the zone of initial impact lay just outside the strong primary locomotive structural members such as underframe/draft gear pocket and collision posts (meeting S-580). This model as shown in Figure 5 represented the first crash scenario used in the development of the overall LS-DYNA modeling technique.

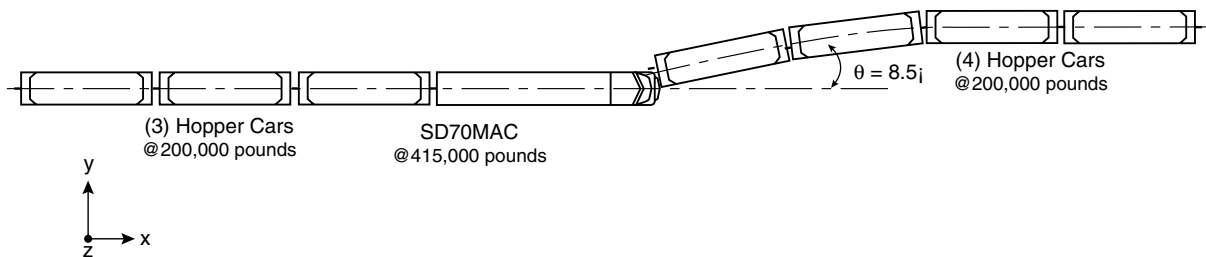


**Figure 5. Collision scenario between primary locomotive consist and hopper car consist**

### *Shifted ISO Container*

A stand-alone ISO type container was utilized for the “shifted load” collision. In this typical scenario, a loose container possibly on the top level of a "double-stack" car is dislodged from a train on an adjacent track, striking the locomotive high and offset on the hood and cab. For the front end of the locomotive in this collision, the container was modeled in detail at the contact end, with some “coarsening” of the model progressing toward the other end. All structural modeling used deformable elements with nonlinear material properties. This was needed for fidelity of the important interaction effects at the crushing/contact interfaces during the collision, which affects overall loads and decelerations.

Many types of such containers exist, in various strengths and in different lengths in the 20 to 40 foot range. An 8 x 8 x 20 foot container was used as a common type, loaded to the 30,000 pound gross weight level. Several trials with different construction weights were made, and the container presently modeled tends toward the lighter end, with ribbed sheet metal sides, square tubular edges, and welded connections, all with lighter gage (10 to 12 gage, or in the range of  $\pm 1/8$  in). Figures 6 and 7 show the orientation of the container and locomotive. The models utilized factored-up material density to produce the desired overall loaded weight.

## **2.3 Development of Finite Element Models**

This section describes the generation of several FE models using HyperMesh. In the development of these models, the primary structures directly involved in a collision were modeled in detail to accurately represent the collision and crushing process. The meshes of these primary structures were fine enough to quantify their stress distribution, and reflect the actual geometry of the individual member layouts, when it was judged necessary to properly represent the structural behavior. The HyperMesh program was used for all modeling work including element generation, contact and material definitions.

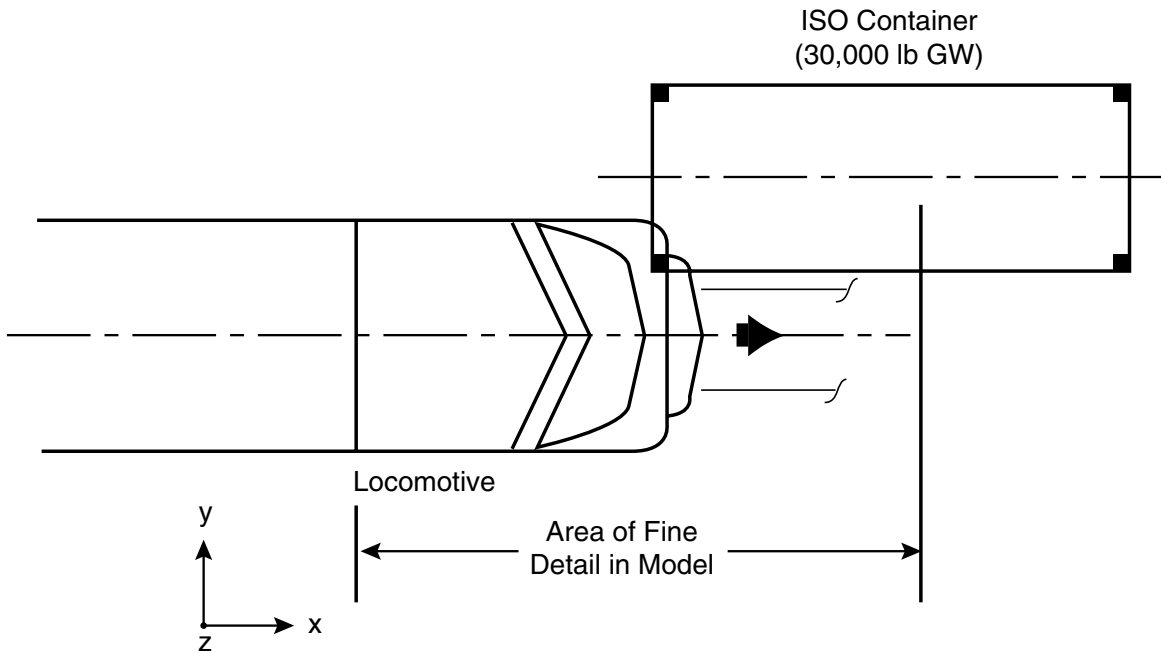


**Figure 6.** *Top view of locomotive front end in collision with ISO type container*

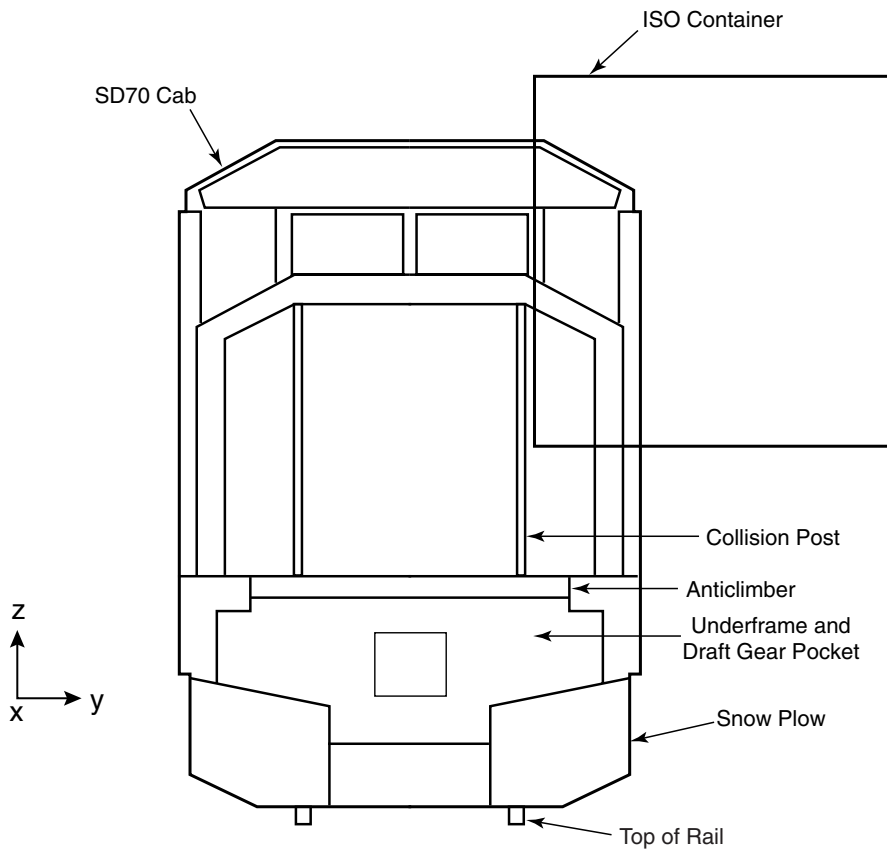


**Figure 7.** *End view of locomotive front end in collision with ISO container*

To properly represent contact surfaces, great efforts were taken to model those structures involved directly in a collision as accurately as possible. This includes both geometric representation and material modeling. The material properties including elasto-plasticity, ultimate strengths (fracture) were precisely represented. These structures modeled in the highest level of detail included the front 1/3 portion of the locomotive and front portions of the leading hopper car and ISO container. For the locomotive, these meshes were fine enough to reasonably quantify their deformations, strains and stresses which would give the insight needed for design evaluations and improvements. These structures included the short hood and collision post, complete cab structure including corner posts, underframe, anticlimber, draft gear and pocket, endplate, and snow plow.

For those structures not directly involved in the primary impact, the FE representations were made simpler, but with their effects on the primary collision process reasonably simulated. Plate-like structures were modeled as “shell” elements and others structures (such as beams, stiffeners, etc.) were represented by proper corresponding elements based on their geometric shapes and functions.

The modelling used units of feet and inches for length, miles per hour for speed, and feet/second<sup>2</sup> for accelerations. These could be converted to SI units using standard software if needed.

### **2.3.1 Finite Element Model of Loco1**

Two models were selected as typical modern large freight locomotives, which are in current production and which incorporate all current (1990) AAR S-580 crashworthiness enhancements. These locomotives are referenced as “*Loco1*” and “*Loco2*” throughout the text of this report. These include specifications for collision post strength, anticlimber, and short hood construction, which are familiar to the industry. Another factor in the selection was that manufacturers provided detailed engineering data for the structure and components thereby enhancing the quality and speed of the modeling effort.

Several sources of information formed the basis for the FE model of the Loco1 locomotive. For some areas of the structure, existing “local” FE models in the ANSYS format were made available. These included models of the underframe, cab, detailed hood structure, and related masses. The model geometry including element thicknesses was transformed to the LS-DYNA format using HyperMesh. Since the origins and purposes of each of these models were slightly different, effort was required to combine and join each of these into an overall consistent model.

The front portion of the underframe was refined to a large extent. The cutout of the top plate for the stairwells was incorporated. The front stairwells themselves are of light construction and do not contribute to the strength of the locomotive. Therefore, they were not included in the model. The mesh of the cab was fine enough to be used directly in the present model with only minor changes. These included refinement of the corner posts and other modifications. After experimentation with the “isolated” cab in preliminary LS-DYNA runs, it was decided to rigidly connect the cab to the underframe using common nodes. The cab-to-frame movements are very small before “bottoming out” so this is satisfactory analytically. This also represents the majority

of existing locomotive construction practice. A new mesh was developed for the long hood structure, including the internal reinforcements and collision post connections. Finally, the many mass elements in the actual locomotive were lumped into fewer mass elements which were then connected to the hood structure.

To complete the locomotive model, the other superstructure components were added manually, based on drawings supplied by the manufacturer. Again, HyperMesh was used to develop these model areas, as detailed in the following paragraphs. The complete FE model of a “Loco1” locomotive is shown in Figure 8.

### 2.3.1.1 Short Hood

The short hood including front, side and top sheets was modeled in detail and appropriately connected to the front end to the cab. The cutout of the entrance door on the front of the hood was added due to the non-structural connection between the door and short hood. The doorframe was included and modeled as beam elements. The sand boxes were also included. The short hood was connected to the underframe and the collision posts were connected to the front and top skins and underframe. Figure 9 shows the resulting local model area.

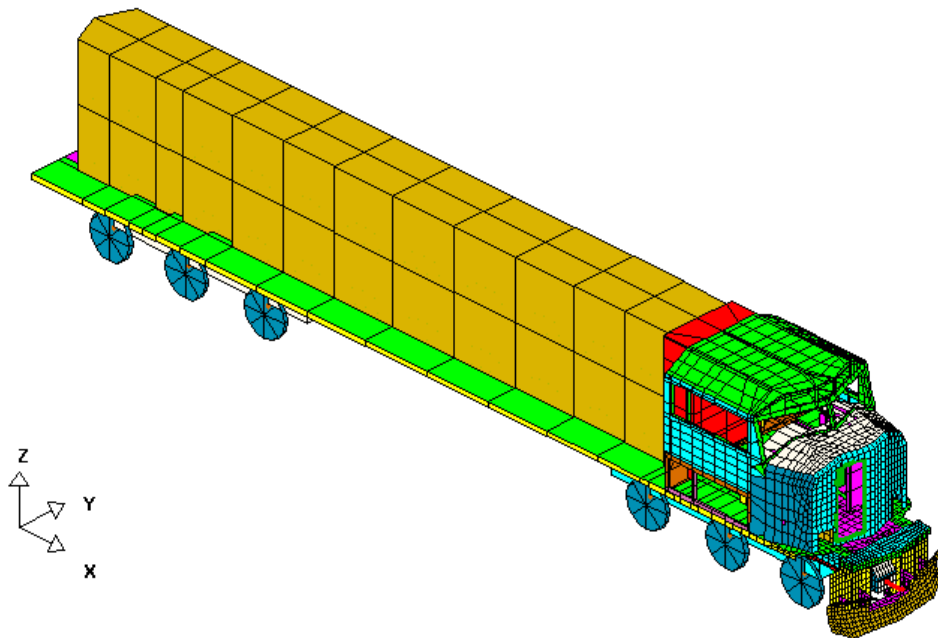


*Figure 8. FE model of the Loco1 locomotive*



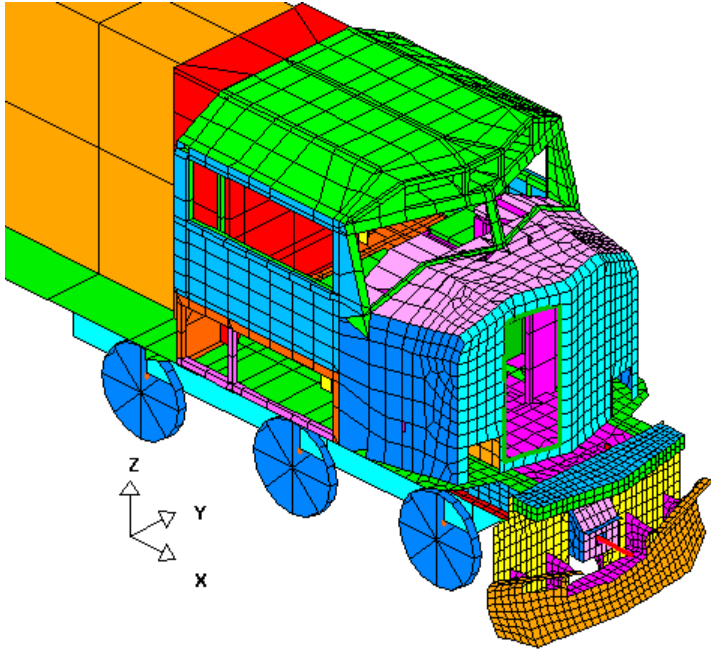


*Figure 9. Close-up of the front portion of Loco1 model*

### 2.3.1.2 Anticlimber

The anticlimber included top plate, front bar, six stiffening bars at the front of the endplate and four bars at the back of the endplate. The front anticlimber was modeled in detail as shown in Figure 10.

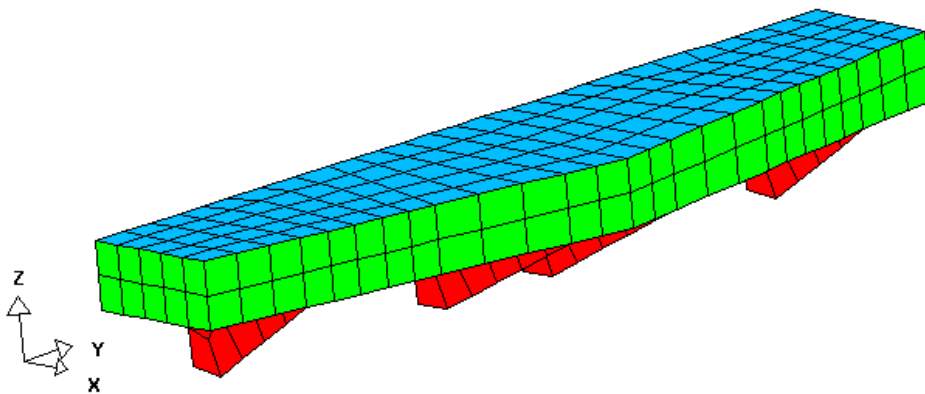


*Figure 10. FE model of the Loco1 anticlimber*



### 2.3.1.3 Draft Gear and Draft Gear Pocket

The draft gear was modeled using beam elements. The draft and buff reactions were represented by a spring, with its stiffness represented by a bi-linear curve as shown in Figure 11, based on the manufacturer's specification. The spring was rigidly connected to the draft gear pocket and its motion range was limited to  $\pm 1.7$  in. The articulation between the draft gear and coupler was modeled by a joint with its rotation ranges limited appropriately. The rotation limits around the longitudinal, lateral and vertical axes were 0,  $\pm 4.4$  degrees and  $\pm 19$  degrees respectively. The draft gear was limited to move only in its axial direction relative to the draft gear pocket. The front draft gear pocket was modeled in detail as shown in Figure 12 and its top was welded to the bottom of the underframe. The possible contact between the coupler and front end of the draft gear pocket was also simulated. The rear draft gear pocket was simply represented by proper constraints between the draft gear/spring and underframe.

### 2.3.1.4 Endplate and Snow Plow

Due to their location, the endplate and snow plow may play some role in crashes involving colliding cars which have a lower underframe compared to locomotives. This is due to the apparent tendency for the primary underframe members of the car to underrun those of the locomotive in offset situations, and the endplate/snow plow resists this to some degree. The endplates were rigidly connected to the draft gear pocket and reinforced by two pipes connected

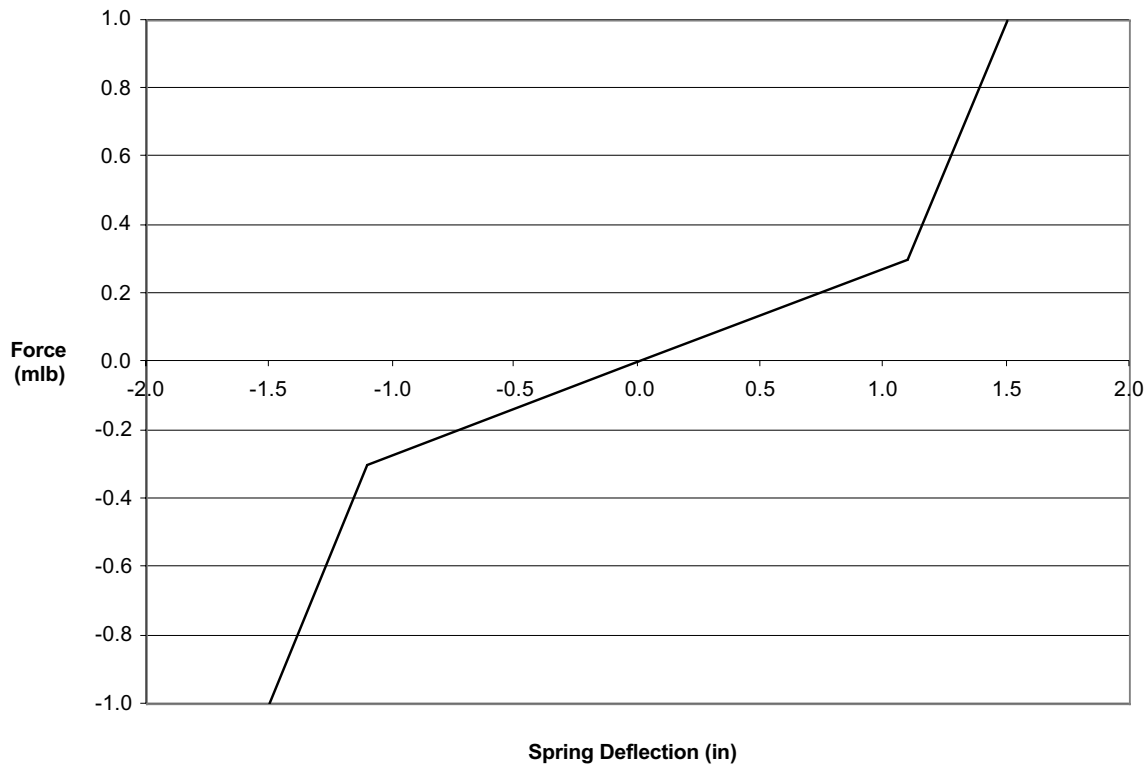


*Figure 11. Draft gear spring stiffness*

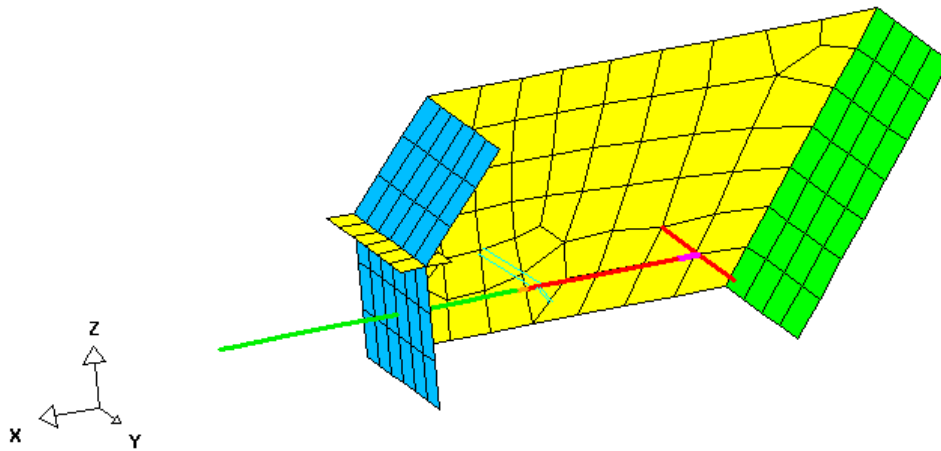


*Figure 12. FE model of Loco1 draft gear and draft gear pocket*

to the bottom of the underframe, as shown in Figure 13. The pipe members were modeled as beam elements with a tubular cross section. The snow plow was connected to the endplate by plates representing the attachment brackets.

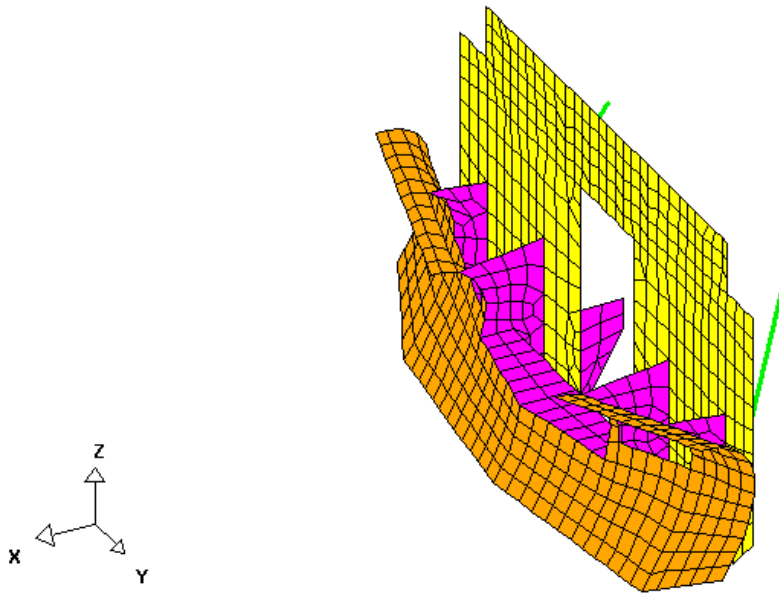


*Figure 13. FE model of Loco1 endplate and snow plow*

### 2.3.1.5 Truck (Bogie) Assembly

The suspension including the primary and secondary springs was simulated in detail. This was required to properly represent the various suspension travel modes, including the nonlinearity of limit stops. The bogies are relatively massive since they contain not only heavy-duty frames and wheels, but also traction motors and gear reduction units.

Six primary and four secondary springs represented suspensions with linear elastic rates before reaching their limiting stops in compression. The rates of the primary and secondary springs were 3125 and 75,000 pounds/in each respectively, and their compression limits 2.0 and 2.75 in. The pivot pin between the truck and underframe was represented in such a way that it limited the relative translation in the horizontal plane while allowed free motion vertically, with a compression limit. The compression limit (0.62 in) was represented by an added soft spring at the pin location. Although the truck frames and wheels were represented by moderately coarse solid elements as shown in Figure 14, they adequately represented the total mass and moments of inertia.

Extensive effort was made to determine if an alternative, simpler representation of the bogie and suspension could be made. This would have to provide the equivalent transnational (primarily bounce/rebound) and rotational (primarily roll and pitch) spring rates to that of the combined primary and secondary suspensions. The requirements in this application are not as stringent as those for exploring wheel/rail interaction or suspension dynamics. However, investigations showed the need for proper connection of the locomotive to the ground plane during the collision process (in 3-D), using proper overall rates and nonlinear limit stops. A straightforward representation of all the individual springs and geometry was adequate, since the important stops and nonlinearities could be incorporated directly.

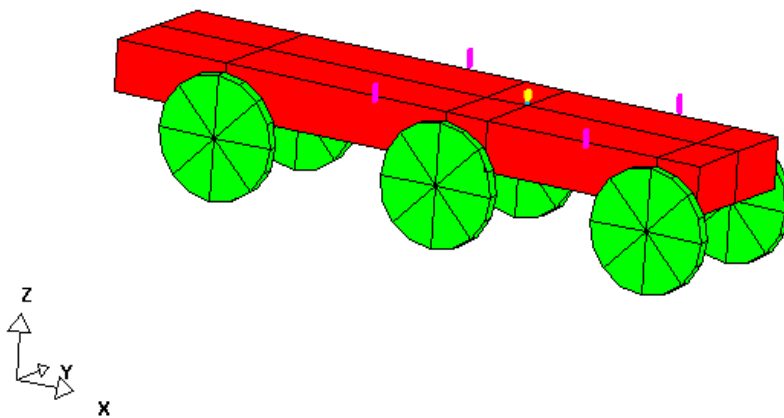


*Figure 14. FE model of the Loco1 truck (bogie)*

### 2.3.1.6 Other Elements

The fuel tank was hung to the underframe and does not provide any reinforcement. The fuel tank was thus only represented by several mass/inertia elements attached at the proper points and in the correct 3-D positions. All other masses in the locomotive were represented as in the actual locomotive. The mass distribution among major subsystems was provided by Loco1 and is listed in Table 1 for reference. The entire FE model had a mass (weight) of 415,000 pounds, which agreed closely with the actual specifications. The length, height and width of the complete model were 888, 188 and 121 in (74 feet-0 in, 15 feet-8 in, and 10 feet-1 in) respectively.

### 2.3.2 FE Model of Loco2

The FE model of the “Loco2” locomotive from the second manufacturer was also developed based on several sources of information. The cab was based on drawings, while the platform was based on an FE model provided by the manufacturer. Some parts of the structures were adapted from the counterparts of the Loco1 locomotive model to reduce modeling efforts. The modeling was performed using the HyperMesh.

Effort was made to represent the cab structures as closely as possible. These structures include short hood, collision posts, windshield and corner post area, and operator cab. As in the Loco1 model, the cutout of the entrance door on the front hand was represented due to the non-structural connection between the door and short hood. The doorframe was included and modeled as beam elements. The sand outlets were also incorporated. Most structures were represented by shell elements with the collision posts modeled as solid elements. The thickness of the collision posts is 3 in, compared to 1.25 in for the Loco1 locomotive. The length of a typical element was around 3.5 in, compared to 5 in for the Loco1 model. The mesh density was determined based on our experience with the Loco1 study with the intention to further improve simulation quality without significantly increasing the computational burden. The mesh became coarser from front towards rear.

The basic geometry of the platform assembly, including the fuel tank and draft gear pockets, was obtained from the FE model provided by the manufacturer. However, the original model was intended for detailed static stress analysis and had too much fine mesh for the present study. The entire platform, beginning with the fuel tank and working outward, was re-meshed and smoothly

*Table 1. Weight distribution of Loco1*

Part	Weight (pounds)
Radial Truck No. 1	58,500
Radial Truck No. 2	58,500
Battery	3,600
Power Plant	60,000
Air Compressor	3,000
Equipment Rack	4,000
TCC1 Cabinet	4,000
TCC2 Cabinet	4,000
Cab Equipment	12,000
Short Hood	34,000
Long Hood (Carbody)	34,000
Underframe	87,000
Fuel Tank	51,000
Draft Gears and Couplers	3,800
Others	28,600
<b>Total</b>	<b>415,000</b>

connected to the superstructures including the cab and carbody. The carbody had a somewhat coarser mesh compared to the front area because it was not directly involved in the collisions. The rear end of the carbody is an adaptation or combination of Loco1 and Loco2 features, since the actual rear end of Loco2 is very complex and significant efforts are needed to truly represent it. However, it was felt that a representative rear superstructure was needed to reasonably simulate the crush interactions in coupled locomotive override situations.

Because the fuel tank for the Loco2 model is welded to the platform, it provides structural strength to the model, and therefore must be modeled explicitly. To complete the model, the anti-climbers, draft gears and couplers, snow plow, and trucks including wheels and springs were added. These structures were adapted from the counterparts of the Loco1 model with proper modifications including spring stiffness. The stiffness values of the primary and secondary springs in the vertical direction for the locomotive are 6,515 and 160,000 pounds/in respectively, compared with 6,250 and 75,000 pounds/in for the Loco1 locomotive. Detailed description on the modeling of these structures can be found in the previous sections.

Two versions of the present model of the Loco2 were developed; one with the detailed rear end as described above (Figure 15), and the other with a much simpler rear end which is just a continuation of the carbody (Figure 16). The simpler version was constructed to reduce the run time of analyses in which the detailed representation of the rear end is not necessary. Some of the components, such as the steps leading up to the front door of the locomotive, were not modeled. These components are mainly sheet metal and do not add to the overall structural

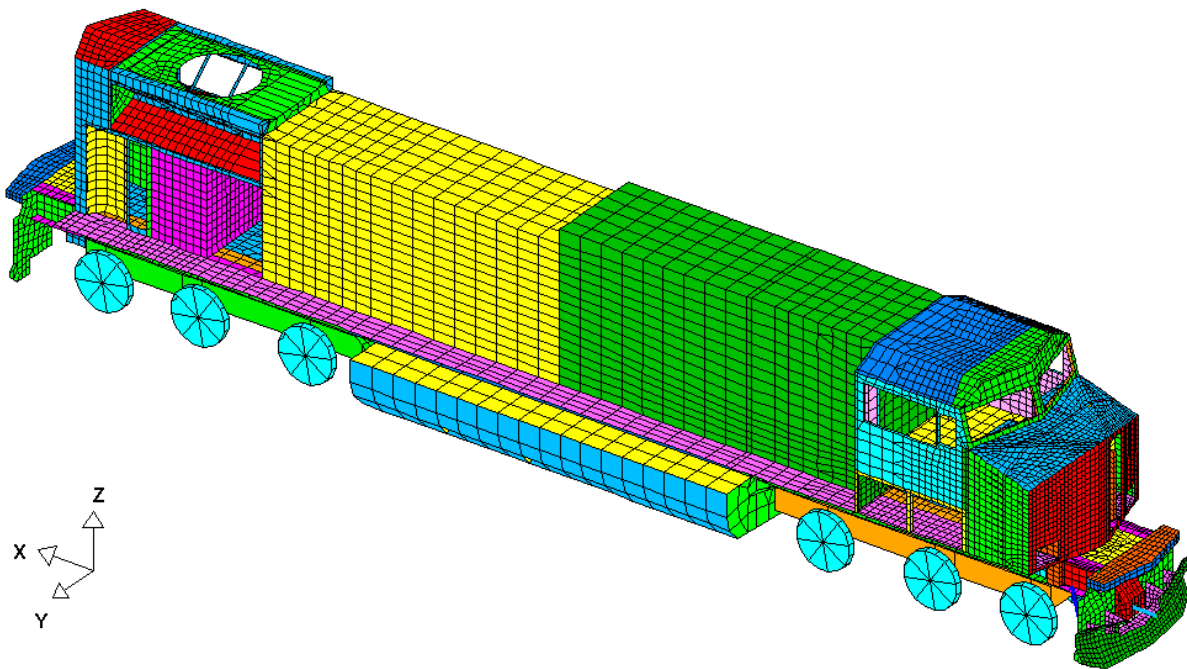


*Figure 15. The FE model of the Loco2 locomotive with detailed rear end*

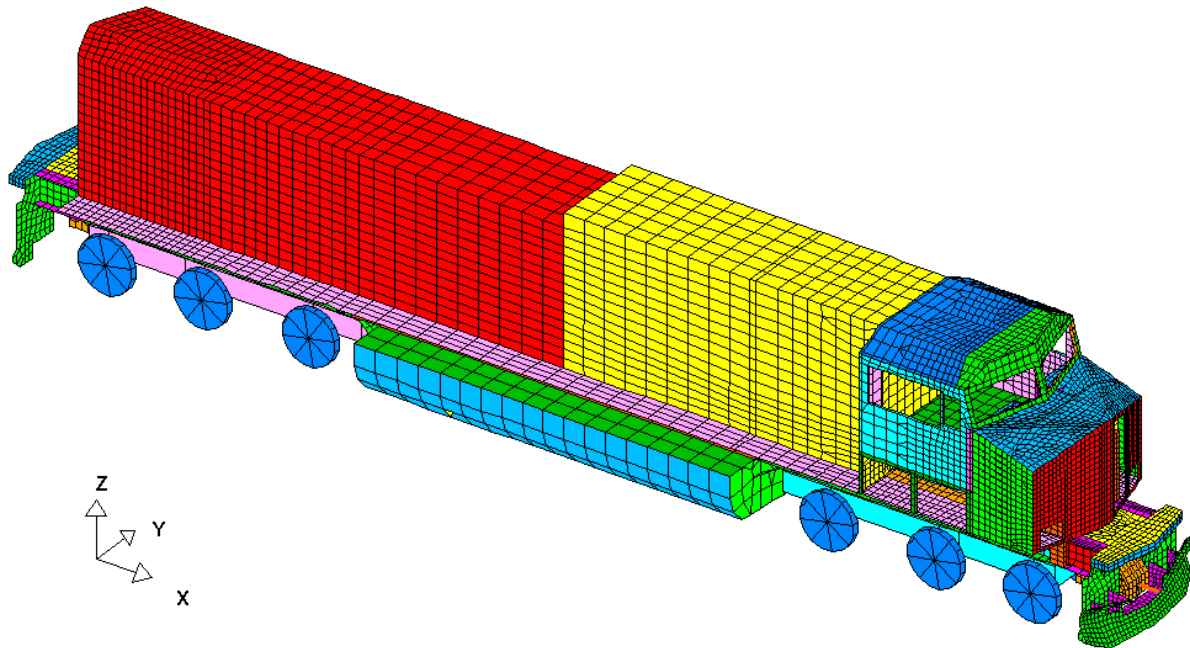


*Figure 16. FE model of the Loco2 locomotive with simplified rear end*

strength. Modeling these parts would just add more elements to the model and slow down the analysis. The total weight of the entire Loco2 locomotive was also 415,000 pounds.

### **2.3.3 Models of Cars and Objects in Collision with Locomotive**

Structural FE models of cars and objects in collision with the “primary” locomotive were also required. The two generalized scenarios used for model development entailed the locomotive-headed primary consist colliding with both a standing freight car consist (offset/oblique partially fouling the right of way) and a shifted load (loaded ISO-type container, high/offset orientation). Therefore, to produce desired fidelity of interaction, each of these objects required relatively detailed modeling of their contact end, progressing to a coarser model towards the other end. “Deformable” modeling elements were used for the entire object which was in direct collision.

The same car models needed for the first scenario were also useful for generating equivalent simplified versions which made up non-colliding cars of both the locomotive-headed (primary) and standing (secondary consists in first scenario). These inherently possess the correct masses/inertias of the full deformable models, but greatly speeding computations. With the provision of the appropriate 3-D nonlinear spring rates for draft gear and suspension, these are entirely adequate to represent the important effects of the “trailing” portions of the consist on the collision zone.

Both hopper and box cars were selected for use in these scenarios. These cars represent car types that could potentially threaten the upper locomotive and cab areas in oblique collisions, due to the relatively high position of the supported mass at the end of the car. This proved to be a relatively challenging modeling effort, although successful, due to early gross bending and fracture of the corner, with “digging in” of the car underframe into the locomotive corner area.

### 2.3.3.1 Hopper Car Models

Sims Professional Engineers supplied geometric information that was the basis of an FE model of an open top hopper car. Data from current Car and Locomotive Cyclopedia (3) was also used. The length, height and overall width of the hopper were 535, 138 and 127 in (44 feet-7 in, 11 feet-6 in, and 10 feet-7 in) respectively. The complete LS-DYNA model developed for the leading hopper is shown in Figure 17.

The carbody and underframe including the center sill were modeled as deformable plate/shell elements. The front (collision) end of the hopper was modeled in detail to get a good representation for the contact simulation between the hopper and locomotive. The contact surfaces change continually during the crushing process. The corner and side beams were included although they are not shown individually in Figure 17 (overlying the plate edges). The trucks, modeled as rigid elements, were located on a simplified suspension relative to the underframe. The draft gears and couplers were simulated in the same manner as the rear end of the locomotive, using 3-D nonlinear springs and stops. The density of the car bodies was scaled to represent loaded goods. The total weight of the hopper was 200,000 pounds, representing an average of 80 percent maximum load. (This can easily be altered if desired.) Similar nonlinear material properties for mild steel were used in different areas to those used for the primary locomotive.

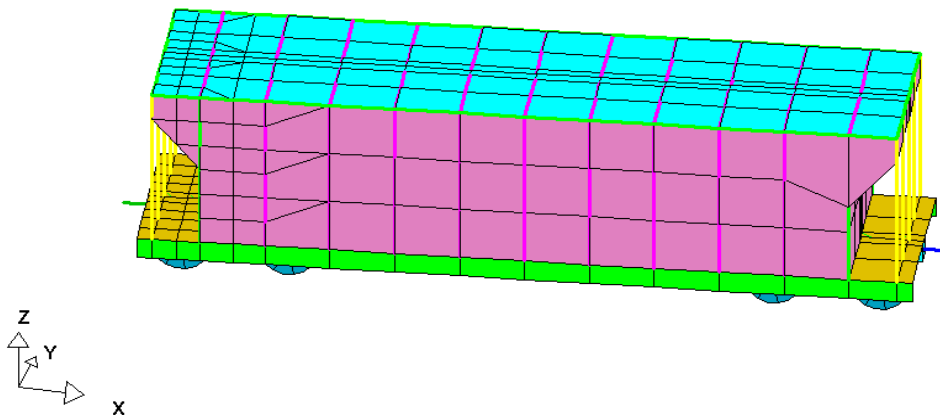


*Figure 17. FE model of the lead hopper car*



### 2.3.3.2 ISO Container Models

A FE model was developed based on the dimensions (8 x 8 x 20 feet) of a “short” style ISO container as shown in Figure 18. All sides including the bottom and top were modeled as shell elements and were stiffened by beam elements. There were also corner beams. The sides and top of the box were assumed to be made from aluminum. The bottom was assumed to be mild steel. The densities of the plates were scaled to represent the weight of a loaded box, which was assumed to be 30,000 pounds for the purpose of this study.

### 2.3.3.3 Consist Models

In the collision simulations, the trailing locomotives and cars should be properly represented in the consist model. Two consist models were generated to represent the locomotive-headed primary consist and standing secondary hopper consist. Three trailing cars for each consist model were included in the current models with the assumption that the effects of succeeding trailing cars become progressively negligible due to the increasing lag in time for their involvement in the collision process. This would be a reasonable compromise between accuracy and computational time required in the FE analysis.

In the current consist models, the leading hopper car model described in the previous section was modestly simplified to represent the trailing cars, which significantly alleviated the computational burden without sacrificing the objectives, since the effects of any local crushing in these trailers are minimal in moderate energy collisions.

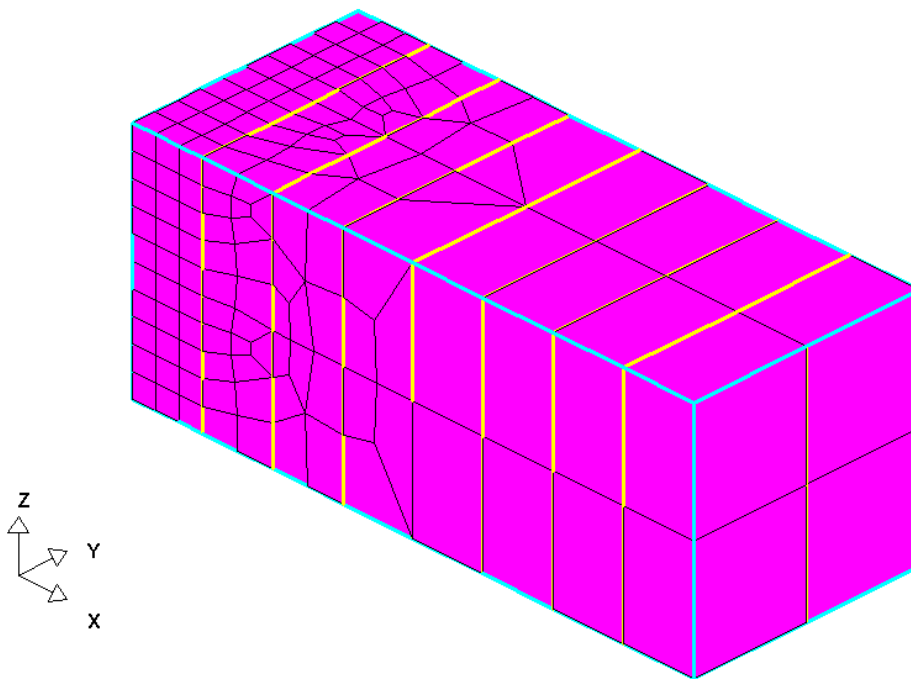


*Figure 18. FE model of the ISO container*



Specifically, the mesh density of the carbody and underframe were reduced and beam elements of the carbody were removed. The density and elastic modulus of the carbody was appropriately adjusted to have the same weight and similar stiffness. The draft gears and couplers were kept the same, to reasonably simulate their functions. The trailing cars were then connected together with the locomotive and leading hopper through couplers to form the two consist models. The primary Loco1 consist model is shown in Figure 19. The interaction between couplers was represented by joint elements with proper rotational stiffness values and limiting stops. The primary Loco2 consist model was created in the same fashion using the Loco2 model with simplified rear end as shown in Figure 16.

### 2.3.4 Modeling of Materials and Other Features

Most structural components in rail vehicles were made from mild steel with their stress-strain relationship represented by a "tri-linear" curve as shown in Figure 20. The first steep section represents the elastic range, with the second and third the plastic range to actual failure at large strains. A piecewise linear plasticity material model in LS-DYNA was used to simulate this kind of material property. The material model can simulate an elastic-plastic material with an arbitrary stress-strain curve and arbitrary strain rate dependency. Failure based on the effective plastic strain was also defined. For mild steel, fracture was assumed when the effective plastic strain reached 0.3. The collision posts and front short hood skin were made from Corten B steel with their stress-strain curve also shown in Figure 20. The failure plastic strain was defined as 0.2 for the Corten B steel, typical for higher-strength steels.

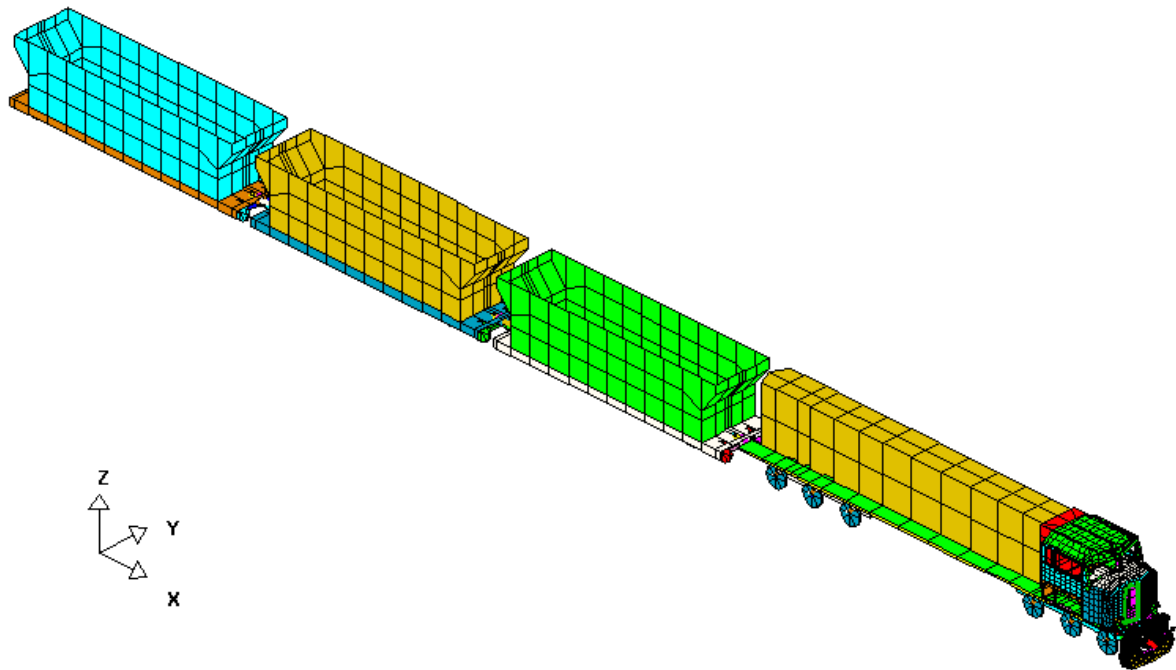


*Figure 19. FE model of the primary Loco1 consist*

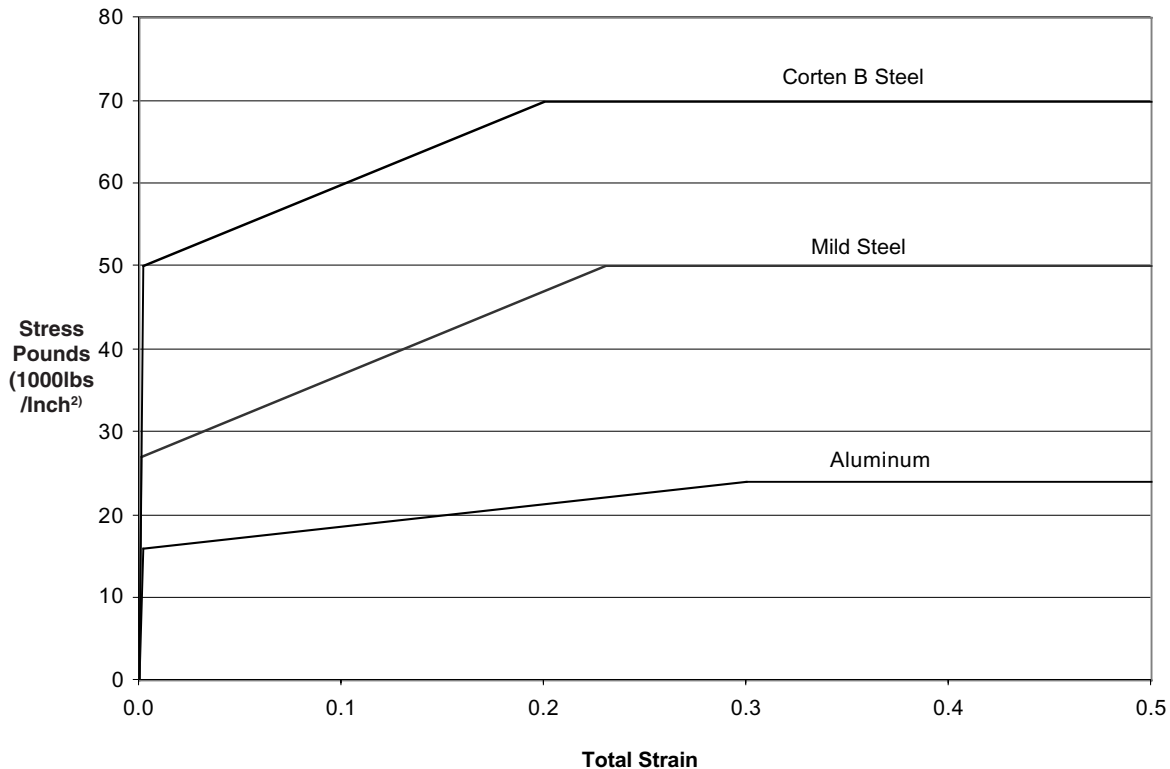


**Figure 20. Elasto-plastic properties of metals**

The contacts between the locomotive and the leading hopper were defined using node-to-surface and surface-to-surface contacts. A friction coefficient of 0.3 was assigned to the contacts. Other contacts among the locomotive, leading hopper and trailing hopper cars were also considered. The effects of weight, mass, and inertias were included and support of both consists in the vertical direction was defined using a ground plane.

For determining an adequate representation of ground friction for derailed vehicles, first a review of existing literature was conducted on the behavior of rail vehicles during and after the derailling process. Then, several trials using single vehicles with an orthogonal friction behavior for the contacts between the consist bogie bodies and the ground plane were conducted. Appropriate values of the friction coefficients were then set at 0.3 in the direction of wheel travel and 0.8 in the perpendicular direction. This provided a reasonable representation of the interaction of the consists with the ground during the collision process. Since the lateral forces needed for derailment (30,000 to 40,000 pounds range for locomotive wheels, a little less for loaded car wheels) are modest and short in duration compared to the collision forces, this approximation seemed reasonable after trials with different factors showed modest sensitivity to this parameter. Animated results from LS-DYNA revealed that these factors were a satisfactory compromise between non-derailed cars, and derailed cars for crush/collision modeling. The start of the expected accordion-type consist shape, telescoping of the draft gear, and contact of car bodies in later stages of the collisions were all, however, observed.

## **2.4 Results of Test Collisions for Development of Simulation Methods**

Two offset collision scenarios were studied: oblique collisions between the locomotive-headed primary consist and standing hoppers consist, and offset/head-on collisions between the same primary consist and shifted load container. The main objective was to evaluate model behaviors by simulating these two kinds of common collisions. Low to moderate speed collisions up to 50 mph were chosen, in which it is possible to enhance crew survivability by improving the structural design. In these speed ranges, crushing and dynamic effects are significant, but not so overwhelmingly destructive. The methodology proposed here is particularly suitable to study the vehicle dynamic response, structural building and crashing in these collisions.

One result that is produced from the LS-DYNA collision simulations is a time history of accelerations experienced in the consist. Decelerations (negative accelerations) in the engineer/crew cab of the lead locomotive can then be used as a general guide to the severity of the collision as it affects the crew. For most of the collisions modeled in this study, the decelerations of the cab floor were used as a general indicator of “environmental” deceleration for the cab and occupants.

The type and degree of injuries that an unrestrained crewmember will sustain depends greatly on the peak deceleration levels (“g-levels”) experienced, their duration and direction, the exact position of the crewmember at the start of the collision, and the specific interior equipment or objects that are impacted by the crewmember. For example, a crewmember seated in the normal forward facing seat, without restraints, could be ejected forward and upward even in a moderate frontal collision producing 3 to 4 peak g’s. Research in the automobile industry has determined the relationships between injury and g-levels for restrained and unrestrained individuals for many types of collisions, impact speeds, vehicle designs, and sizes and positions of the occupants. Similar research remains to be done for the railroad industry. Based on experience in other industries, such as auto and aircraft, humans can undergo environmental deceleration levels in the 3 g range without serious injury, if the surrounding interior is reasonably “crash friendly.” Injuries are likely to increase significantly with higher g-levels, especially in cases where there are repeated g-load peaks, multiple directions of the decelerations, and unprotected interior equipment or other features.

### **2.4.1 Baseline Simulation with Loco1**

#### **2.4.1.1 Collision with Hopper Consist**

These scenarios simulate low-angle collisions occurring during the presence of a consist fouling a turnout, projecting into the main line Right Of Way (ROW). The initial collision configuration is shown in Figure 21. The consists were offset two-thirds of the standard 10 foot rail vehicle width in the lateral direction, with the left side of the leading hopper about 10 in inside (overlying) the left collision post of the locomotive. The relative angle between the consists was 8.5 degrees.

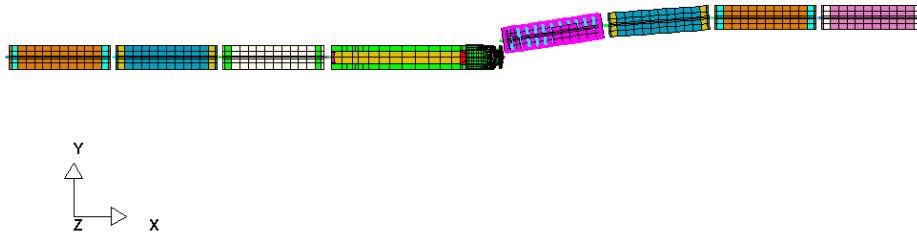
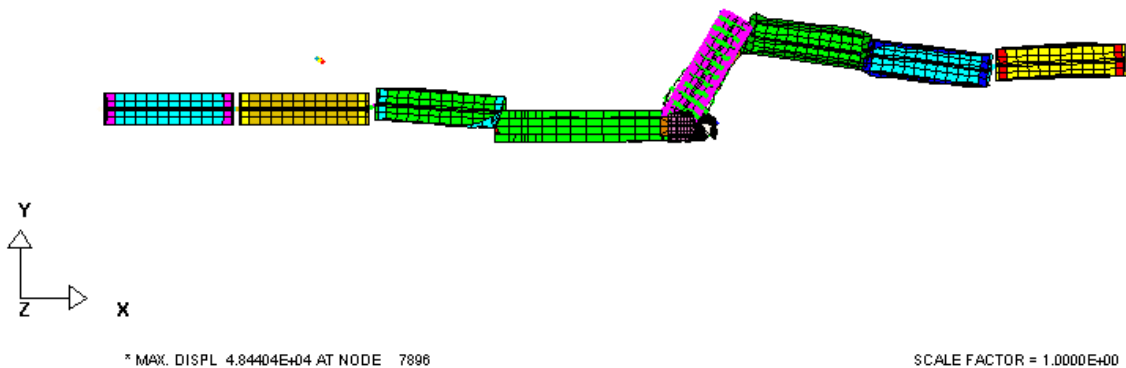


**Figure 21. Collision configuration between Loco1 and hopper car consists**

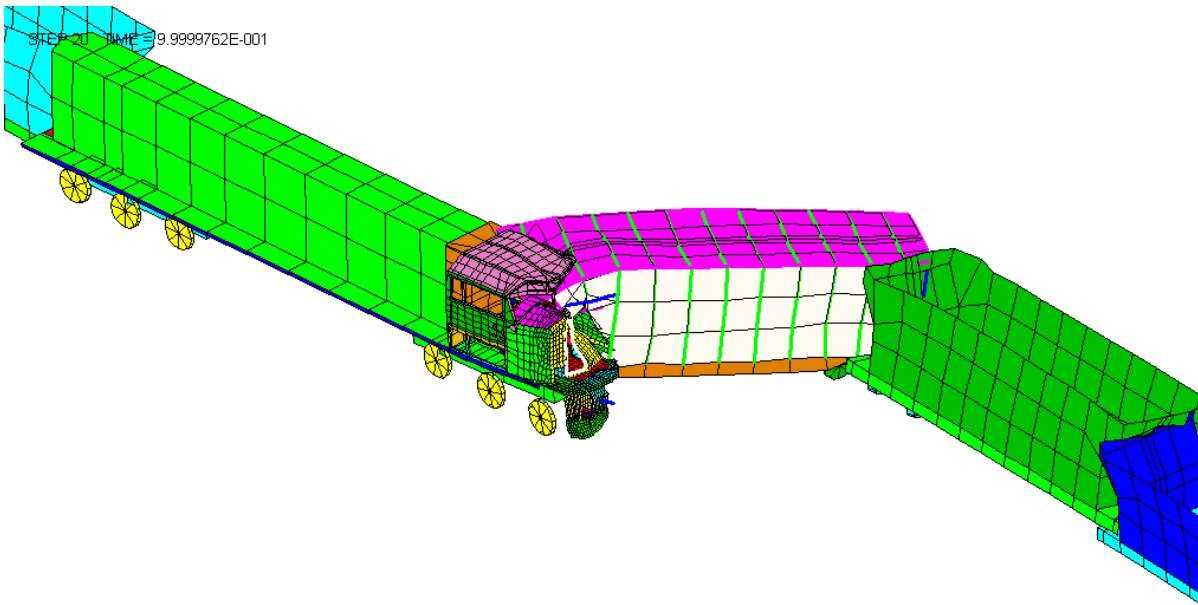
Two cases have been used for the development process, with the primary consist traveling at 30 and 50 mph impacting the stationary hopper consist. The results for the 50 mph case are discussed here in detail; the results at 30 mph are similar with significantly less damage.

Figure 22 shows the top view of both consists 0.8 seconds after collision. Much larger motions occurred for the hopper consist than for the locomotive-headed consist, consistent with the higher locomotive weight and momentum. There were large deformations in the short hood of the locomotive and carbody of the leading hopper, which are shown in Figure 23. Secondary collisions also occurred between the lead vehicle and trailing cars in both consists as the

STEP 20 TIME = 9.9999762E-001



**Figure 22. Top view of the 50 mph collision between Loco1 and hopper car consists at 1 second**



*Figure 23. Close-up view of the 50 mph collision between Loco1 and hopper car consists at 1 second*

successive car draft gears compressed ("telescoped"); this realistically reflected behavior in higher-speed collisions. The collision sequence can be observed from the velocity profiles of the locomotive and all hoppers in the locomotive axial direction as shown in Figure 24. The floor acceleration profile (g's) in the region of the locomotive cab floor (engineer's side) in the locomotive axial direction is shown in Figure 25. The resultant contact force between the locomotive and leading hopper is shown in Figure 26.

#### **2.4.1.2 Collision with ISO Container**

This scenario simulates a shifted load type of collision between the locomotive in consist and a container from a flat car that has shifted partially into the path of the locomotive. The container was offset laterally just outside the collision posts, and overlapped the windshield/corner post and short hood, as shown in Figure 27. The position of the ISO container is fairly high up on the locomotive, representing the top-level container on a two-high stack, which is a common rail configuration. The height of the center-of-gravity (CG) of the container was close to the height of the short hood top. This high position presents a potentially more dangerous situation for the crew members, since the center of the oncoming mass was at the windshield level of the locomotive.

Two cases have been used for the development process, with the locomotive-headed consist traveling at 30 and 50 mph impacting the "suspended" container. The results for the 50 mph case will be presented. The results for 30 mph showed similar but less violent behavior.

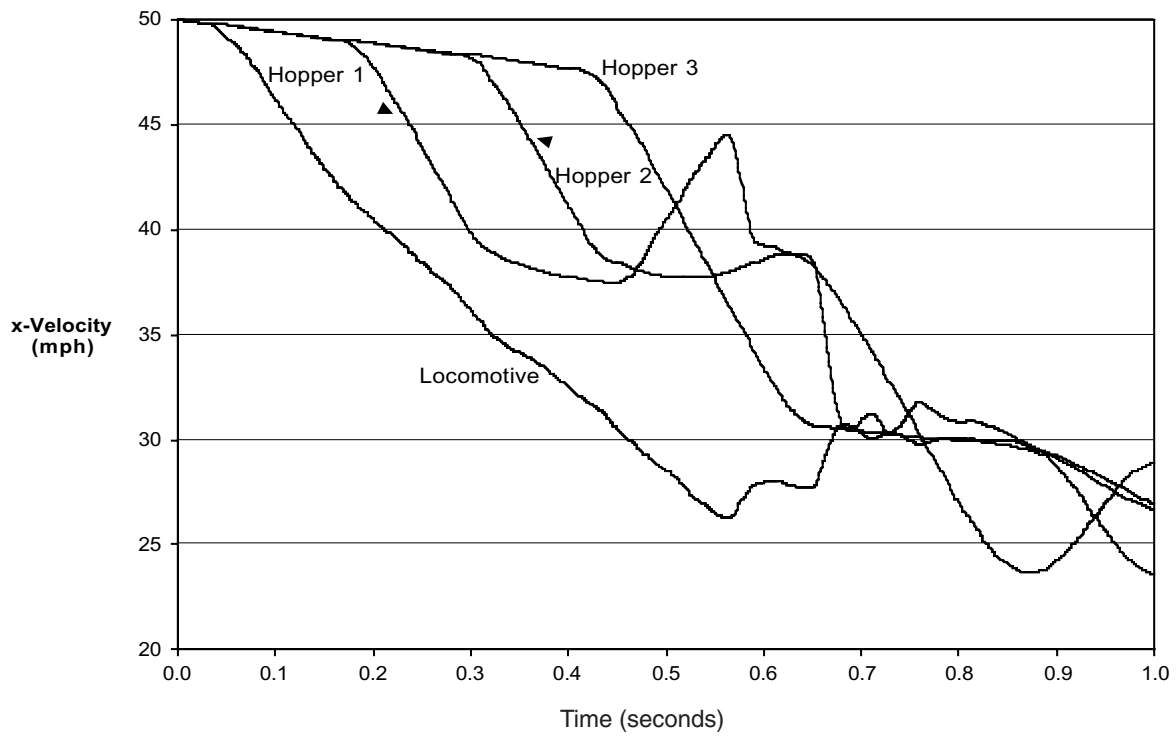


**Figure 24.** *Velocity profiles of locomotive and hopper cars of the Loco1 consist*

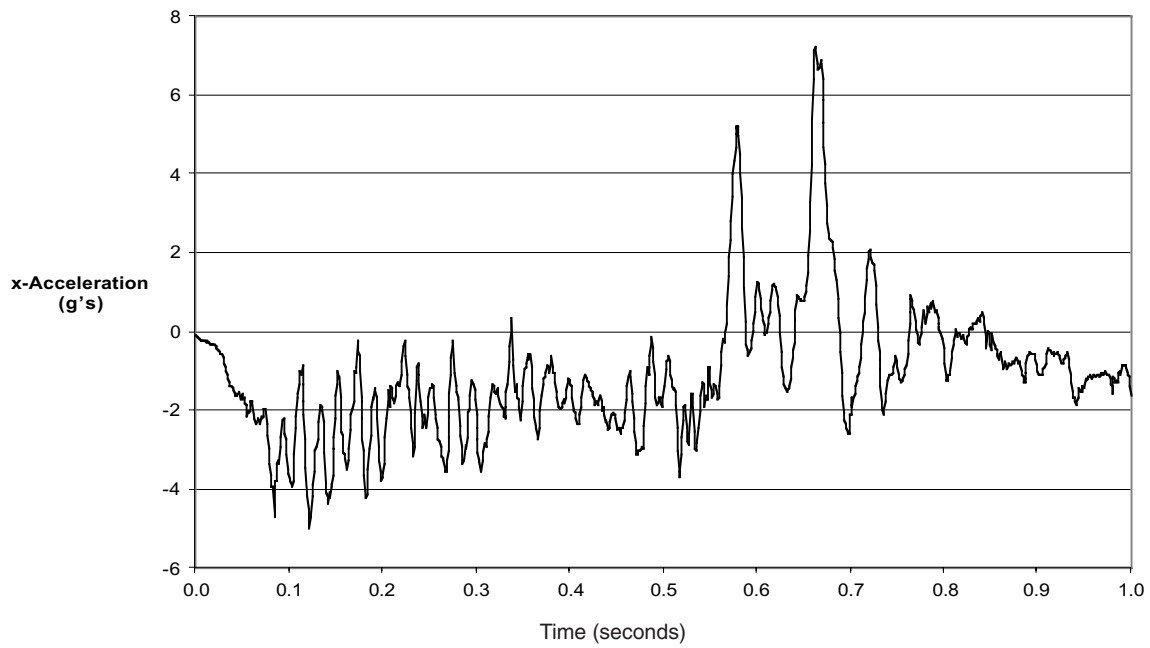


**Figure 25.** *Cab floor deceleration for the 50 mph collision between Loco1 and offset, standing hopper car consists*

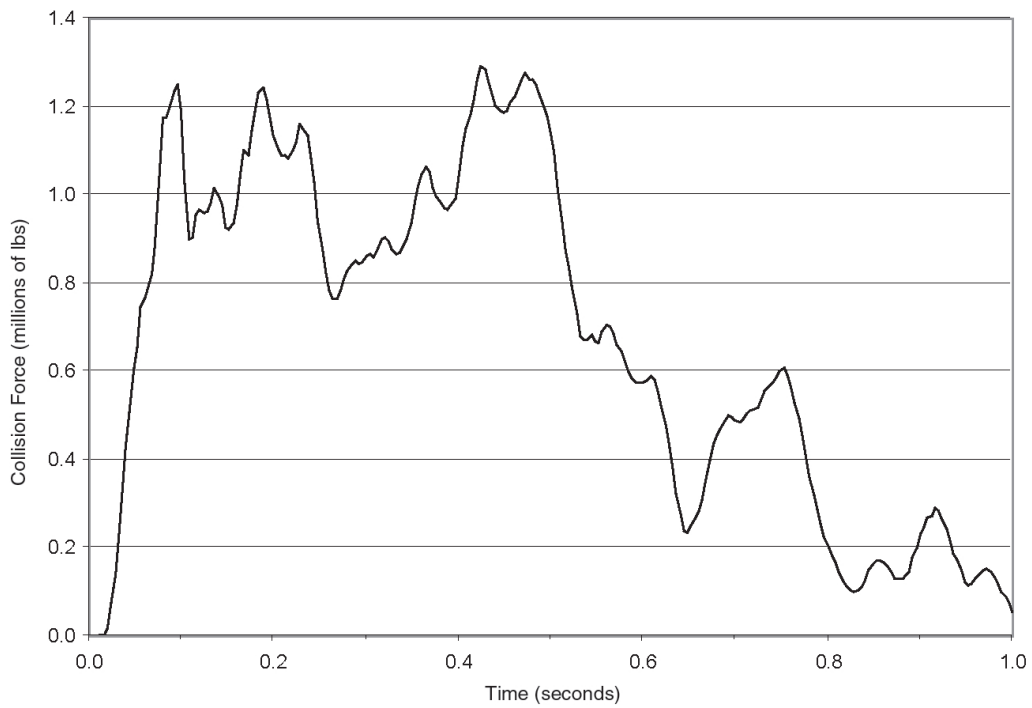


**Figure 26.** *Total collision force between Loco1 and offset, standing hopper car consists*

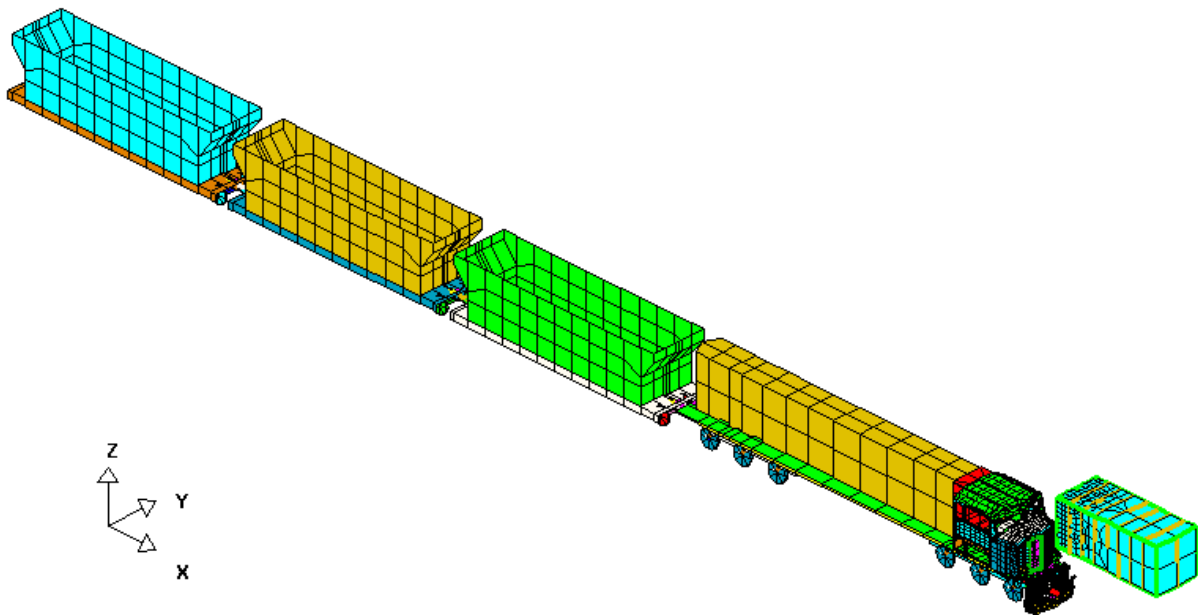


**Figure 27.** *Collision configuration between Loco1 consist and suspended ISO container*

The maximum deformation stage for both locomotive and container in the 50 mph collision is shown in Figure 28. The primary collision process between the short hood and container was followed by the secondary collision between the corner post, windshield, cab roof, and container. The acceleration profile (g's) at the proximity of the engineer's feet along the locomotive axial direction is shown in Figure 29. The floor acceleration experienced by the engineer in this case was much lower than the one in the consist collision described above. The resultant contact force between the locomotive and container is shown in Figure 30.

## 2.4.2 Baseline Simulation with Loco2

The two collision scenarios that were previously studied using the Loco1 were repeated here using the consist headed by the second U.S. locomotive (Loco2). They are collisions of the primary locomotive consist with the secondary hopper/box car consist or with the ISO container. The same initial configurations as in the Loco1 simulations were used. The collisions were again analyzed using LS-DYNA and the results are presented.

### 2.4.2.1 Collision with Box Car Consist

The deformations of both locomotive and box car at the end of simulation (1 second) for the 30 mph collision are shown in Figure 31. In this case, the locomotive underframe sustained severe damage, while the short hood and cab sustained very limited damages (Figure 32).

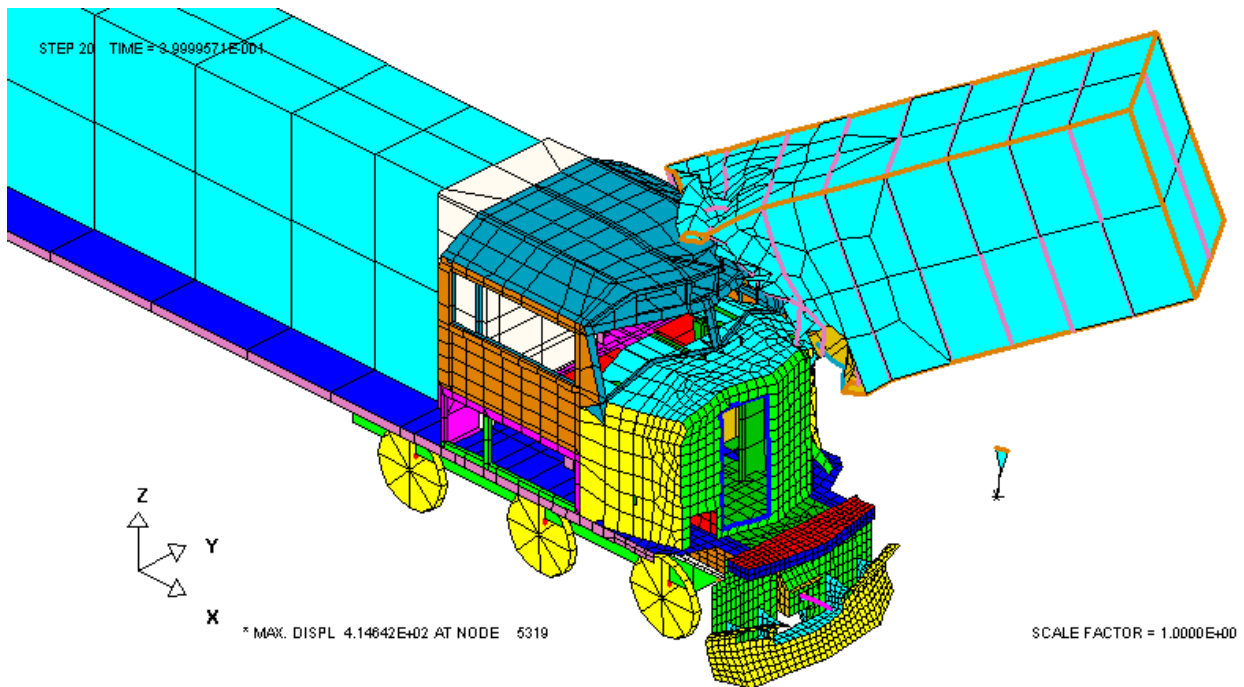


**Figure 28.** Close-up view of the 50 mph collision between Loco1 consist and container at 0.4 seconds



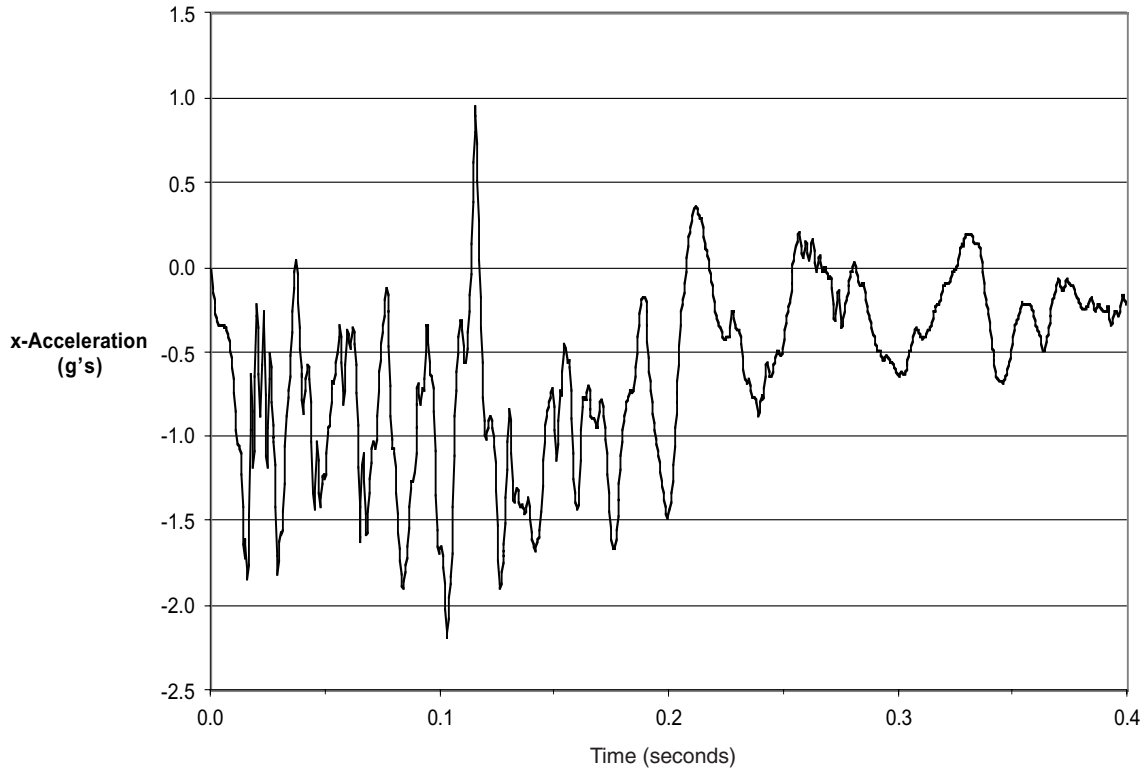


**Figure 29.** Cab floor deceleration for the 50 mph collision between Loco1 consist and container

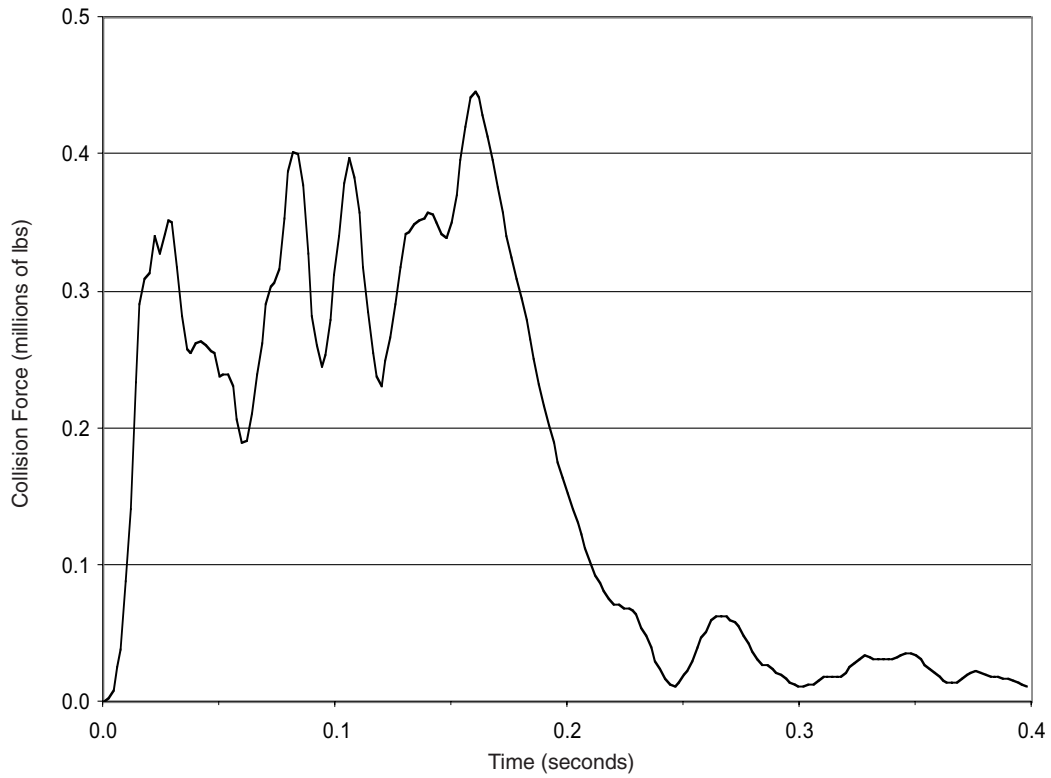


**Figure 30.** Collision force for the 50 mph collision between Loco1 consist and container

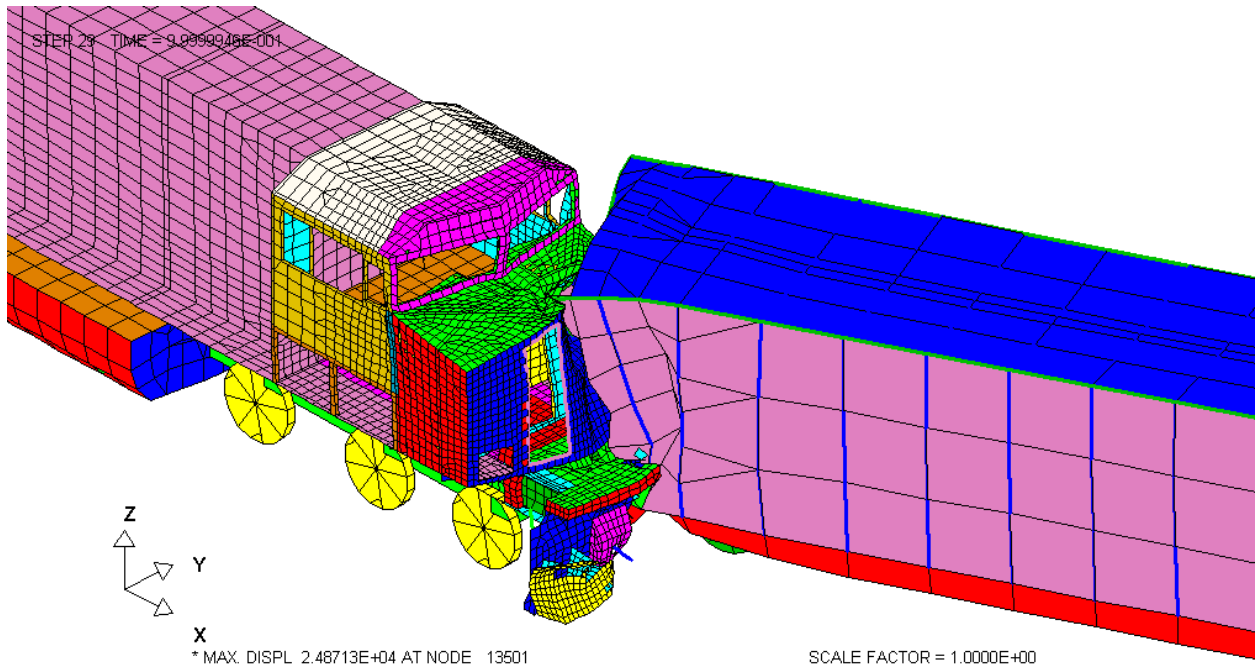


**Figure 31.** Close-up view of the deformations of locomotive and box car at the end of simulation (1 second) for the 30 mph case

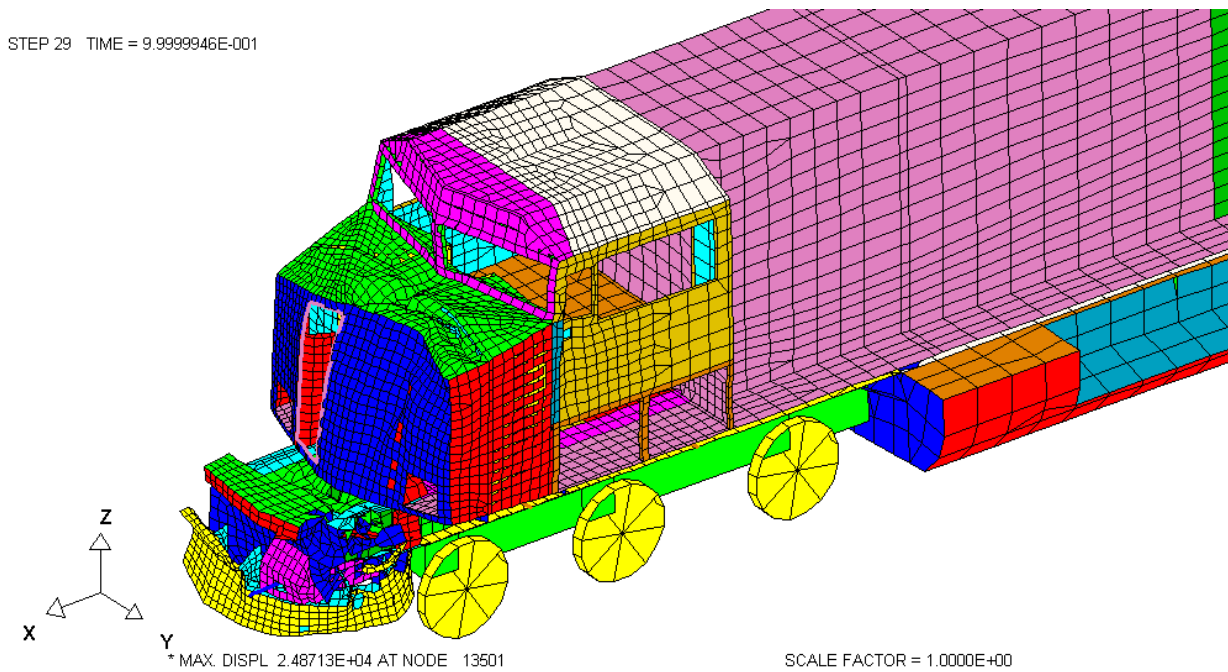


**Figure 32.** Deformed locomotive at the end of simulation (1 second) for the 30 mph case

However, significant damage was done to both short hood and cab including a large cab volume loss for the 50 mph case as shown in Figure 33. The collision forces and cab floor decelerations for both cases are comparable to those of the Loco1 locomotive study.

### 2.4.2.2 Collision with ISO-Type Container

The container was placed about 32.5 in above the top of the locomotive underframe and just missed the left collision post laterally, exactly the same position as in the Loco1 locomotive study. The initial speed of the Loco2 consist was 50 mph and the container was assumed stationary. The deformations of both locomotive and container at the end of simulation (0.5 seconds) are shown in Figure 34. The lateral view of the deformed locomotive at end of simulation is shown in Figure 35. It can be observed that the windshield/ corner post area, the top of the cab, and the short hood sustained significant damages. The front portion of the container was totally torn off. These observations are similar to those of the collision between the Loco1 locomotive consist and container, with the exception that the damages to the Loco2 are somewhat more severe. Similar collision force and deceleration for the locomotive cab floor were also obtained.

### 2.4.2.3 Collision with Loco1 Consist

The same Loco1 consist as in subsection 2.4.1 was used as the collision object. The Loco1 and Loco2 consists were assumed to have one-third offset (40 in) laterally and the two locomotives had a relative angle of 8.5 degrees. The platform of the Loco2 was about 3.75 in higher than that

STEP 25 TIME = 9.9999684E-001

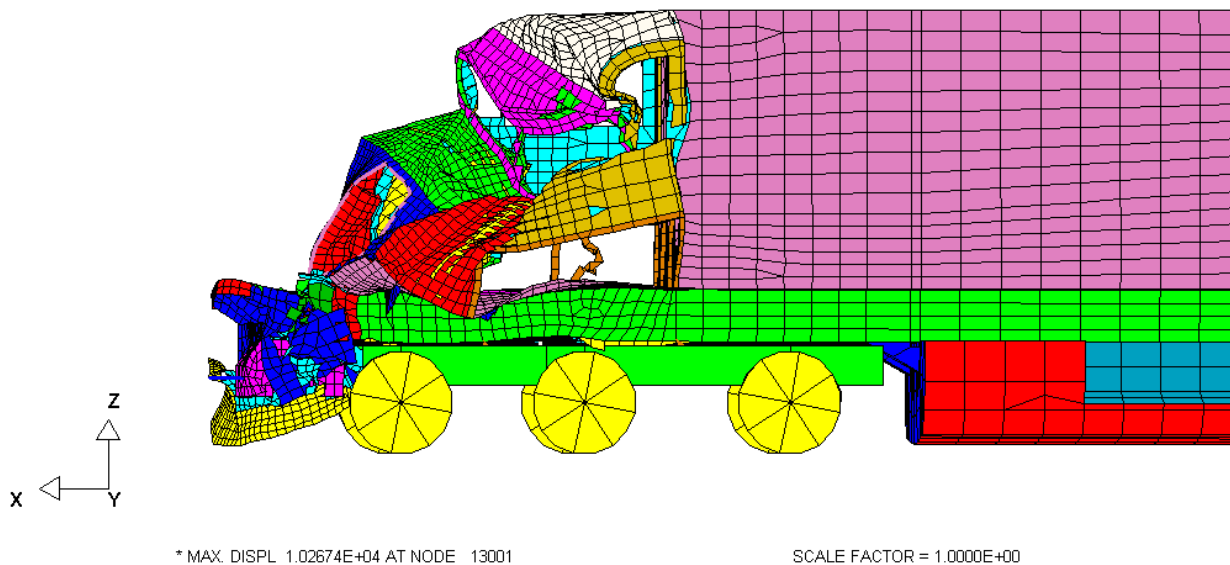


*Figure 33. Deformed locomotive at the end of simulation (1 second) for the 50 mph case*

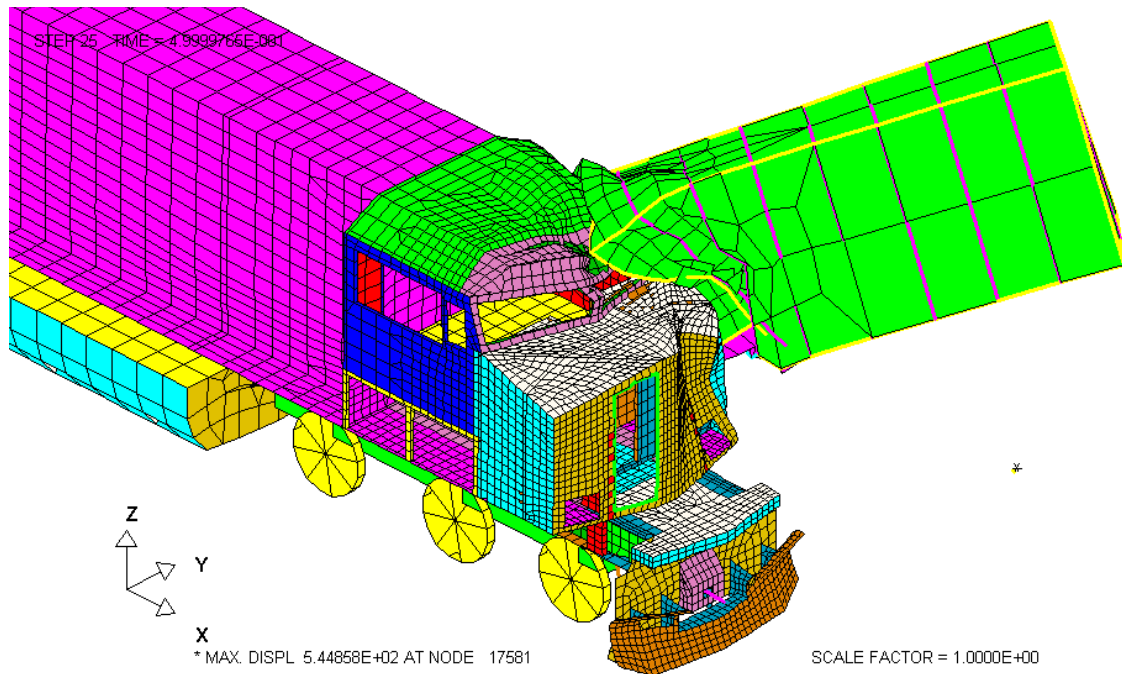


**Figure 34.** *Deformations of the locomotive and container at the end of simulation (0.5 second) for the 50 mph collision*

STEP 25 TIME = 4.9999765E-001

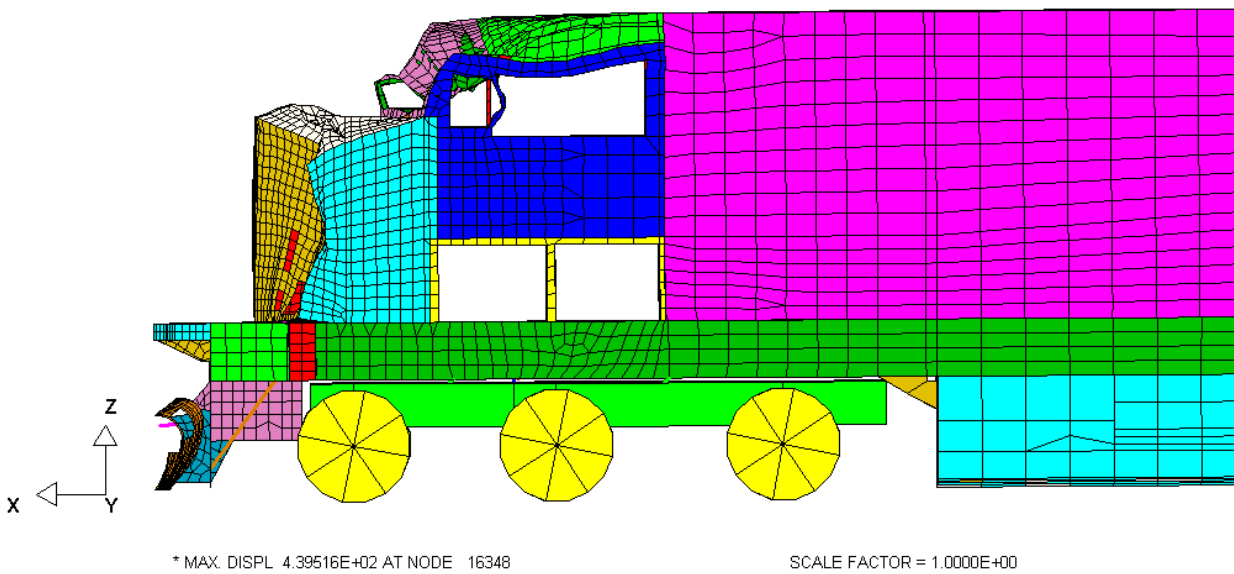


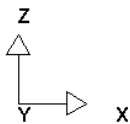
**Figure 35.** *Lateral view of the deformed locomotive at the end of simulation (0.5 second) for the 50 mph collision*

of Loco1. The Loco1 consist assumed an initial velocity of 50 mph while the Loco2 consist was assumed stationary. The lateral view of the consists at the end of simulation (1 second) is shown in Figure 36, while the deformations of both locomotives are shown in Figure 37. Most damage to both locomotives occurred in the front portion of the underframes and short hood areas. The cabs of both locomotives remain basically intact. Injury to the crew members due to direct intrusion is minimal. However, the deceleration at the cab floor was about 9.5g as shown in Figure 38, and injury due to this high g-load and secondary collisions between the crew members and the cab interior is highly possible.

## 2.5 Summary of Test Collision Studies

Two common off-center collision scenarios were simulated and their results presented using the “model-in-model” approach with LS-DYNA. The accelerations of the underframe floor were quantified to get estimates on the impact levels crewmembers would experience. For specific representation of the behavior of human crew occupants in the locomotive cab, further detailed modeling could be performed using computerized human “dummies” with actual interior structures and systems. This approach would be used to estimate injury and survivability levels with various combinations of interior arrangements (seat construction, spacing from interior, even restraints or air-bag type measures, if deemed practical). A variety of probable collision scenarios can be used and the injury levels of the crew can be predicted using the methodology developed.

STEP 25 TIME = 9.9999905E-001



\* MAX. DISPL 4.17598E+04 AT NODE 2766

SCALE FACTOR = 1.0000E+00

**Figure 36.** Side view of the two locomotive consists at the end of simulation (1 second) for the 50 mph collision

STEP 25 TIME = 9.9999905E-001

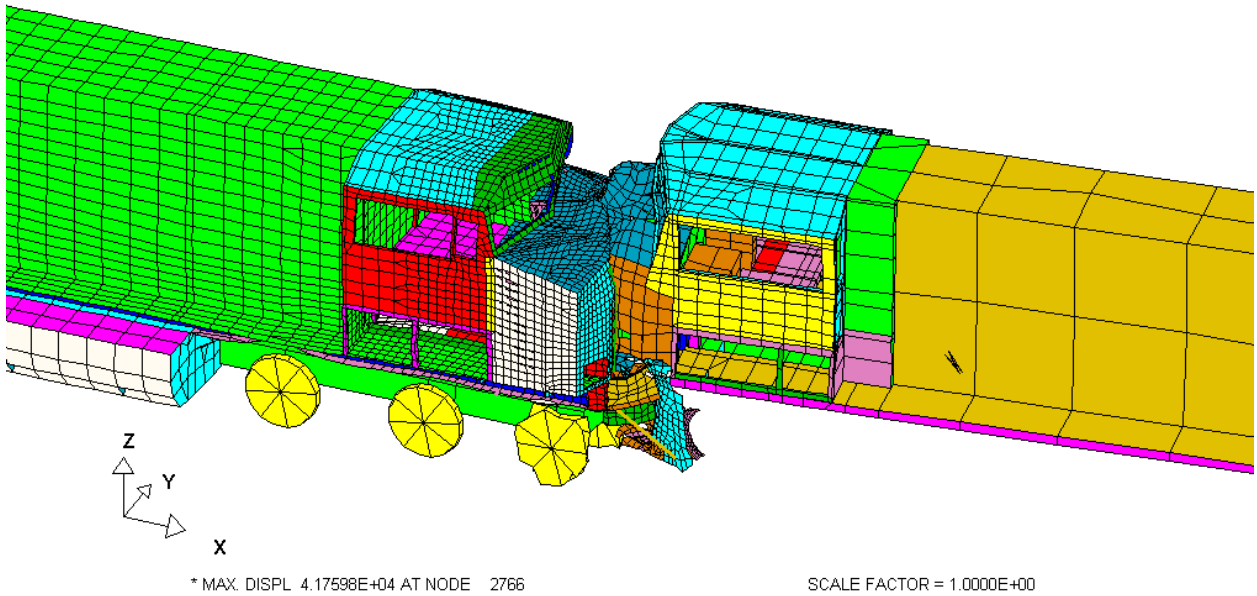


**Figure 37.** Close-up of the deformations of both locomotives at the end of simulation (1 second) for the 50 mph collision

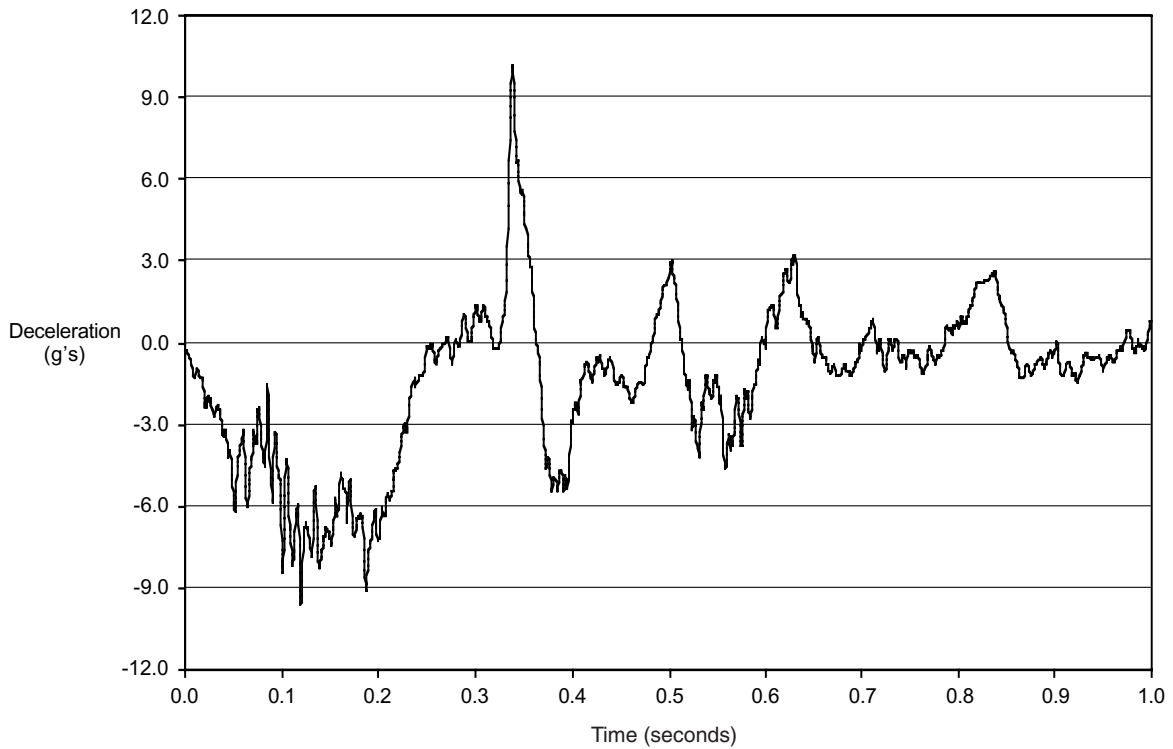


**Figure 38.** Time history of deceleration at the Loco2 cab floor for the 50 mph collision

An ISO container was used in the current study, since these are often found in single and double stack intermodal rail cars. The strength and weight of a container will of course affect the crushing of the short hood and cab and involvement of the corner posts in a collision.

A similar methodology has been widely used in the automotive industry. Although not validated by actual accident data at this stage, the predicted results are reasonable. Some trial runs of head-on collisions between two locomotives, and a locomotive to a rigid wall were conducted and reasonable behaviors were also observed. Of course, a complete comparison between the predicted results and either accident or experimental data should be made before any final conclusions can be drawn. Similarly, the current models can be properly modified to simulate recorded accidents to assess the fidelity of the present modeling approach as reported in Section 4. When fully validated, the current approach and models could be used as an integrated part of the design process for safer locomotives.

This analytical method for simulation of rail vehicle collisions appears promising for evaluating detailed structural behavior of locomotives and other rail vehicles, and will also aid in the prediction of survivability for train crews. This method involves use of recent computerized models already proven in the automobile industry. The method can account for the coupled behavior of multiple-vehicle rail consists, and the many types of collisions, which can threaten train crews. The scenarios can include collisions with other trains (head-or tail-end), shifted loads from adjacent trains, and grade crossing collisions. The method is very useful in identifying key parameters affecting the collision consequences.

### **2.5.1 Simulation Method Developed for Rail Vehicle Collisions**

The current method utilizes a full 3-D, nonlinear, dynamic FE structural modeling approach with the LS-DYNA program system, supplemented by a preprocessor for model generation, and postprocessor for color graphic animated depiction of the collision process.

The principal new development in this method is the use of detailed 3-D structural models of the vehicles (and/or objects) in direct collision, embedded within an overall dynamic model of the colliding consist(s) and objects. The simulation of the complete collision and the local structural effects is therefore performed in a single step. This inherently considers the interaction process of the multiple vehicles and objects together with the localized detailed dynamic crushing behavior of the structures, which are directly affected by the collision. This approach, using LS-DYNA with embedded detail models in overall consist models is producing encouraging results with generalized accident scenarios.

### **2.5.2 Guide to Modeling Characteristics for Simulations**

Accurate prediction of the consequences of a collision requires first that the modeling process include representation of large nonlinear deflections, buckling, and kinematics, such as provided by LS-DYNA. Specifically, adequate modeling of train consists in collisions requires the following:



- (a) The overall LS-DYNA model for train consists to provide realistic 3-D nonlinear spring rates between vehicles representing the effect of draft gear deformations, travel stops, and clearance (initial free travel).
- (b) Data on all consist vehicles, bogies, and 3-D suspension stiffnesses between bogies and body, travel stops, and clearances.
- (c) Overall masses and 3-D inertias for each vehicle in the consist with separate items for loaded carbody with draft gear, and for bogies.

Together, (a) through (c) permit representation of the interacting forces within the consists during the collision plus the yaw, pitch and roll motions of the vehicles in a reasonably realistic manner. These are needed primarily to produce the proper forces and impulse in the collision zone. Results on the consist deflections (telescoping and “accordion” pattern) during the collision event with relatively simple ground interaction rules (“orthotropic friction”), are encouraging.

- (d) Control and definition of the surfaces that contact during the collisions. This can be accomplished by having at least one of any two contacting surfaces be “deformable” (i.e., have defined, finite structural load-deflection characteristics). LS-DYNA has means of defining contact surfaces.
- (e) Nonlinear material characteristics for all deformable structures modeled as plates, shells, beams, etc. The nonlinearity (assuming metallic components) in the elasto-plastic behavior with a typical “piecewise linear” stress-strain curve embodying the elastic, elasto-plastic, and ductile (if applicable) ranges up to fracture (ultimate strength). Incorporating these material characteristics will provide a means of separation at critical joints, welds, etc., due to crashing, buckling and excessive deformations.
- (f) Adequate finite-element “mesh” size for the contacting structures both on the locomotive and the other object or vehicle in the collision. The structures most heavily involved in the deformation/collapse process would require relatively fine meshes; other far away structures from contact areas can be modelled with coarser meshes. Locomotive structures which should be modeled in considerable detail include the front end areas such as hood structures, cab, draft gear pocket, collision posts, anticlimber, etc. Impacting structures such as the hopper car bodies and ISO containers would also be fully deformable fine meshes, increasing in fineness towards the impact area. The structural models described earlier in this report indicate the degree of fineness, which has resulted in realistic crash behavior, although it is possible a reduction in fineness (i.e., number of FEs) could be made with further trials.

Items (d) through (f) generally provide for realistic collapse and crushing of the contacting structures, which fail through a combination of yielding, buckling, plasticity and fracture (local separations). This is a direct way of assessing the forces, deflections and damage during the



many types of collisions, some of which involve only local (but critical) areas of the locomotive such as the cab, hood and windshield structures.

### **2.5.3 Summary**

The modeling approach for comprehensive simulation of rail vehicle collisions has been demonstrated and appears to produce realistic and usable results in complex situations such as off center and oblique conditions. The results to date indicate that the method can be successfully used to evaluate and guide development of crashworthiness and survivability improvements.

Use of this methodology is helpful in conducting parametric studies to determine the effects on collision behavior for primary variables such as: impact speed, type of freight car in collided with, strength and weight of shifted load, and location and orientation of colliding object or vehicle on primary locomotive frontal area.



### **3. PARAMETRIC STUDIES OF LOCOMOTIVE CRASHWORTHINESS**

The finite element method has been used to simulate several rail vehicle collision scenarios to evaluate the detailed structural behavior of locomotives and other rail vehicles. These collision scenarios include collisions of a locomotive-headed consist with a hopper/box car consist and shifted loads. Detailed three-dimensional models of vehicles involved in direct collision, such as the lead locomotive and hopper/box car, were embedded within overall dynamic models of the collision consists. The simulation of the complete collision involving multiple vehicle interactions and localized detailed structural crushing is performed in a single step. The approach has produced encouraging results for the simulated scenarios.

To better understand collision dynamics and increase the fidelity of the simulation approach, parametric studies were performed to evaluate the effects of various factors on the overall collision process and local structure behavior. These factors include collision speed, strength and weight of struck objects, struck car end structures, and offset. These parametric studies were conducted using the previously generated finite element models. These models include a locomotive-headed (Loco1) consist, a hopper/box car lead consist, and an ISO-type container. Readers are referred to Section 2 for complete description of these models including material properties.

#### **3.1 Collisions with Standing Hopper/Box Car Consist**

This scenario simulates a low angle collision during the presence of a consist fouling a turnout (S-type), projecting into the main line ROW. The top view of the collision configuration between the primary Loco1 consist and standing hopper car consist is shown in Figure 21. The first two cars of the hopper consist are on the turnout with the remaining two cars on a parallel track. The relative angle between the lead hopper car and locomotive consist was 8.5 degrees and the angle between the first and second cars of the hopper consist was 4.25 degrees. The lead hopper car was offset laterally two-thirds of the standard 10 foot rail vehicle with respect to the locomotive.

##### **3.1.1 Effects of Collision Speed**

Two cases were studied: the locomotive consist moving at 30 and 50 miles per hour, colliding with the standing hopper consist.

- The top view of the consist at the end of simulation (1 second) for the 30 mph collision is shown in Figure 39. The top view of the consist for the 50 mph collision was previously shown in Figure 22. The rotations (in the horizontal plane unless specified) of the lead

STEP 21 TIME = 9.9999762E-01

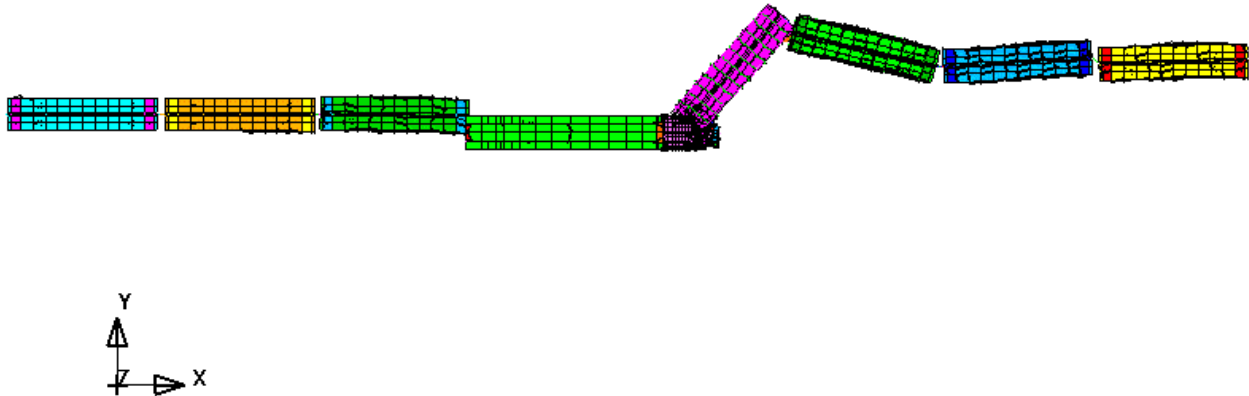


*Figure 39. Top view of the locomotive and hopper consists at  $t = 1$  second for the 30 mph case*

hopper car were 30 degrees and 55 degrees for the 30 and 50 mph cases, respectively, at the end of analysis. There was no obvious rotation for the locomotive in both cases.

- The deformations of the locomotive were considerably less at the lower speed collision compared with the higher speed collision as shown in Figures 40 and 41 (lateral view). The collision post and short hood deformed a lot. The top plate failed for the 50 mph case. There was significant damage to the windshield/corner post area for both cases due to the projecting top of the hopper body. The corner post was torn apart at the higher speed. There was also noticeable damage to the locomotive underframe and some cave-in of the cab roof for the 50 mph case.
- Maximum longitudinal deceleration at the cab floor were 4.5 and 5.0 g's. Although there was not much difference in their maximum values, the duration was much longer for the 50 mph collision. Peak contact force levels were 1.45 and 1.55 million pounds for the 30 and 50 mph cases, respectively.
- Direct injury is possible to unrestrained crew members for the 50 mph case.

### 3.1.2 Effects of Car End Consist: Box Car versus Hopper Car

The lead hopper of the hopper consist was replaced by a box car to form the box car consist. The trailing hopper cars were kept the same. The box car was adjusted to have the same weight as a

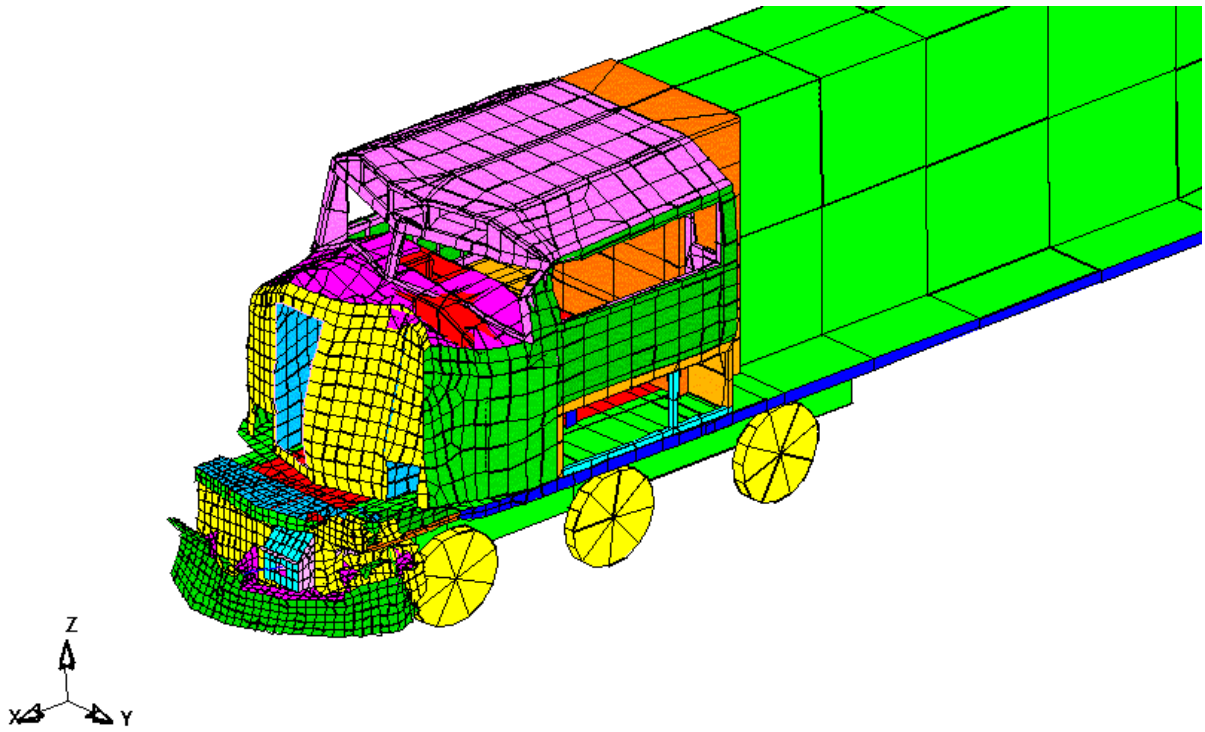


*Figure 40. The deformed locomotive for the 30 mph collision with the standing hopper consist*

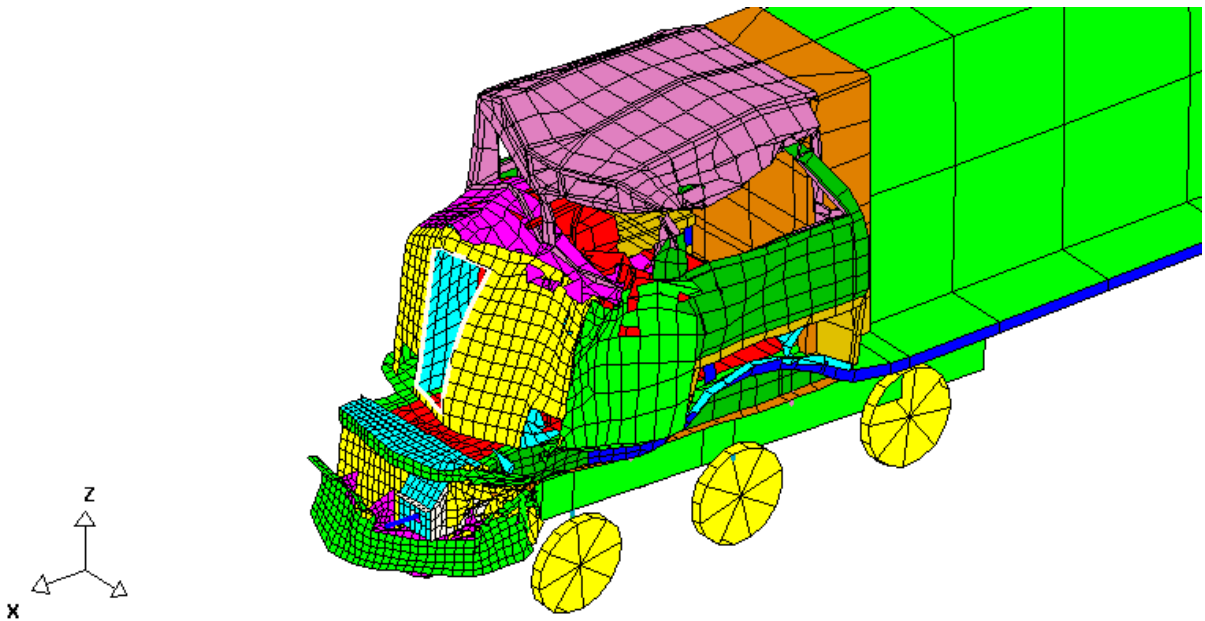


*Figure 41. The deformed locomotive for the 50 mph collision with the standing hopper consist*

hopper. Thus, the only difference between the two consists is their end model construction. The box car had a flat front side, compared with the cave-in shape of the hopper. A collision speed of 50 mph was selected to study the effects of the different car end structure.

- Similar overall motion patterns for the locomotive consist occurred, but with less rotation (45 degrees) for the lead box car.
- Large twisting and inward deflection in the left collision post occurred for both cases (Figures 41 and 42). Similar deformation patterns in the short hood were also predicted. The twisting motion of the hopper/box car resulted in collision with the side of the locomotive and caused considerable damage to the underframe.
- A little higher contact force (1.7 million pounds) and cab floor deceleration (5.8 g's) for the box car case was predicted.
- Injury is possible to the crew members due to intrusion and secondary collisions with the interior.

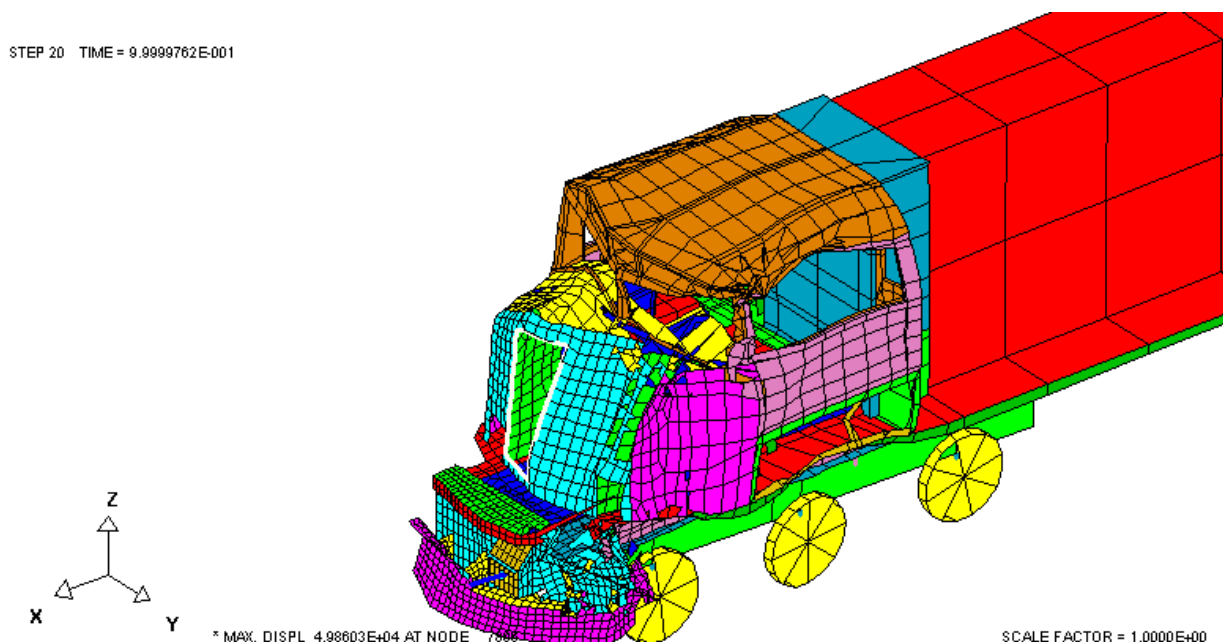


**Figure 42.** *The deformed locomotive for the 50 mph collision with the standing box car consist*

## **3.2 Collisions with ISO-Type Containers**

This collision scenario simulates a shifted load type collision between the locomotive consist and a container from a flat car that has shifted partially into the path of the loco. The container was offset laterally just outside the collision posts, and overlapped vertically the windshield/corner post and short hood as shown in Figure 7. The mid-section (CG) of the container was approximately at the height of the short hood top.

Two other versions of the base model were generated to study the effects of container strength and weight on collisions between the locomotive consist and container. For one version the plates and beams were considered to be made from mild steel. For the other version the weight of the base model was increased to 60,000 pounds by scaling the densities of all plates.

### **3.2.1 Effects of Collision Speed**

Two cases were analyzed: the locomotive consist moving at 30 and 50 mph collided with the stationary baseline container. The following results were obtained:

- The container rotated toward the windshield/corner post area around the front edge of the short hood in addition to the longitudinal crushing for both collision speeds. The deformed shape of the locomotive and container at the end of the simulation (0.4 seconds) for the 50 mph collision was shown in Figure 28. No contact between container and the windshield/corner post area was observed for the 30 mph case.
- Some deformations occurred in the short hood for the 30 mph case (Figure 43), while part of the short hood was sheared off along the collision post edges for the 50 mph case (Figure 44). Some deformations occurred in the windshield/corner post area for the higher speed collision. The collision posts were not involved much in either case.
- Cab floor decelerations were below 2 g's for both cases. Severe injury from direct intrusion collision seems unlikely away from the impact-side forward cab area, but flying debris, interior equipment or secondary collision between the crew and interior could occur.

### **3.2.2 Effects of Container Strength**

Two collision cases were evaluated: the locomotive consist moving at 50 mph colliding with the stationary baseline container and with the all-steel container. Comparison is as follows:

- The container had more pitch motion for the all-steel container case. The container actually hit the cab roof resulting in some cave-in for this case.
- Deformation patterns were similar for both cases, although more deformations occurred for the stronger case, especially in the windshield/corner post area and cab roof (Figure 45). Not much involvement for the collision posts occurred for either case.

STEP 21 TIME = 3.9999571E-01

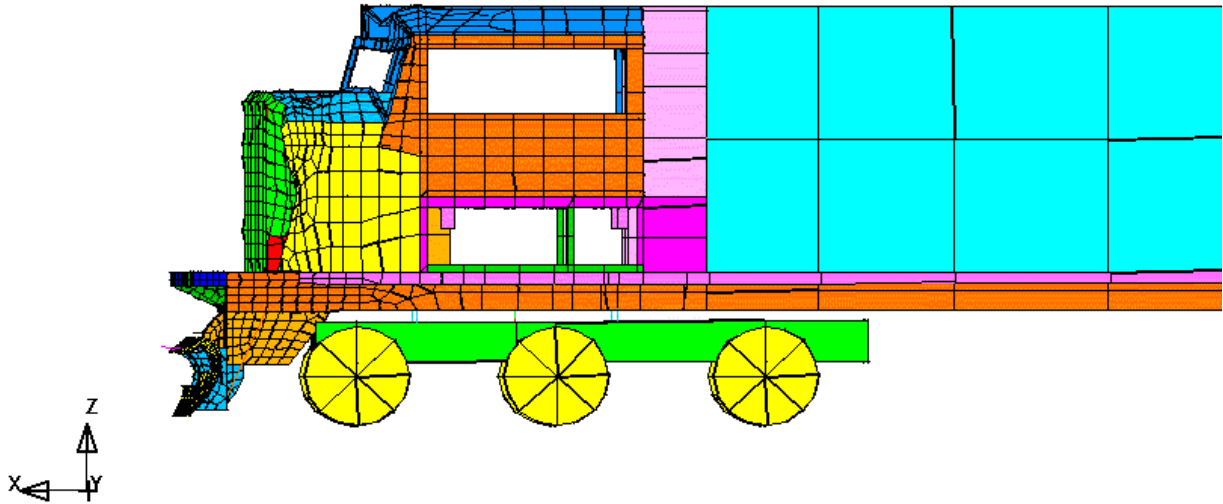


*Figure 43. The deformed locomotive for the 30 mph collision with the 30,000 pound aluminum container*

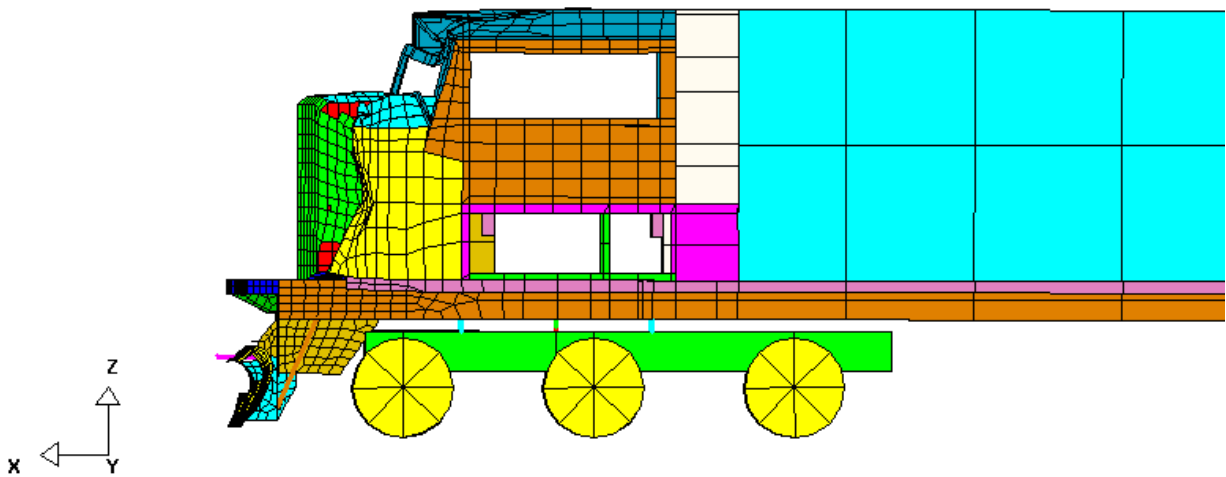


*Figure 44. The deformed locomotive for the 50 mph collision with the 30,000 pound aluminum container*



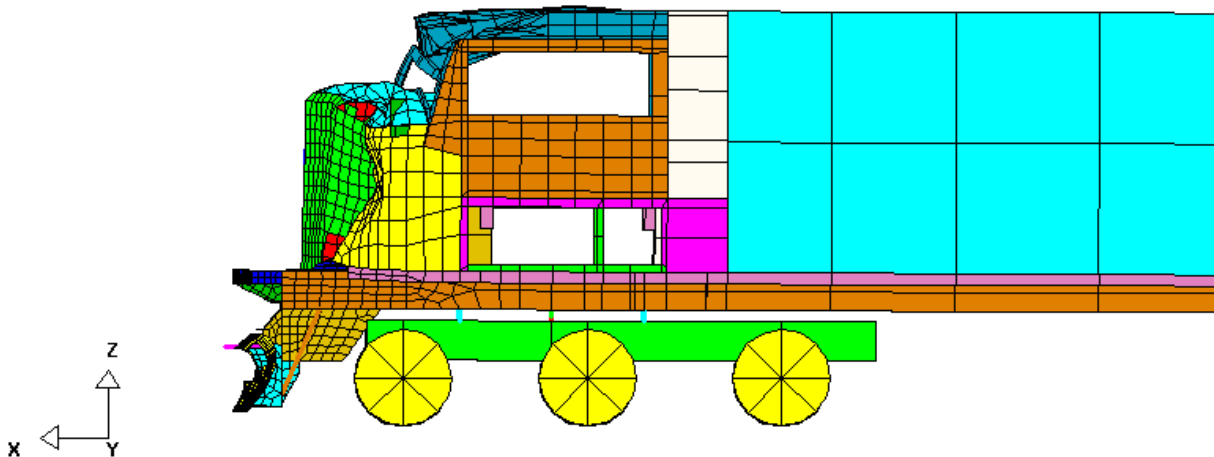


*Figure 45. The deformed locomotive for the 50 mph collision with the 30,000 pound all-steel container*

- Maximum contact forces were 400,000 and 500,000 pounds, and longitudinal decelerations were 2 and 2.5 g's respectively for the baseline case and all-steel container case. Severe injury from direct intrusion or secondary collision is still unlikely.

### 3.2.3 Effects of Container Weight

Two cases were evaluated for a locomotive consist moving at 50 mph colliding with a stationary container: 1) the baseline 30,000 pound container, and 2) a similar 60,000 pound container. Comparison is as follows:

- While the pitch motions were similar for both cases, the heavier container penetrated the locomotive cab more along the longitudinal direction.
- More damage occurred to the windshield/corner post area, especially the cab roof for the heavier container case as shown in Figure 46. The collision posts did not significantly affect the outcome, similar to the studies of collision speeds and container strengths.
- The maximum cab floor deceleration was about 3 g's for the heavier container case. Direct injuries to the crewmembers are possible due to significant cab penetration by the heavier container.

STEP 20 TIME = 3.9999571E-001

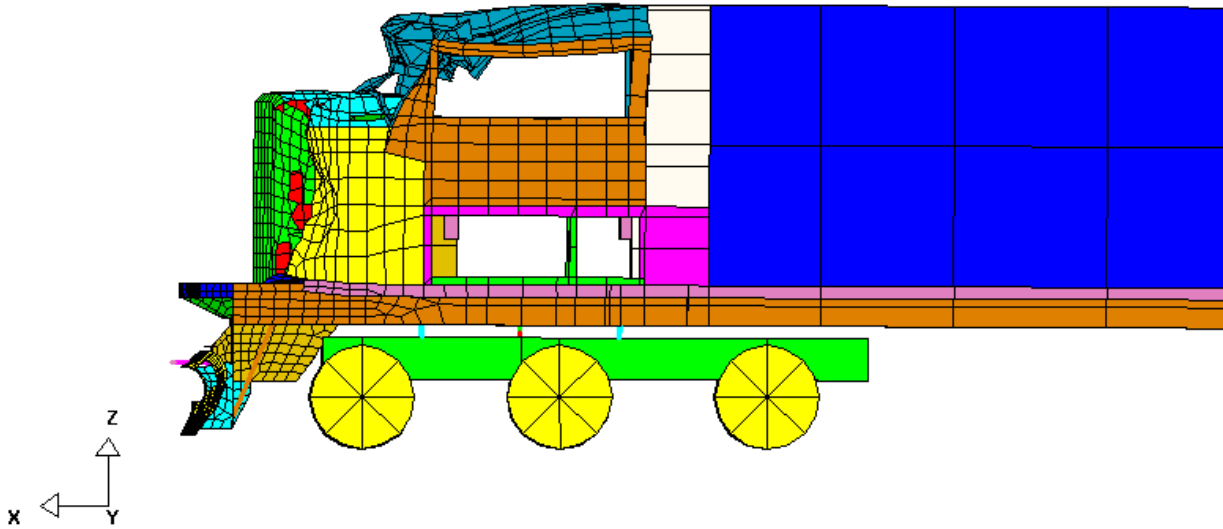


*Figure 46. The deformed locomotive for the 50 mph collision with the 60,000 pounds aluminum container*

### 3.3 Locomotive-to-Locomotive Collisions in Consists

Locomotive-Locomotive Collisions representing high-energy collisions were also simulated in the parametric studies. These are comprised of a locomotive-headed consist impacting an equivalent standing consist. Each of the locomotive consists was represented by the Loco1 consist as described in Section 2. A 6 in difference in sill height was introduced to represent a typical vertical offset in this kind of collision. The primary engagement is still between locomotive underframes. Three collision scenarios were evaluated:

1. Two-third lateral offset oblique (80 in).
2. One-third lateral offset oblique (40 in).
3. Head-on collision.

The configuration of case 1 was the same as in the previous collisions between the Loco1 and Loco2 consists. The only difference between cases 1 and 2 was the lateral offset value.

### 3.3.1 Two-Thirds Lateral Offset

In this study, the two locomotives engaged each other side-along-side without obvious rotation as shown in Figure 47. This motion pattern is significantly different from those observed in both locomotive-hopper and locomotive-box car collisions due to lateral “nesting” of the box-like underframe structures, sliding along without too much resistance. After the failure of the snow plow and endplates (both are relatively weak), there was not much other engagement between the two locomotive consists, except between the underframe of the higher locomotive and short hood of the lower locomotive, and between short hoods. The short hood of a locomotive, however, is narrower than the car body of the hopper/box car and oblique, which makes it easier for the locomotives to pass each other.

### 3.3.2 One-Third Lateral Offset

The lateral view of the deformed locomotive consists at the end of simulation (1 second) showed upward motions in the consists (Figure 48). Again more damage to the short hood and collision posts of the stationary locomotive was observed (stationary locomotive is on the right in Figure 49). No yaw of either locomotive was noticed.

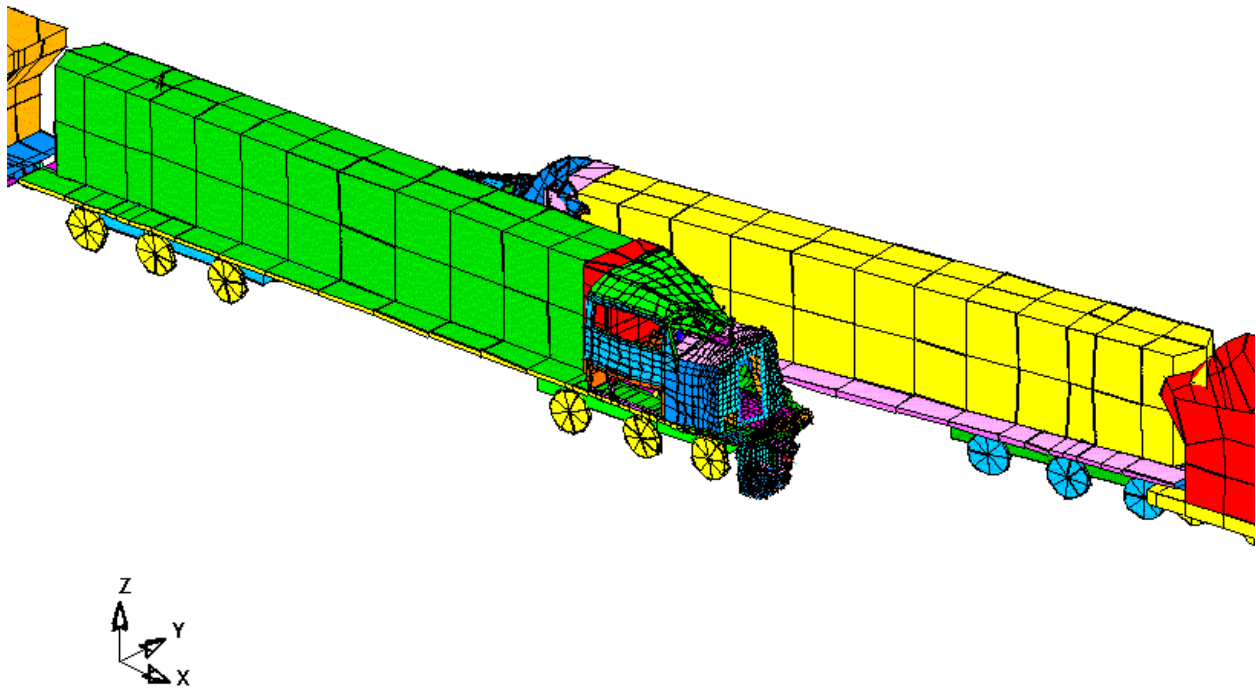


*Figure 47. The deformed locomotives at the end of simulation for the 50 mph two-thirds offset collision*

STEP 20 TIME = 9.9999762E-001

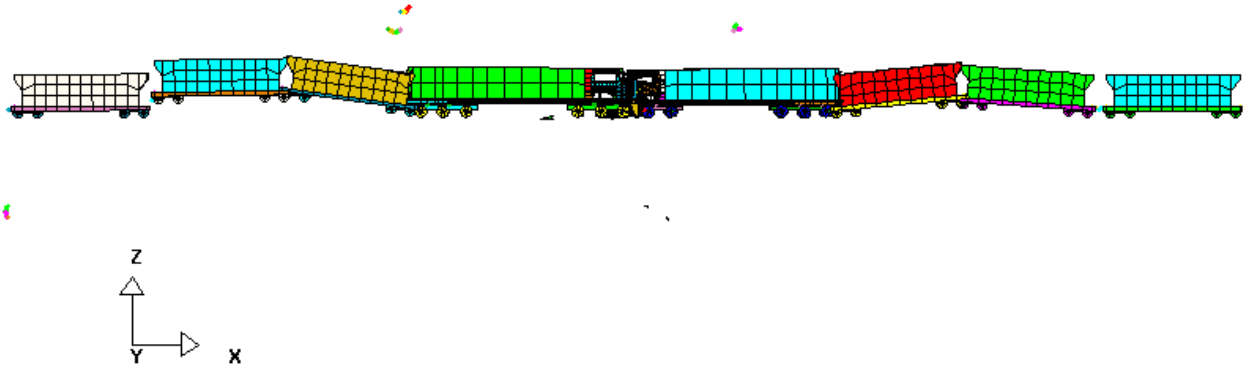


*Figure 48. Lateral view of the deformed two locomotive consists at the end of simulation for the 50 mph one-third offset collision*

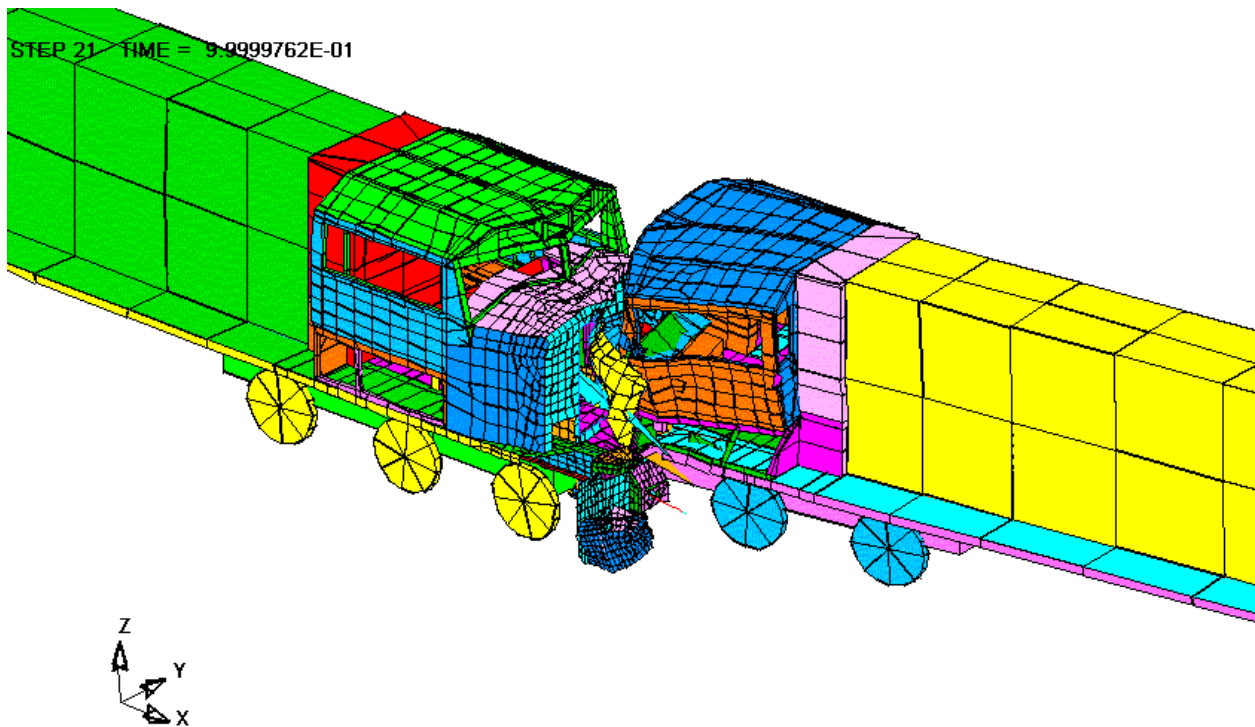


*Figure 49. The deformed locomotives at the end of simulation for the 50 mph one-third offset collision*

### 3.3.3 Head-On Collision

Heavy damage occurred to the short hood and collision posts of the lower stationary locomotive due to direct impact of the underframe of the higher, moving locomotive (Figure 50). There was several inches of override by the moving locomotive.

### 3.3.4 Cab Deceleration During Locomotive-to-Locomotive Collisions

The peak cab decelerations were estimated to be in the 4.5, 7.5 and 11 g's range respectively for the above three collision cases. The peak contact forces were about 1.8, 3 and 5 million pounds, respectively. All of these values were obtained after “filtering” of the raw results with “SAE” filtering, which is basically a low-pass type of scheme in which variations above 80 to 100 Hz are filtered out. Removal of the high frequency content facilitates easier understanding of the gross response of the structures.

## 3.4 Discussions on Parametric Studies

Several collision scenarios were selected to study the effects of speed, container strength and weight, freight car end construction, and offset on system kinematics and local structural crushing. The severity of collision increased with the increase of collision speed, container strength and weight. The hopper car caused less damage to the short hood and collision posts, but more damage to the windshield/corner post area compared to those caused by the box car.

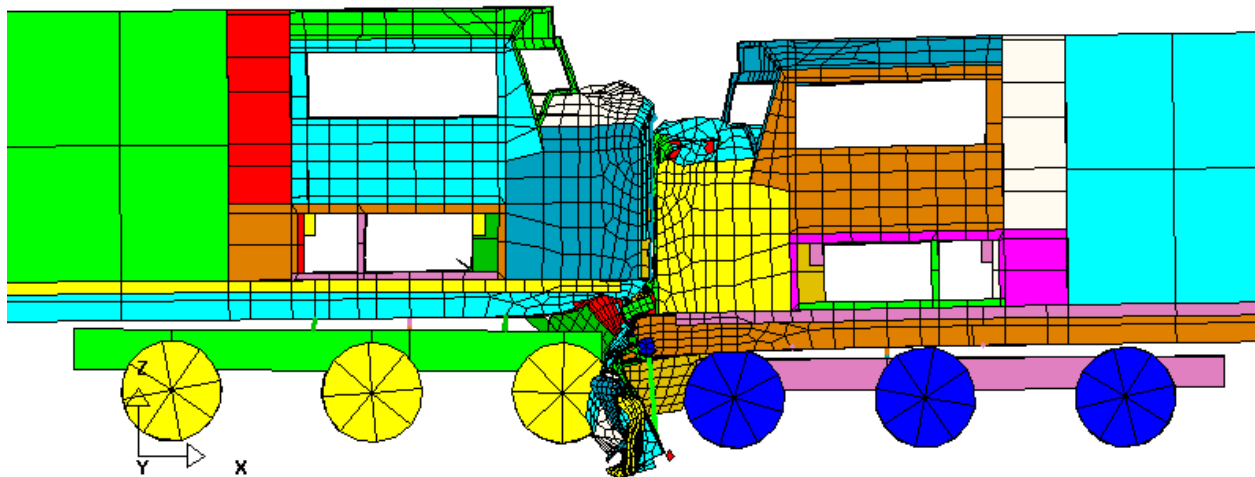


*Figure 50. Lateral view of the deformed locomotives for the 50 mph head-on collision*

In addition to the structural damage evaluations, in-cab decelerations were also determined. An example of deceleration data obtained in the simulations of the locomotive collision with the box and the hopper cars is shown in Figure 51. Slightly higher levels of deceleration in the cab were seen in the case of the collision involving the box car.

The kinematic behavior of locomotives involved in the 2/3 offset oblique collision seems to be in agreement with observations. As the locomotives became more centered relative to each other, the collision forces and severity rapidly increased, as expected from increasing engagement of primary structures. The "lower" locomotive was most affected, with its collision post on the engagement side struck primarily by the top plate of the moving locomotive underframe. The off-side collision post of the lower locomotive was not severely affected, as were the posts of the "upper" locomotive.

The load distributions, both axial and lateral, on the struck locomotive collision posts in these scenarios were also assessed. The majority of the collision forces (with the 6 in vertical offset) remained in the underframe engagements rather than the collision posts with these locomotive designs (i.e., several hundred pound range in collision posts compared to overall maximum collision force in the 3 million pound range). This indicates some general confirmation for the magnitude and nature of the proposed RSAC collision post strengthening requirements.

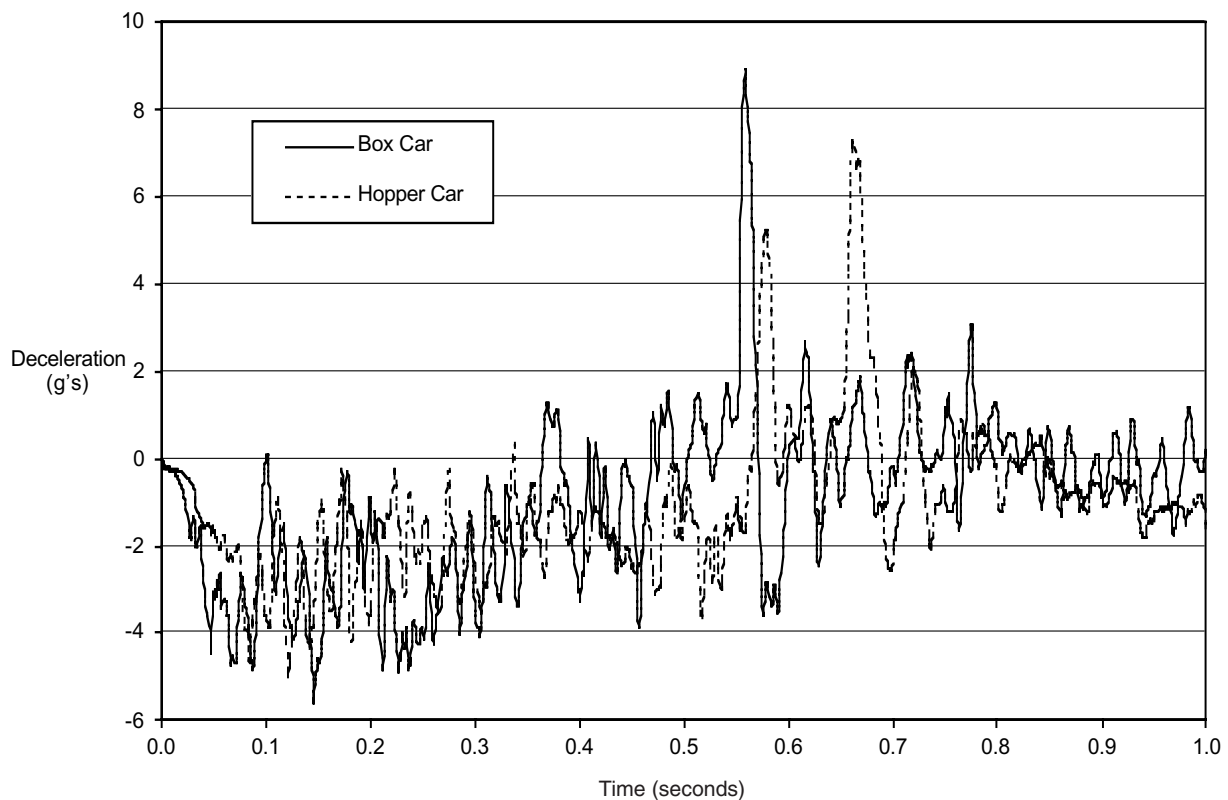


**Figure 51.** *Example of cab floor decelerations for collision between locomotive consist at 50 mph with stationary hopper and box car consists*

## 4. MODEL VALIDATION STUDIES

---

### 4.1 Objectives

Representative models of locomotives, other rail vehicles, and other potential colliding objects (such as intermodal containers) have been studied in a variety of collision scenarios. The basic modeling approach utilized the LS-DYNA program. When properly used, this approach can evaluate the effects of collision interactions, critical nonlinear structural behavior, buckling, fracture, kinematics and wayside interactions of the vehicles. The approach is valuable since the effects of varying parameters such as collision speeds, location and other characteristics of the colliding vehicles, and structural improvements can be quantified and visually displayed.

The types of collisions for which these techniques have been developed to date have included: different locomotive-headed consists striking standing consists obliquely fouling the *right of way* (ROW) — both with freight cars and other locomotives; freight locomotive-headed consists striking loose, loaded intermodal containers dislodged from opposing adjacent track; and multiple coupled locomotive overrides in direct collisions. These studies showed how the analytical methodology using the “model-in-model” approach with LS-DYNA can successfully simulate these typical rail collision scenarios. They also showed how crashworthiness improvements in the structural design can be examined by comparing behavior of standard versus modified locomotives in the same collision scenario.

The model validation is important because a generalized validated model provides a valuable tool that can be exercised in future studies on safety and crashworthiness of all vehicles. Expensive full-scale experiments can be eliminated. Numerous types of locomotive structural improvements can be evaluated. The tool will be useful to the industry in new designs. Model validations can be performed on the basis of the following methods:

1. Simulation of historical accidents.
2. Laboratory testing.
3. Limited full-scale field testing.

The first method is used here. Numerous accident scenarios of rail vehicle collisions were reported by the NTSB. In some cases, reasonable data was provided that can facilitate the reconstruction and analytic simulation of the accident.

The laboratory testing under equivalent static loads gives a means of understanding the crash behavior of the locomotive structure. Full-scale dynamic field testing provides validation which will be used in subsequent studies.

## **4.2 Historical Accident Candidates for Validation Simulations**

Literature studies and meeting discussions involving government, labor and industry were conducted, and three crash scenarios which could be used as representative crash scenarios for validation purposes were selected. Criteria for selection were based on:

- Adequacy of accident data including detailed descriptions of rail vehicles, collision conditions, and post-accident photos and measurements.
- Locomotive designs that represented reasonably recent and common configurations, preferably with the primary locomotives meeting S-580 standards.
- Conformance of the locomotives and other vehicles involved with the existing analytical models.

The following two crash scenarios were initially selected based on the above criteria:

- *Scenario 1*— Westfield, WV: Occurred on August 20, 1998, shown in Figure 52. This represented a coupled locomotive override crash scenario, in which the second locomotive in the moving consist overrode the lead locomotive from behind, destroying much of the lead locomotive superstructure above the underframe.
- *Scenario 2* — Phoenixville, PA. Occurred on August 23, 1996, shown in Figure 53. This involved a standing freight consist containing trailing flat cars designed for carrying highway truck\* trailers. This consist was struck in a rear-end collision by a SD80M locomotive-headed consist. The struck spine car buckled, and overrode the hood/cab area of the locomotive, with substantial damage to the locomotive before the spine car rolled off to the side.

## **4.3 Accident Selection for Validation**

Both of these accidents represented an important and distinct accident type, each of which has occurred several times in historical and anecdotal records.

### **4.3.1 Assessment of Coupled-Locomotive Override (Scenario 1)**

The actual accident involved two different locomotives in the first two positions in the consist, and a third in the colliding consist.

---

\*These specialty cars will be referred to as "spine cars" reflecting their construction for carriage of highway trailers.





Coupled-Locomotive  
Override Collision

Location: Smithfield, WV  
Date: August 20, 1998

*Figure 52. Accident Scenario 1*



Damaged Trailer Car after Collision

Location: Phoenixville, PA  
Date: August 23, 1996

*Figure 53. Accident Scenario 2*

Due to the complexity involved in modelling three different types of locomotives, it was decided to simplify the scenario and represent it in a “generic” fashion. This provided verification of the modeling approach in two important areas: the ability to simulate coupled-vehicle override, and the simulation of realistic crushing behavior of the rear end of the locomotive (the number 1 unit in the consist).

#### **4.3.2 Assessment of Locomotive Collision with Standing Spine Car (Scenario 2)**

The “rear-end” spine car accident (Phoenixville, PA, 1996) was studied in detail in the simulation. This accident had sufficient photographic and numerical information to best support the simulation. The configuration of the Loco1 locomotive, already modeled in detail, closely conformed to the accident locomotive. Appropriate data was obtained to create an LS-DYNA spine car model for use in this simulation. The scenario contained only one locomotive, making the overall model size more manageable and contributed to the decision for selection of this scenario.

#### **4.4 Simulation of the Spine Car Accident (Scenario 2)**

##### **4.4.1 Modeling of Spine Car and Consist**

The first FE model of a typical intermodal spine car was developed. This was based on a combination of drawings and partial structural models available from manufacturers. Again, this used the LS-DYNA system, plus Hypermesh for the meshing and characterization of the FE model.

Several spine car and intermodal car manufacturers were contacted; two of these (Gunderson, Inc. in Portland, OR and Johnstown America in Johnstown, PA) kindly agreed to provide sufficient drawings and data suitable as a good starting point for the modeling. Gunderson furnished a basic chassis LS-DYNA model of their intermediate-size car. Additional drawings of the end regions, and approximate numerical data for suspension rates were also obtained from them. Simplified structural modeling of the end beam regions, plus incorporation of freight car tandem-style bogies was completed.

The spine car model represented a composite, or generic model which incorporated the actual spine car structure with features such as standard bogies and structural ends. It closely resembles the spine car found in the accident used for these validation studies. A depiction of this FE model is shown in Figure 54.

The overall model of the full collision scenario is shown in Figure 55. This model consisted of the locomotive-headed consist moving at 32 mph, plus the stationary freight car consist, with the detailed spine car at the end, on the same track (in-line collision). The same consist headed by the Loco1 with three car hopper consist as developed in previous tasks comprised the model of the moving consist. The stationary consist was modeled with the detailed spine car on the collision end, and continued forward as a loaded 3-car hopper consist, again as developed before. The front car of this stationary consist had additional mass to represent the weight of three

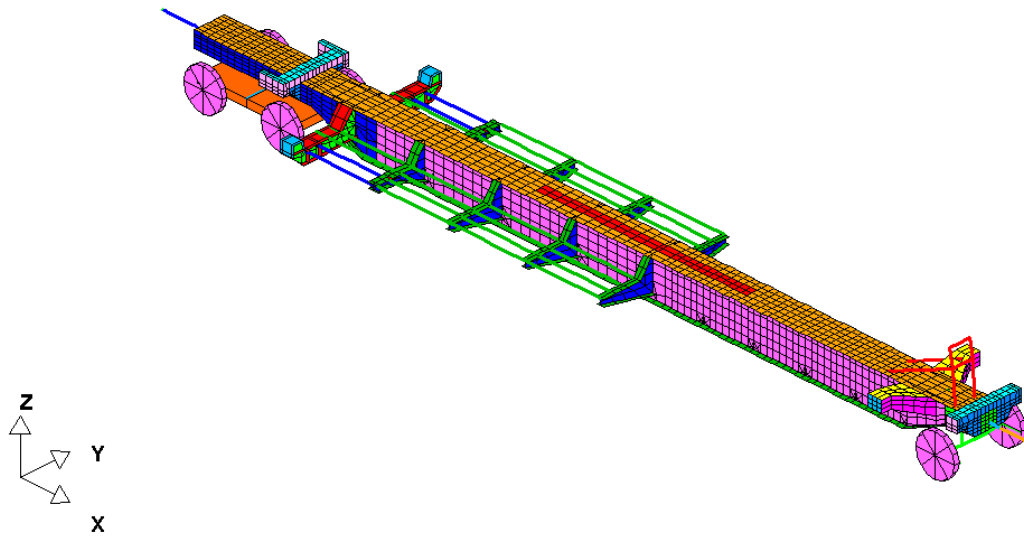


*Figure 54. FE model of the intermodal spine car*

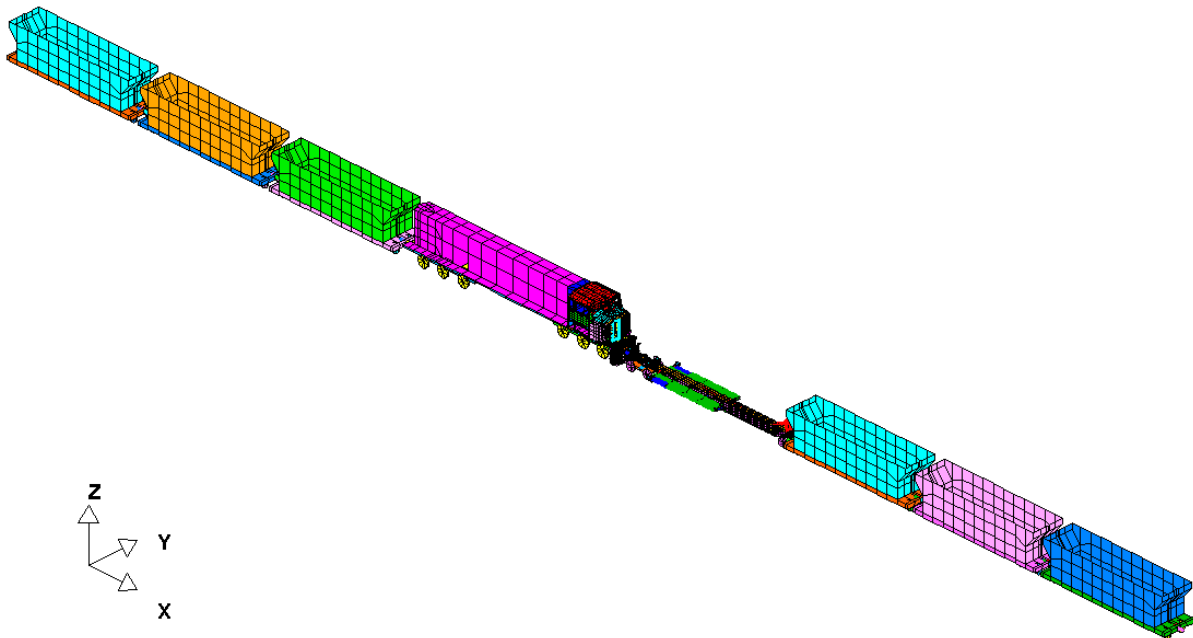


*Figure 55. Collision configuration between the moving Loco1 and stationary spine car consists*

additional cars, since the actual consist comprised many more cars. (Based on our experience with these models, the effects of more distant cars naturally diminishes due to draft gear compression, time delay, etc., so this is a reasonably good representation.) The overall model used in our analysis, comprised both consists, set on a 2 degree curve representing the crash conditions. There was a slight angle at impact in the overhead view, which lent a slight non-symmetry to the collision, and which was incorporated into the analysis. The rolling friction on the rail was lower than lateral derailed resistance, in accordance with the orthogonal friction behavior concept described in subsection 2.3.4. Figure 56 shows a close-up view of the model in the collision zone, before impact.

#### 4.4.2 Comparison of Simulation and Accident Outcomes

The LS-DYNA simulation of the actual crash as described showed the following sequence. First, the initial contact was via the draft gear, which compressed to the limit and then failed sufficiently to produce body-to-body contact. The end structure of the spine car, much lower than the underframe of the locomotive, contacted the draft gear pocket and end plate of the locomotive. Also, the end of the “spine” of the car appeared to be trapped by the locomotive anticlimber above. The loads were less than needed to fail the anticlimber upward, so the locomotive-headed consist proceeded forward, and the high axial loads produced upward buckling failure of the spine car at the point where the reduced-depth end section over the bogie transitioned to the deeper mid-section (Figures 57 and 58). It buckled upward because 1) the bogie and suspension bottoming on the spine car prevented the downward movement of the car; and 2) the height of the structural bending center of the reduced section (“neutral axis”) is above that of the deeper central section, producing an eccentric bending moment in the spine car frame.

As the locomotive continued forward, slowing slightly, the spine car was naturally restrained from moving by the inertia of the remaining cars ahead. The high axial loads on the sill of the

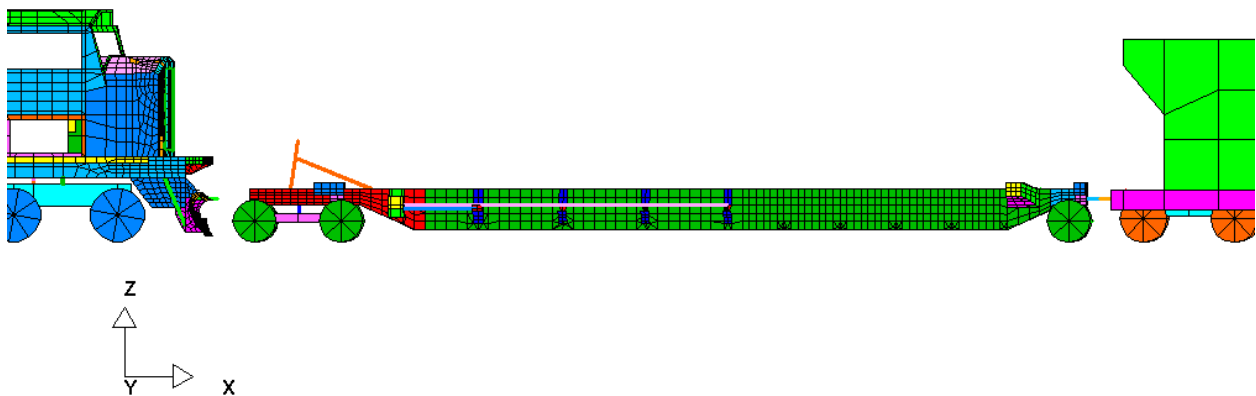


*Figure 56. Lateral view of collision zone*

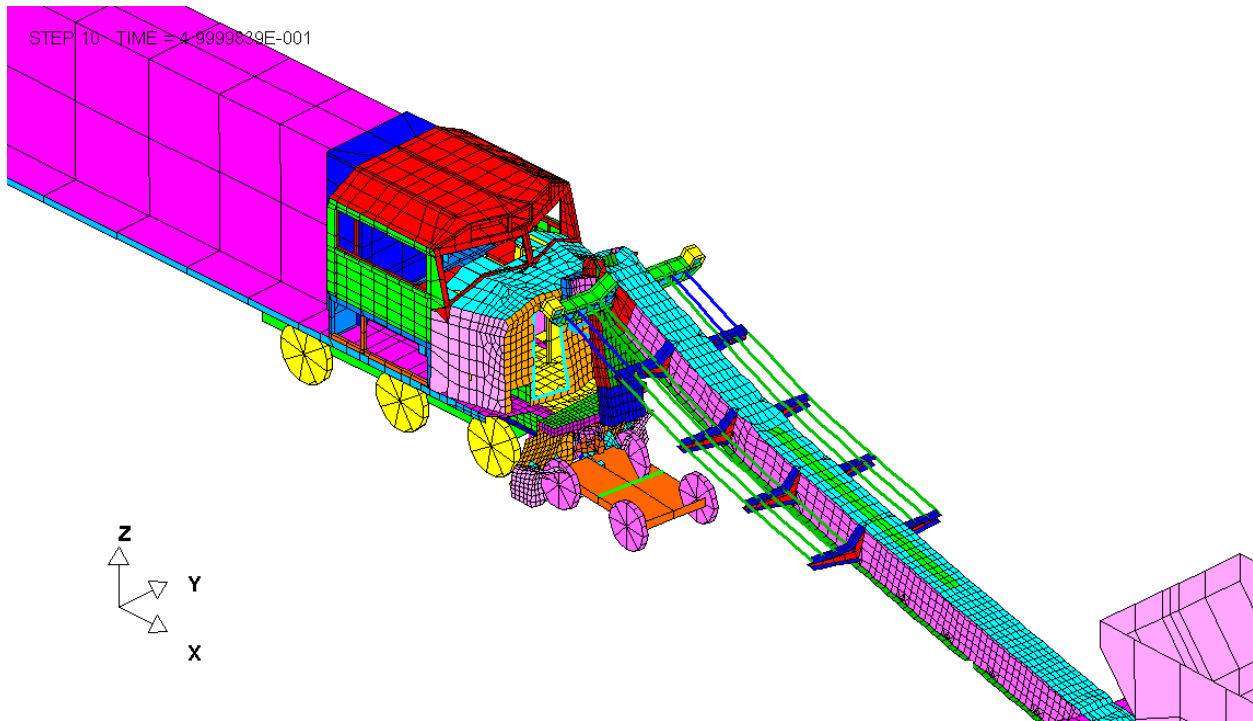


*Figure 57. Isometric view of collision showing spine car buckling upward ( $t = 0.5$  seconds) midway in collision*

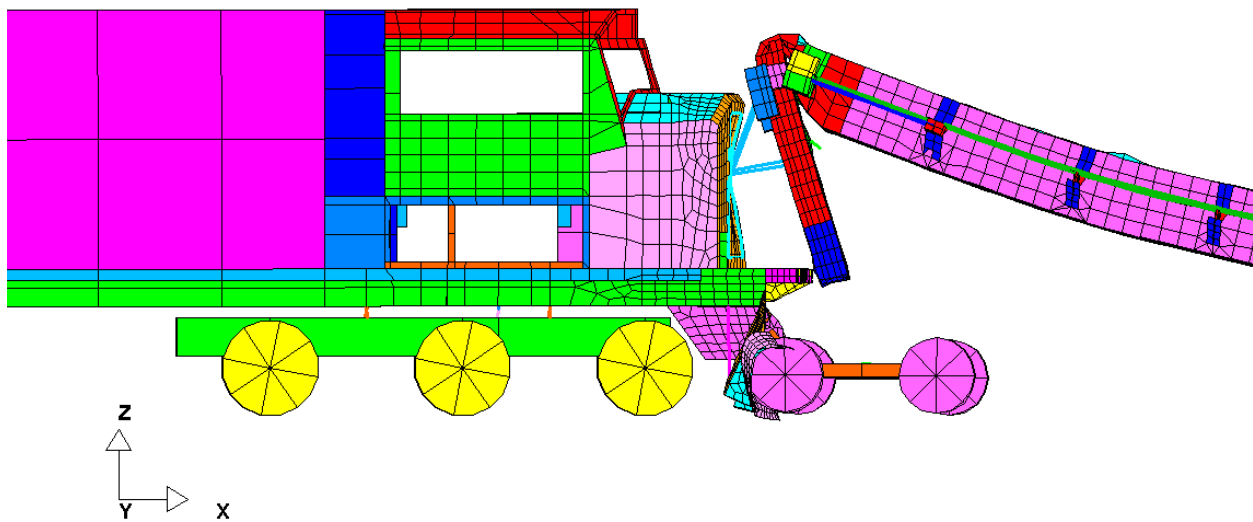


*Figure 58. Lateral view showing buckled spine car and early contact with short hood ( $t = 0.5$  seconds)*

spine car folded it upward almost 180 degrees, projecting the carbody up and over the locomotive short hood and then against the windshield as shown in Figure 59. The locomotive continued to move forward even though decelerating due to the collision forces and braking. The spine car continuously moved up and forward and simultaneously rolled over to the side (Figures 60 and 61). The height of the override between the spine car and the trailing hopper car as well as the stiffness of the front end of the spine car were assumed in the model. The results indicated that there was some sensitivity to these parameters.

Since our interest is primarily during the initial portion of the collision in which the collision damage and important vehicle motions occur, the analyses were conducted over a timeframe of 1.5 seconds. This reflects a balance of reasonable computational time and simulation of both the crushing/damage and the kinematics (motions) of the multiple vehicles involved.

Several detailed observations of the analytical sequence help explain the actual damage to the locomotive and the spine car.

First, the structural members mounted on top of the spine platform to support the trailer “fifth wheels” were responsible for some locomotive windshield damage. After the front end of the spine car failed and buckled upward, these steel members projected downward from the buckled section, and raked the locomotive windshield as the locomotive passed beneath. This accounted for much of the windshield frame damage. Figure 60 clearly shows the damage and loss of volume in the cab and windshield area of the locomotive (this loss of volume was not great in the actual accident, consistent with the simulation predictions).

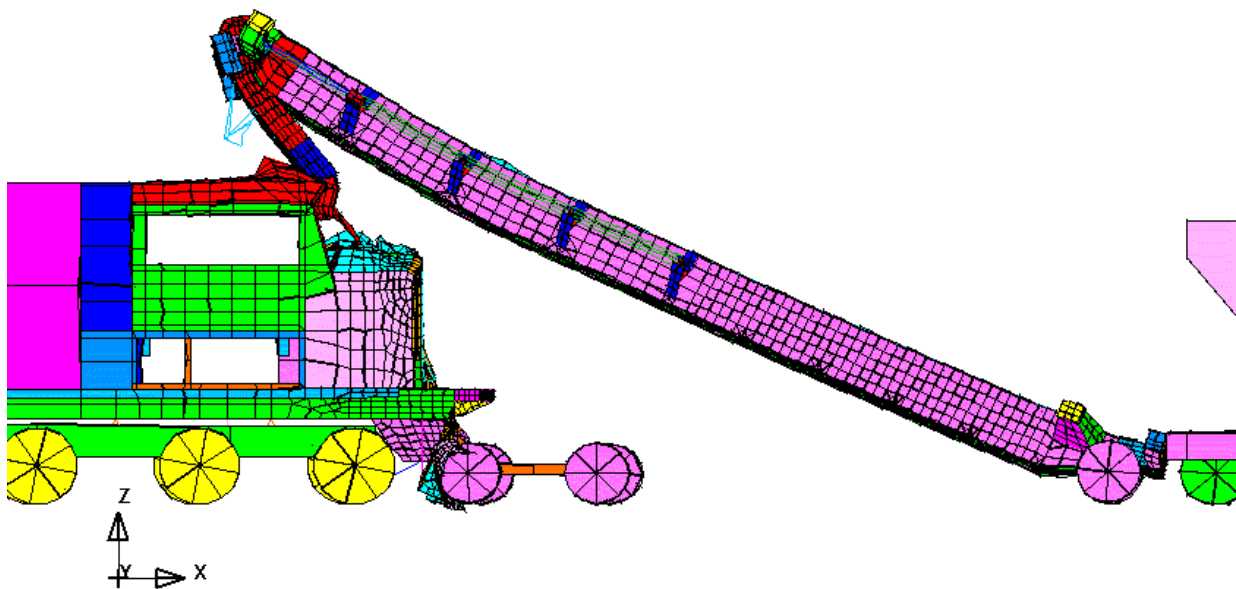


*Figure 59. Lateral view showing the movement of the spine car up and over the locomotive hood and cab (t = 1.0 second)*



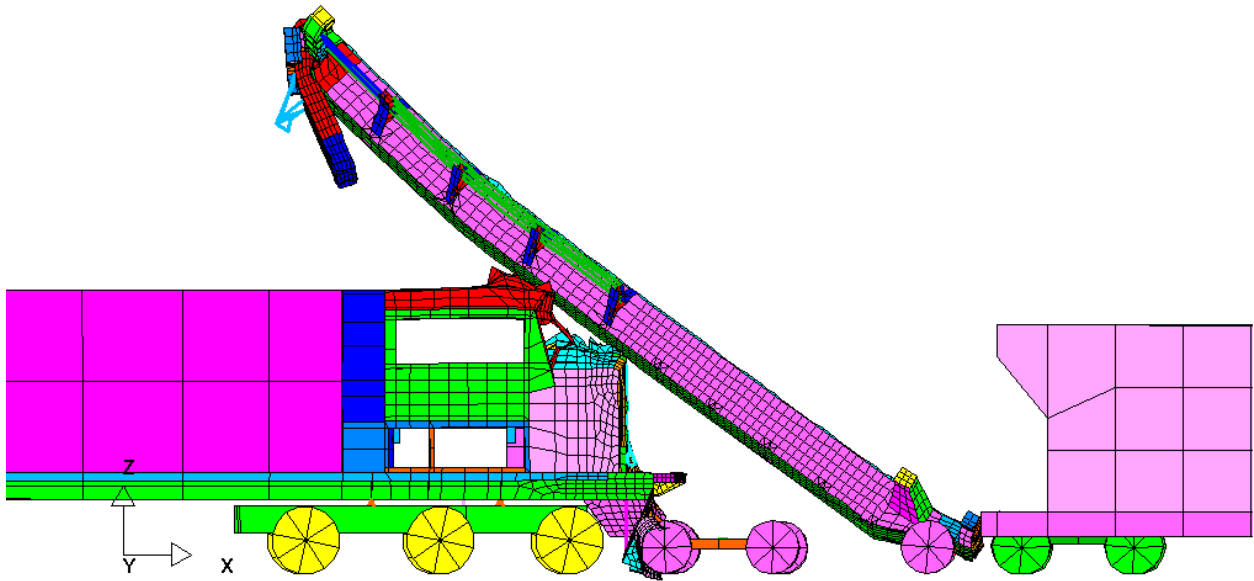


**Figure 60.** *Later view showing the damage to the locomotive windshield and roof area ( $t = 1.5$  seconds). Spine carbody is rolling off away from the viewer*

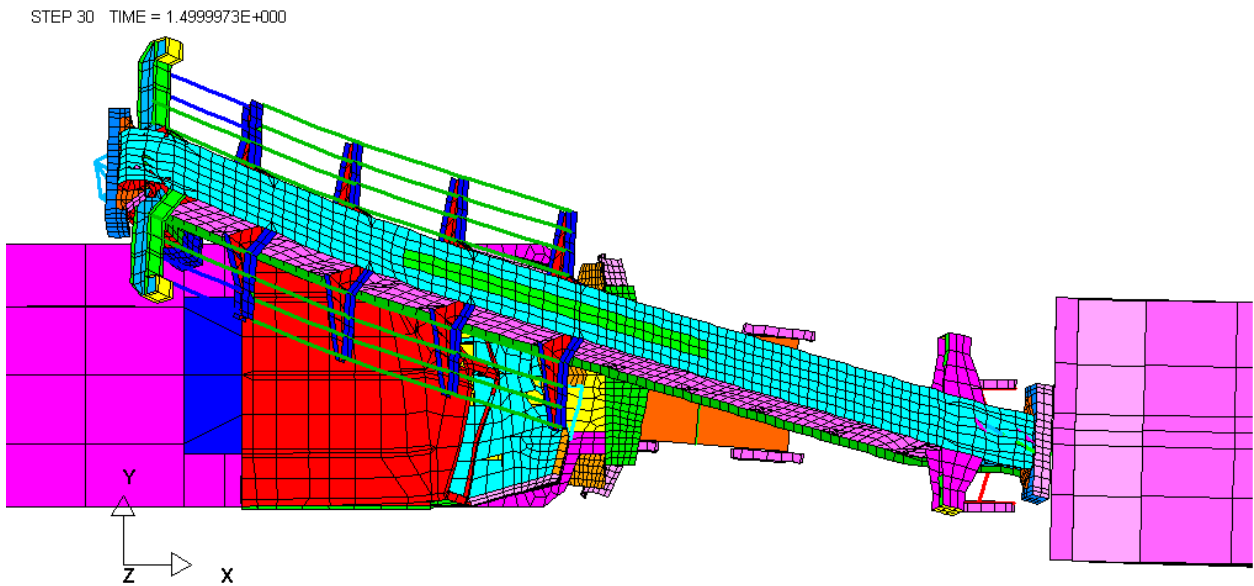


**Figure 61.** *Top view showing spine car rolling off to the left of locomotive ( $t = 1.5$  seconds) before it falls inverted on the wayside*

Second, the substantial upward momentum created by the upward buckling allowed the locomotive to move well under the spine car body, with the top front of the locomotive hood striking the underside of the spine car central beam. This is consistent with both locomotive and spine car damage observed in the accident photos.

Finally, the slight angle of contact in plan view due to the curved track did produce a “roll-off” of the carbody during the collision in the direction expected; however, the initial movements allowed the buckled carbody to project over the cab before rolling off, doing the damage seen.

#### **4.5 Supplemental Validation Studies: Coupled Locomotive Override (Scenario 1)**

This class of collisions represents cases in which multiple locomotives at the head of the same consist, are involved in strong head-on collisions. These consists are typically long, heavy freight trains which require the multiple locomotives for adequate traction and operation. If speeds and momentum are high enough, a trailing locomotive can override the lead locomotive, especially if they are of differing design with underframe height mismatches. Since they are coupled, and in motion on the tracks before the collision (although heavy braking is likely), the locomotives are in-line and so the initial collision behavior also shows an in-line tendency.

The sequence is typically collapse of the draft gear, then contact of the draft gear pockets, which are incorporated into the relatively massive underframes. Following this the override can either continue, or consist buckling can occur at the contact and/or other locations, depending on the many structural-dynamic factors of the consist (crush interactions and forces, location of car masses, coupler geometries, etc.). The tendency for override of one locomotive over another during the crushing process seems to be greater if the underframe of the trailing locomotive is higher than that of the lead locomotive.

##### **4.5.1 Modeling Approach**

The same general approach was used to study the “coupled-locomotive” override phenomenon. A consist consisting of two locomotives and two loaded trailing hoppers was first generated. The lead locomotive is similar to the one in the previous work (Loco1), but with a much more detailed representation of the rear end structure. This rear end (bodywork and equipment) was completely modeled in detail to include all the necessary equipment weights and structural details as shown in Figures 62 and 63. The anticlimber, endplate, draft gear packet, and underframe of the rear end were modeled to the same level of detail as those of the front end.

The locomotive height above the rail was assumed for each of the locomotives. The actual locomotives in consists can have different sill, or underframe, heights. (An example is found in Loco2 versus Loco1 locomotives, but sill heights can also vary with locomotive types from the same manufacturer.) The bogie height and primary and secondary spring heights were adjusted slightly to represent this "vertical offset." This was needed to simulate the interactions between the two locomotives during override.



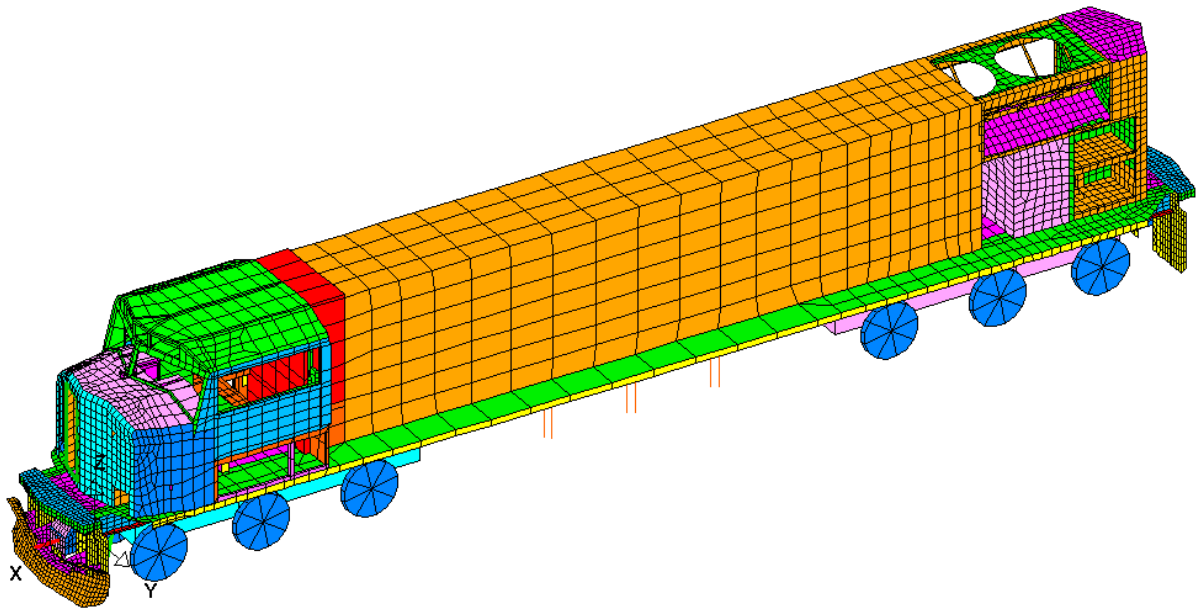


*Figure 62. Leading Loco1 locomotive with detailed rear end*

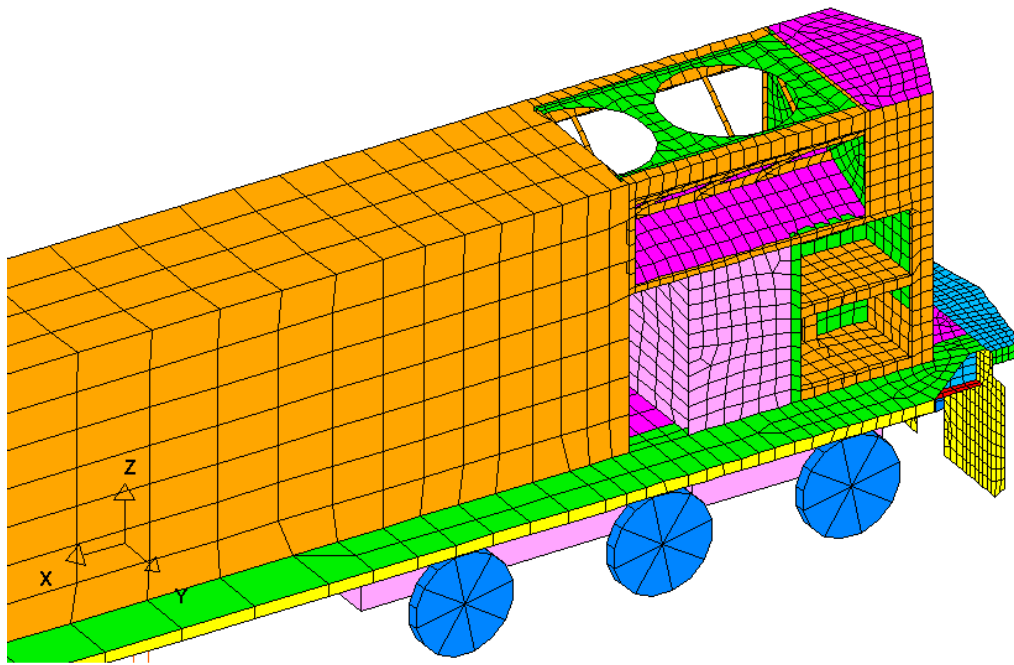


*Figure 63. Close-up of rear end of the lead locomotive*

Each locomotive weighed 415,000 pounds; each trailing car weight was 200,000 pounds (representing average loaded consist, not maximum possible weight). Figures 64 and 65 depict the lead and trailing locomotives, and the consist.

The trailing locomotive used is the same as the one in the previous work but with the underframe and superstructures raised relative to the bogies to provide a height mismatch between the locomotives. The couplers and draft gears, however, were kept at the same height for proper connections. Height mismatches of 6 in and higher were modeled to investigate the tendency for override. As in real practice, the overall depth of the underframe structures is in the range of 16 in to 18 in, so that the majority of the underframe still overlaps in the side view. No change

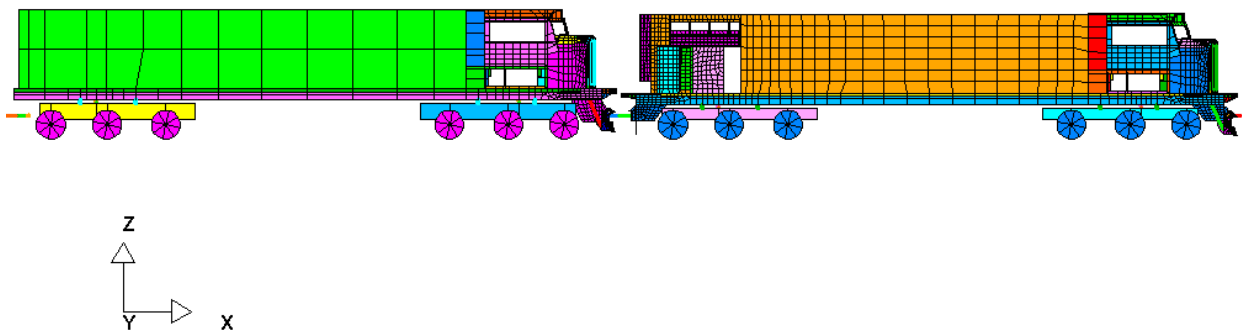


*Figure 64. Lateral view of the lead and trailing locomotives*

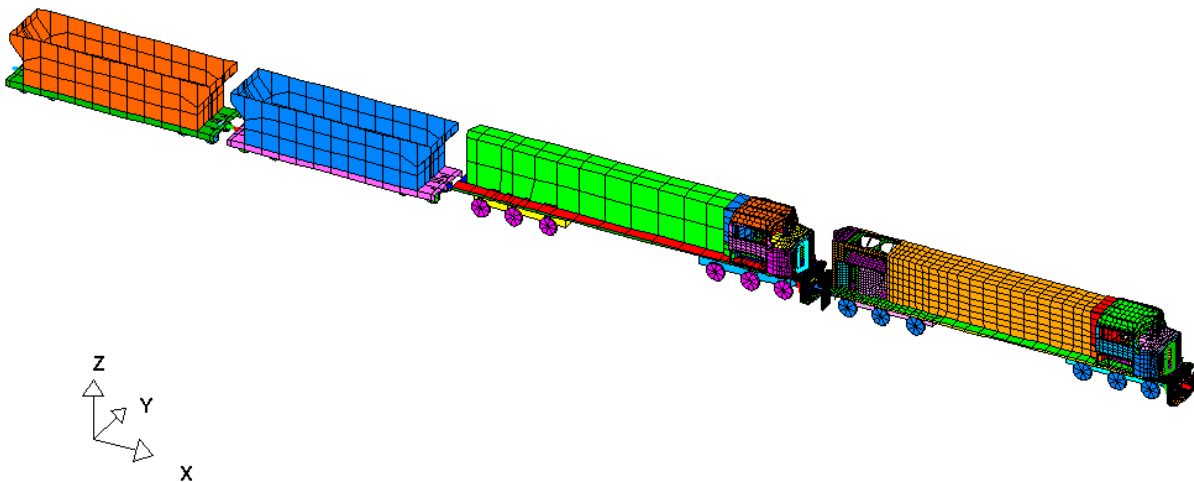


*Figure 65. Locomotive consist for override analysis*

was made to the two trailing hoppers compared to the ones used in previous consist analyses. Other features including material and joint properties and interactions between the consist and track were the also the same as in the previous simulations performed in this program.

An idealized collision scenario between this consist and a vertical wall was used for initial override simulations. The consist was given an initial velocity and then collided with the rigid wall. This scenario would be similar to the head-on collision of the same two consists traveling at the same speed, admittedly a severe situation. The simplification, however, alleviated the computation burden dramatically, since here are now two relatively complex locomotive structural-dynamic models embedded in the consist. Four cases have been analyzed so far: the consist traveling at 30 and 50 mph with the height offset between the two locomotives being 6 in and 10 in. For reference, the vertical thicknesses of the anticlimber and underframe are 6 in and 16 in respectively; thus there is still a significant engagement between the underframes for both height offset cases. Further, the draft gear pockets are aligned with each other in plan view, and these project further downward, producing a significant direct engagement of the primary underframe structures.

#### **4.5.2 Observations**

In all cases, the front portion of the lead locomotive underframe buckled downward due to the very high loads developed. This agrees with anecdotal observations of large locomotives in collisions such as this. While no obvious override was observed for the 30 mph collisions, there were significant overrides for both 50 mph collisions. There was not enough inertia/energy from the trailing locomotive and cars to make override occur in the 30 mph cases, likely due to the low consist weight. The override of the 10 in offset case was only marginally more than that of the 6 in offset case.

The collision sequence in the simulations clearly shows the initial contact, compression/failure of the draft gear, and crushing of the anticlimbers (used both on the front of the Loco2 and the rear of the Loco1). Then, the underframe of the Loco2, in which downward bending was already starting, overrode that of the Loco1, crushing and penetrating the aft bodywork and equipment area of the Loco1. The debris of the crushed locomotive ends seemed to assist the override as a ramp, albeit with heavy friction and resistance. As noted, the anticlimbers and related structures were destroyed early in the collision and did not appear to absorb significant amounts of what was admittedly a very large crash energy during impact. Given more consist weight, it appeared that further crush would occur, since the aft bodywork would continue to fail. The next major resistance would be the mass of the prime mover (diesel engine and alternator, weighing close to 50,000 pounds) being contacted by the Loco2 frame and body.

The results of these simulations are shown in Figures 66 to 71. Simulation results in "movie" format aided in the evaluation of results.

STEP 10 TIME = 1.9999868E-001

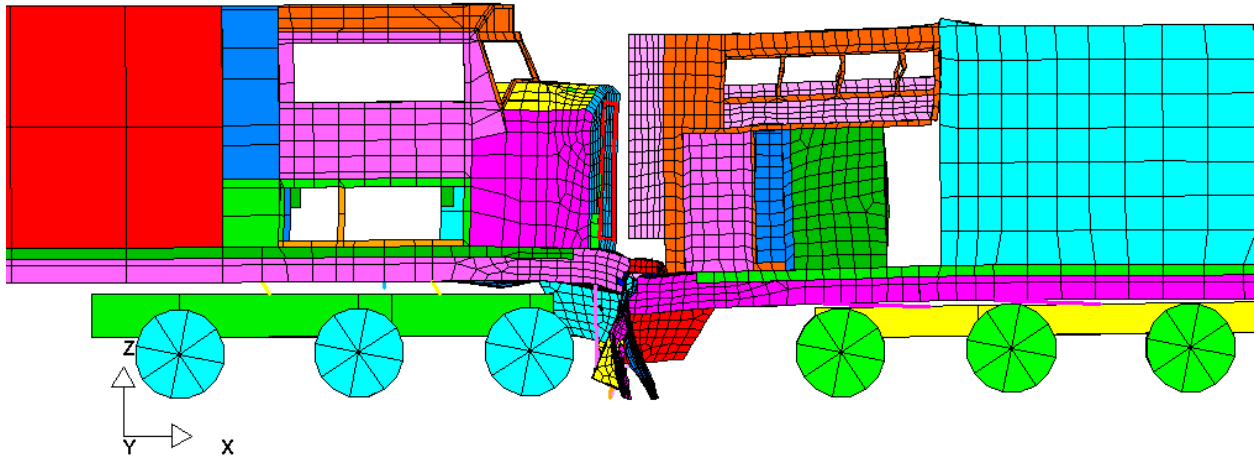


**Figure 66.** Deformed shape showing rear end of lead locomotive and front end of trailing locomotive at 0.2 seconds for 30 mph collision with 6 in height offset

STEP 26 TIME = 5.0000024E-001

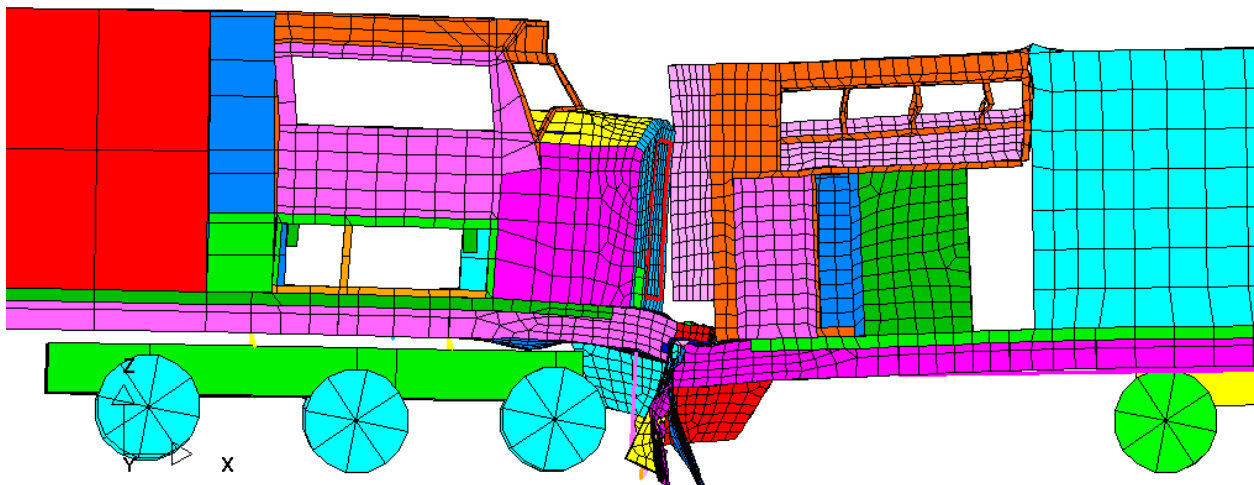


**Figure 67.** Deformed shape showing rear end of lead locomotive and front end of trailing locomotive at 0.5 seconds for 30 mph collision with 6 in height offset

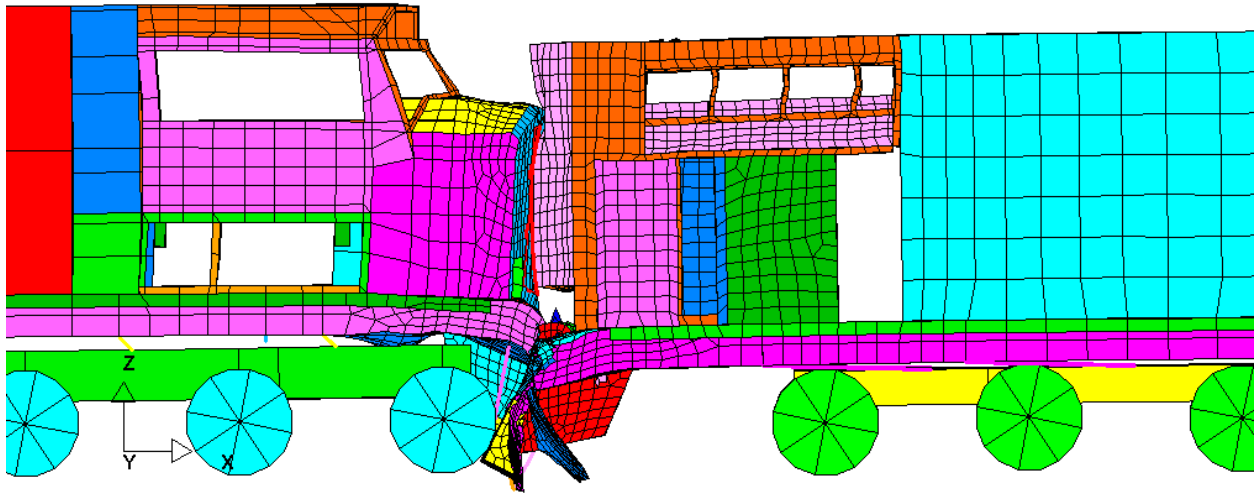


*Figure 68. Deformed shape showing rear end of lead locomotive and front end of trailing locomotive at 0.18 seconds for 50 mph collision with 6 in height offset*

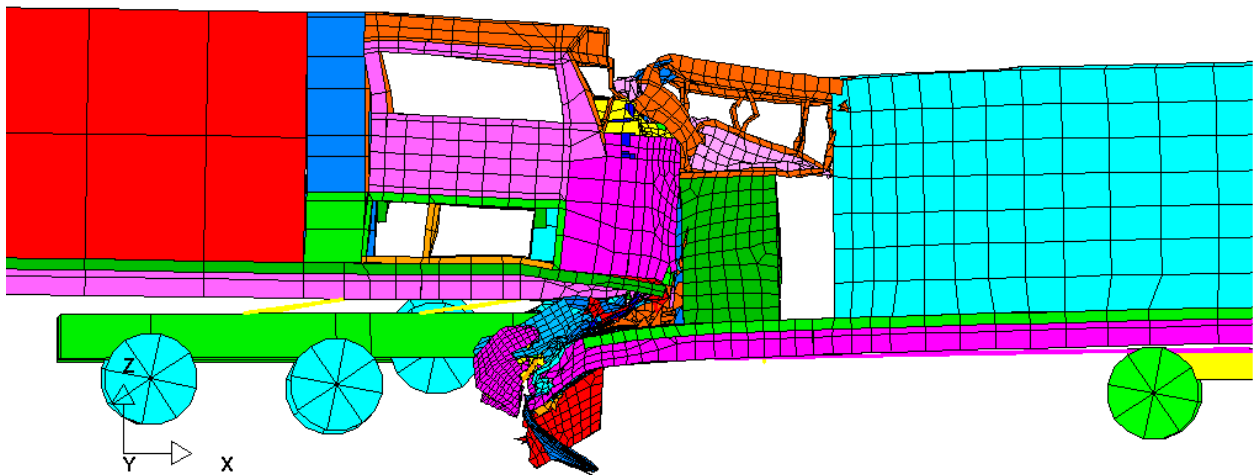


*Figure 69. Deformed shape showing rear end of lead locomotive and front end of trailing locomotive at 0.5 seconds for 50 mph collision with 6 in height offset*

STEP 26 TIME = 5.0000024E-001

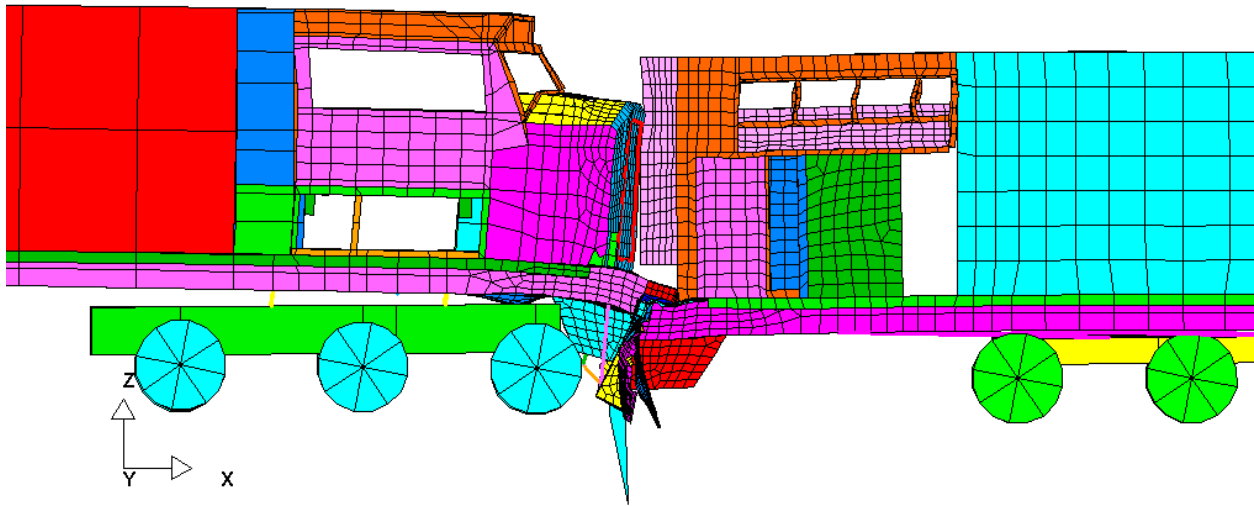


*Figure 70. Deformed shape showing rear end of lead locomotive and front end of trailing locomotive at 0.5 seconds for 30 mph collision with 10 in height offset*

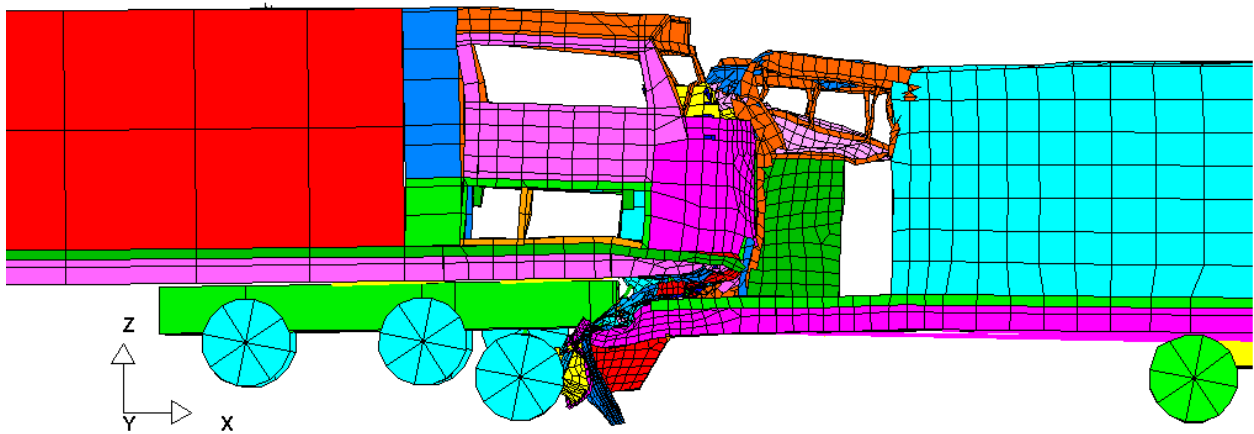


*Figure 71. Deformed shape showing rear end of lead locomotive and front end of overriding coupled locomotive at 1.5 seconds for 30 mph collision with 10 in height offset*

## 4.6 Summary

Using the 1996 Phoenixville, PA accident, a verification study showed the finite-element simulation of crash behavior to be very consistent with the NTSB accident report and other photo records. During the accident, the front end of the spine car was folded under and projected the car up over the short hood and against the windshield of the locomotive.

The simulated kinematics of the crash (taken over the initial 1.5 seconds of the accident, capturing all primary behavior) were consistent with the accident observations. The buckled-under spine car end raked the hood and windshield (including the effects of the fifth-wheel support structure on the car). The simulation correctly predicted the areas and degree of damage to the locomotive in these areas. The impacted carbody then began rolling inverted towards one side, with the simulation predicting the motion evidenced in the actual collision outcome.

This verification study showed that the collision simulation technique using the LS-DYNA modeling of consists, with additional modelling details in the collision zone, can be expected to reproduce the major elements of an actual accident. Such simulations can predict significant damage to the locomotive and other vehicles impacted in the collision. This methodology demonstrates the ability to re-create the likely sequence of events during a complex collision process involving multiple vehicles or objects.

Additionally, the output from the simulation can furnish data such as the dynamic forces at the contacts, internal stresses, and the g-load environment in the cab or other areas of the locomotive. This is very valuable information for the designers and operators, since these parameters can be seen as they varied in the collision, and can also be related to the final consequences. Further, modifications or improvements could then be developed and evaluated based on factual knowledge of the accident process, as seen in an actual accident. This complements the capabilities shown in earlier program efforts in which the effects of several design modifications in hypothetical accidents were shown.





## 5. POTENTIAL LOCOMOTIVE STRUCTURAL IMPROVEMENTS

---

### 5.1 Strengthening Studies of Large Freight Locomotive 1 (Loco1)

Four types of strengthening on Loco1 locomotive structures were considered, and their effects on improving crashworthiness have been assessed based on several collision scenarios. These are not intended as final designs—rather, each improvement was selected to demonstrate the way that the analytical simulation technique using LS-DYNA can be used with a realistic crash scenario to observe differences in outcomes “before and after” the improvement.

Naturally, using different scenarios would show the different effect of each type of improvement. Table 2 shows examples of different scenarios that were used to “test” these different improvements. Many more combinations are possible, and the locomotive designer could tailor these choices to their expected operational environments.

Details of these four strengthened configuration examples are:

1. Increasing the thickness values of the sheet metal forming the corner posts, cab front frame (windshield top) and cab side wall all to 1/4 in, from 1/8 in, 1/8 in and 3/16 in respectively.
2. Doubling the thickness of the short hood components: the top from 3/16 in to 3/8 in, and the side plates from 3/8 in to 3/4 in.
3. Interconnecting (“tying”) the top edges of the collision posts together with a 5/8 in Corten steel plate (not representative of a final design, but only to see the effect).

*Table 2. Trial structural improvements*

Trial Structural Improvement	Locomotive Collision Scenario
Strengthening of windshield/corner post structures (increase section properties)	ISO Containers (high/offset “shifted load”)
Strengthening of short hood (thickness increase)	ISO Containers (high/offset “shifted load”)
Interconnection of collision posts	Box-car consist (oblique/offset, fouled ROW) Locomotive-locomotive consists (oblique/offset, fouled ROW, plus height differential)
Add lateral flanges to collision posts	Box-car consist (oblique/offset, fouled ROW)

4. Adding flanges on both front and back of the collision posts, to form an “I” section. The thickness of the flanges is 1.25 in, the same as that of collision posts. Both 5 in and 10 in flange widths were evaluated.

Items 3 and 4 were identified also in the published literature on crashworthiness. Our studies evaluated specific trial upgrades for all items 1 to 4, and their actual performance in the simulated collisions relative to “baseline” configurations. These simulated collision scenarios used were described in Section 3 of this report.

#### *Future Effects of New RSAC-Recommended Crashworthiness Standards*

It should be noted that the newly-adopted version of the AAR crashworthiness standard S-580 for locomotives (to take effect in 2003) includes new strength requirements for most of these areas. The present 1990 standard involves only the collision posts, anticlimber and short hood. Meeting these standards could involve the same kind of design improvements, only using conventional static analysis. The dynamic scenario-type simulations developed in this program would be valuable in assessing the design improvements under a wide variety of realistic scenarios, not just the regulatory static scenarios. There is extensive provision in the new S-580 for doing exactly that, via either testing or acceptable analyses such as this as an *alternative* to the static conditions. This would be fulfilled by such simulations as validation efforts are continued.

#### **5.1.1 Strengthening of Windshield/Cab Corner Post Area**

Collision between the moving Loco1 consist (50 mph) and a stationary aluminum ISO-type container (60 pounds) impacting high/offset on the front hood and windshield was used to evaluate the benefits of strengthening the windshield/corner post area. The reasoning is based on the observations of the baseline simulations seen earlier, which appeared consistent and rational. In these, the deformation and free-body pitching/yawing motion of the containers was significant due to the strike of the lower inside part of the highly placed container; the pitch and yaw of the heavily-deformed container into and downward onto the windshield top, corner post and nearby roof produced conditions which taxed these areas.

Much less deformation occurred with the strengthened windshield/corner post area (Figure 72), compared to the baseline model (Figure 46). The cave-in of the cab roof was also less for the strengthened model. (The crushing in the short hood was similar for both.) Thus, this design modification could be very effective in reducing the damage to the cab and enhancing safety of crew members, and it was seen that this type of collision would “test” the windshield and roof structure, thereby being a useful case for design evaluations.

#### **5.1.2 Strengthening of Short Hood**

The same collision scenario between the Loco1 consist and container as above was used to assess the benefits of strengthening the short hood. Although less damage to the strengthened short hood was observed, there was no noticeable benefit in protecting the cab after

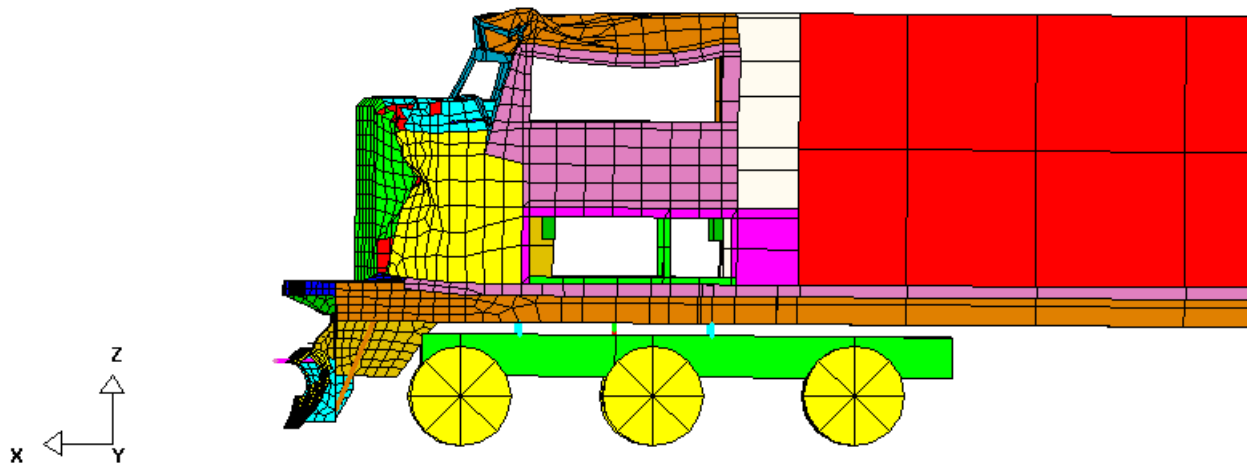


**Figure 72. Locomotive with strengthened windshield/corner post in 50 mph collision with 60,000 pound all-aluminum container ( $t = 0.4$  seconds)**

strengthening the short hood. This is shown in Figure 73. The stronger short hood front deformed much less, forming more of a fulcrum which increased the down-and-in pitch/yaw motion of the container. Thus, any benefits of the hood strengthening in deflecting/deforming the container might be offset or negated by the increased damage to the cab roof, corner post and windshield area caused by the more violent container motion. It would seem, therefore, that hood strengthening which could be useful for lower impacts and collision post reinforcement should then be coupled with cab windshield, roof and corner post strengthening to also preserve improvement in these potential “high” shifted load-type impacts. Strengthening of the short hood *only* would not be recommended without evaluating improvements in windshield top, corner post top connection, and adjacent roof strength, to deal with this type of collision.

### 5.1.3 Interconnection of Collision Posts

This was another strategy thought to have potential to improve front end strength through providing help of one collision post to another in offset situations. The one-third offset (40 in offset) collision between two Loco1 consists with a closing speed of 50 mph was used, with the stationary locomotive being positioned 6 in lower (as done in prior uses of this collision). In this collision, the moving, upper locomotive taxes the front end of the fouling, lower locomotive severely. However, the underframes contact directly, providing the great majority of the contact force compared to the collision posts, so this is not an ideal scenario.

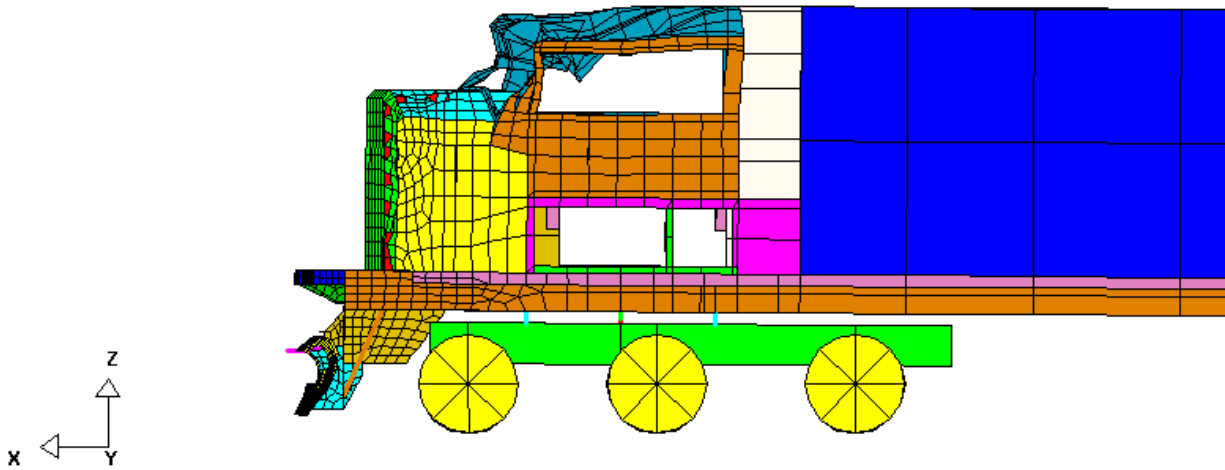


**Figure 73. Locomotive with strengthened short hood in 50 mph collision with 60,000 pound all-aluminum container ( $t = 0.4$  seconds)**

Significant benefits were not observed in this particular situation. The deformed collision posts are shown in Figures 74 and 75 for the baseline case and the case with tied collision posts. The total collision forces between the consists (Figure 76) and cab floor accelerations were also about the same level. Although the tied collision posts provided somewhat more resistance, their contribution was still only 15 percent of that provided by the underframe as shown in Figure 76. Thus, the additional interconnection of the collision posts in this collision scenario was not notably beneficial. (It should be noted that the posts are already tied together to a degree in the baseline case via the top of the short hood.)

Tying the collision posts together could be beneficial for collision scenarios in which they play a major role. However, the conclusion is that the approach of individually strengthening the lateral bending and twisting modes of the collision posts would be more beneficial, via forming a box-like or flanged configuration. This latter approach is therefore described below.

#### **5.1.4 Adding Stiffening Flanges to Collision Posts**

More effort was focused on evaluating the possible benefits of stiffening flanges added to the collision post plates. Two degrees of stiffening were tried: addition of both 5 in and 10 in wide flanges (front and rear), the same thickness as the posts. This was not optimum, but gave two data points for assessing the possible benefits in heavy frontal-offset collisions, in which the higher lateral (flexural/shear) strength could come into play.

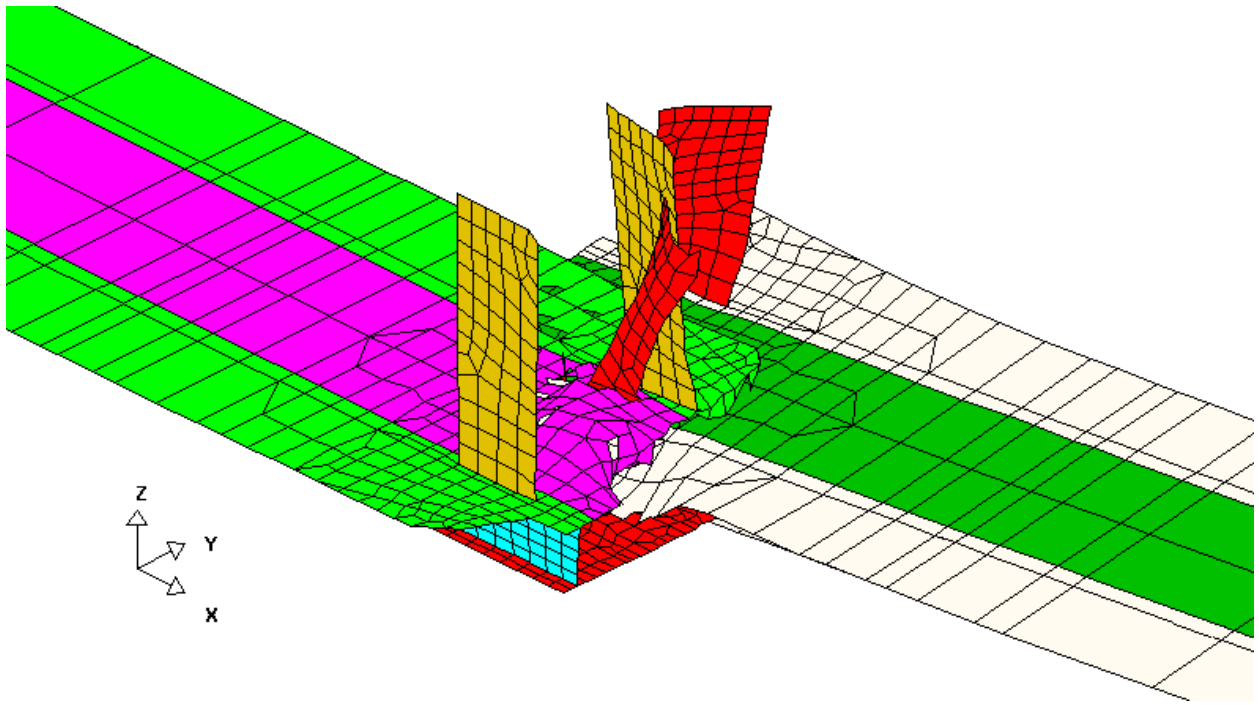


**Figure 74.** *Baseline collision posts for 50 mph one-third offset (40 in) collision between Loco1 consist and standing locomotive-headed consist (t = 1 second)*

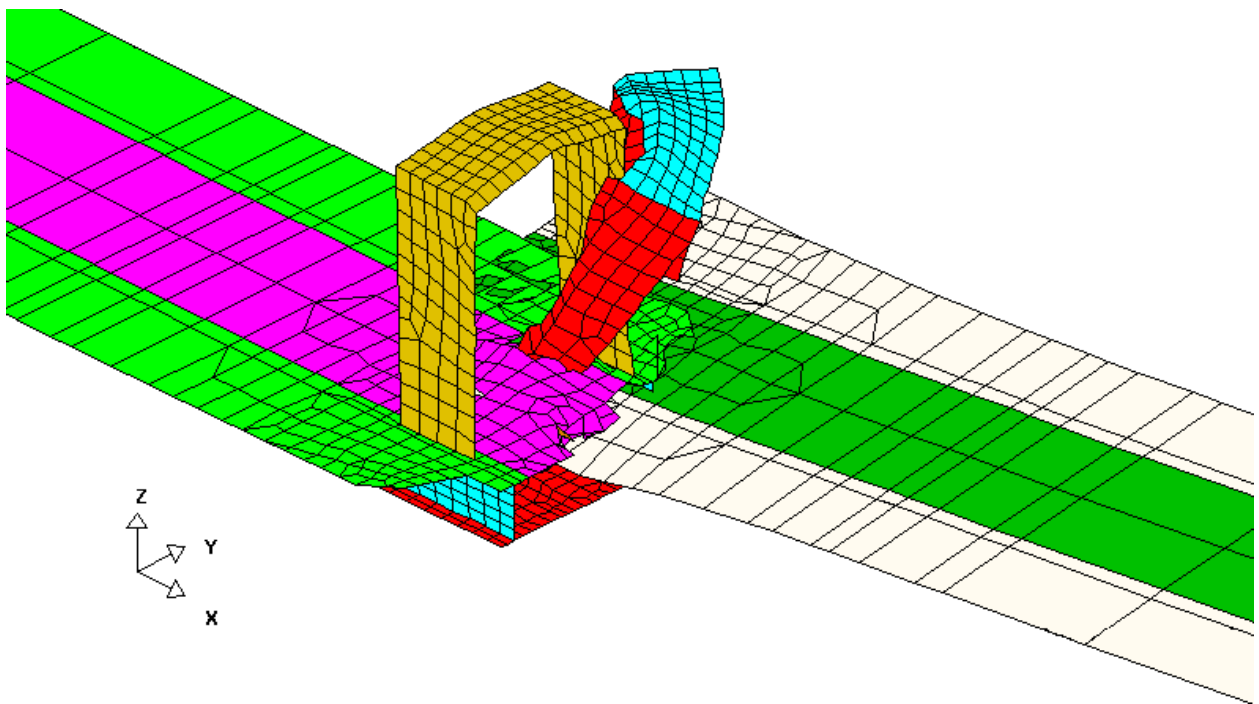


**Figure 75.** *Interconnected collision posts for 50 mph one-third offset (40 in) collision between Loco1 consist and standing locomotive-headed consist (t = 1 second)*

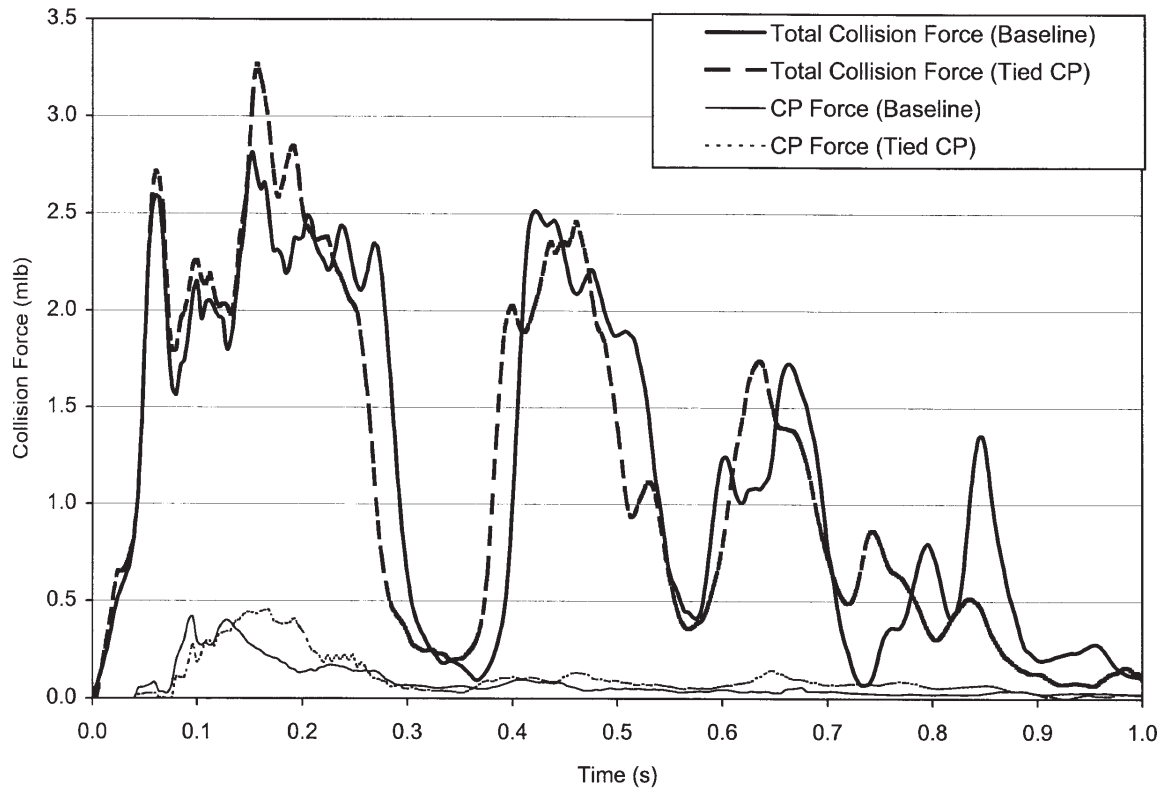


**Figure 76.** *Total collision force between two loco consists and force borne by collision posts (CP) of the stationary locomotive for a 50 mph collision*

For the case in which 5 in wide flanges were added, there was only a small difference in the overall behavior of the consists and the crush response of the locomotive compared with the baseline case. Similar deformation patterns of bending and twisting for the left collision post (impact side) were observed as shown in Figure 77 compared to the baseline case. The aft displacement of the top frontal corner of the left collision post was 48.2 in and 50.7 in for the strengthened versus baseline case. Adding the 5 in flanges did not apparently change total collision force and cab floor deceleration either. In summary, the addition of the 5 in flanges to the collision posts were not sufficient to materially affect the outcome in this collision scenario.

For the case of the 10 in wide added flanges, much more benefit was seen. Although the overall consist behavior remained similar, much less crush was observed in the short hood and cab areas. The relative translation of the top frontal corner of the left collision post was only 27.0 in, mostly from rigid body rotation around the collision post base due to weakening of the base area (Figure 78). Wider flanges will be beneficial, but must have an accompanying strengthening of the base area to utilize the benefit. Total collision force and maximum cab deceleration were somewhat higher compared to the baseline case.

In summary, the 10 in flanges added to the collision posts for the selected collision scenario reduced the aft/inward crush by almost 50 percent, a significant improvement. The base

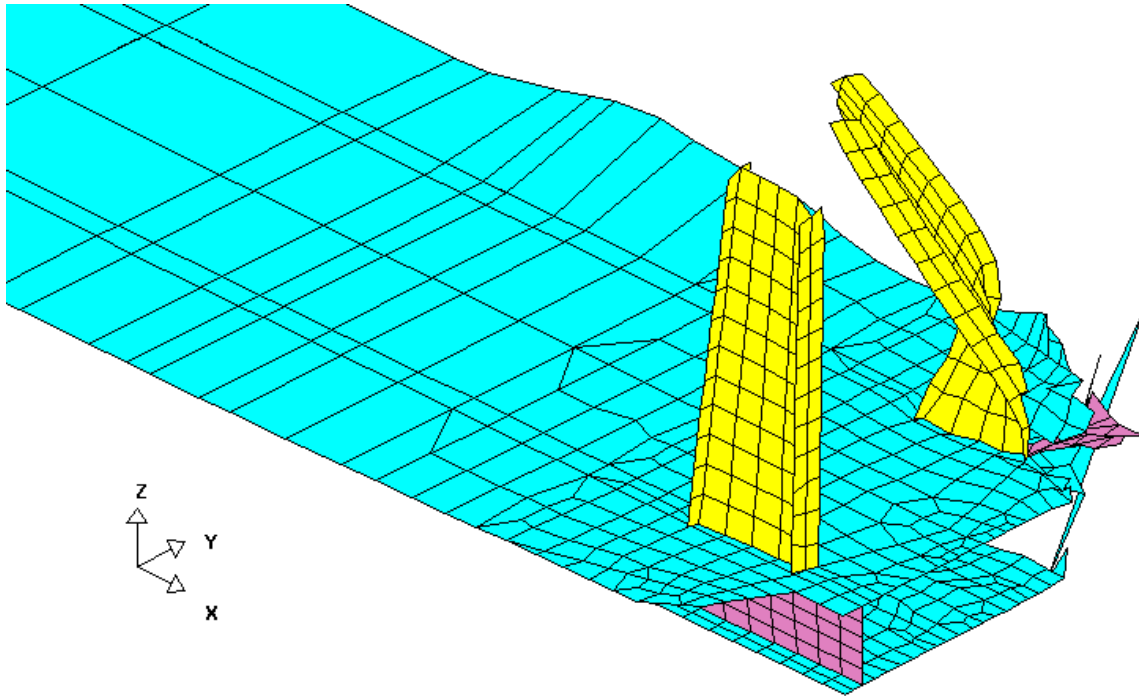


*Figure 77. Deformed collision posts with 5 in flanges at  $t = 1$  second for the 2/3 offset 50 mph between the moving Loco1 consist and stationary box car consist*

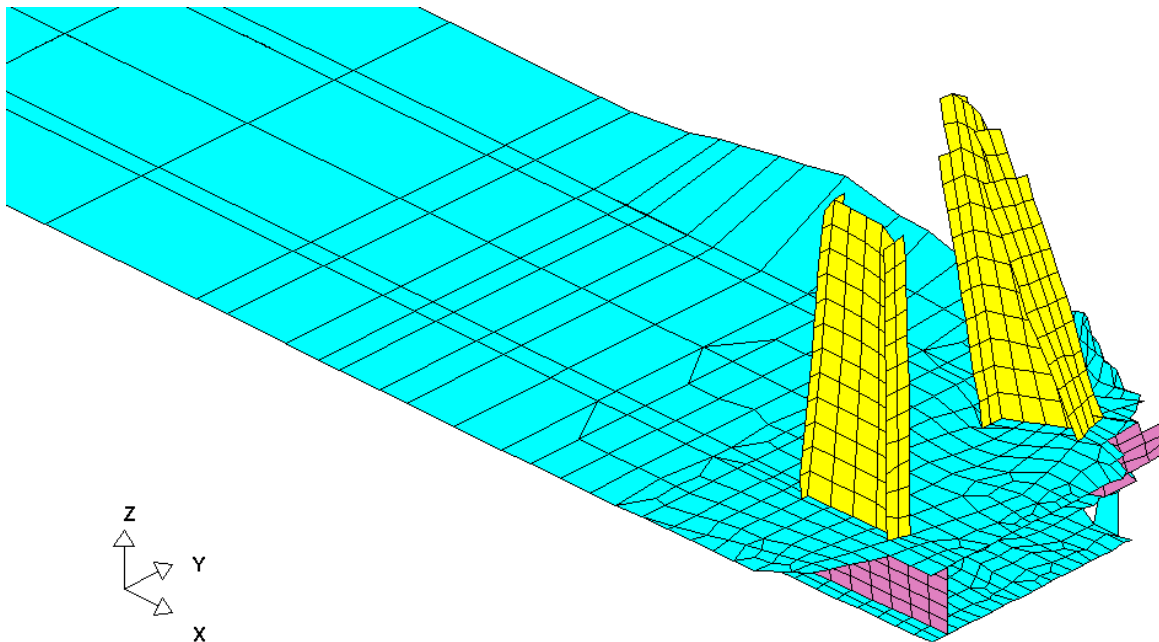


*Figure 78. Deformed collision posts with 10 in flanges at  $t = 1$  second for the 2/3 offset 50 mph between the moving Loco1 consist and stationary box car consist*



connection to the underframe would also require strengthening to realize fully this benefit. This gives a good idea of the magnitude of the flange size needed to significantly affect the accident outcome in this type of head-on/offset situation. Possibly even more benefits would be observed when the collision posts would be more directly involved in “higher” collisions, since some collision forces here still were transmitted directly through underframe contacts.

## **5.2 Strengthening Study of Second Large Freight Locomotive (Loco2)**

Loco2, also produced by a U.S. manufacturer, was similar to Loco1. This second study was done to apply the same general type of strengthening approaches to a different locomotive design. Three types of strengthening on the “Loco2” locomotive structures were made and their effects on improving crashworthiness have been assessed based on several collision scenarios. As before, these are not intended as final designs; rather to show the value of the simulation method and the general magnitude of the potential benefits.

The three strengthening configurations were:

1. Increasing the thickness values of the frontal windshield frame and side wall of the cab to 1/4 in from 0.09 in and 1/8 in, respectively.
2. Doubling the thickness of the top and side plates of short hood from 1/4 in and 3/8 in to 1/2 in and 3/4 in, respectively.
3. Increasing the height of the collision posts to the level of the top short hood plate. (In this locomotive, the collision posts do not extend to the top of the hood; the strengthened case did not add welds to the inside of the hood, although this could be done also.)

The same scenarios as for Loco1 were used. To evaluate the effectiveness of the first two strengthening approaches, the high/offset collision scenario between the Loco2 consist and the ISO-type container was selected. The offset collision scenario between the Loco2 consist and the standing, fouling box car consist was selected to assess the third strengthening approach.

### **5.2.1 Strengthening of Windshield and Corner Post Area**

The collision between the moving locomotive consist at 50 mph with a high/offset aluminum ISO-type 30,000 pound container was used to evaluate the benefits of strengthening the windshield/corner post area. Much less local deformations occurred with the strengthened windshield/corner post (Figure 79), compared to the baseline model (Figure 35). The cave-in of the cab roof was also minimal for the strengthened model. The crushing in the short hood was similar for both models, since it remained unchanged. Thus, this design modification is very effective in reducing the damage to the cab and could enhance the safety of crew members.



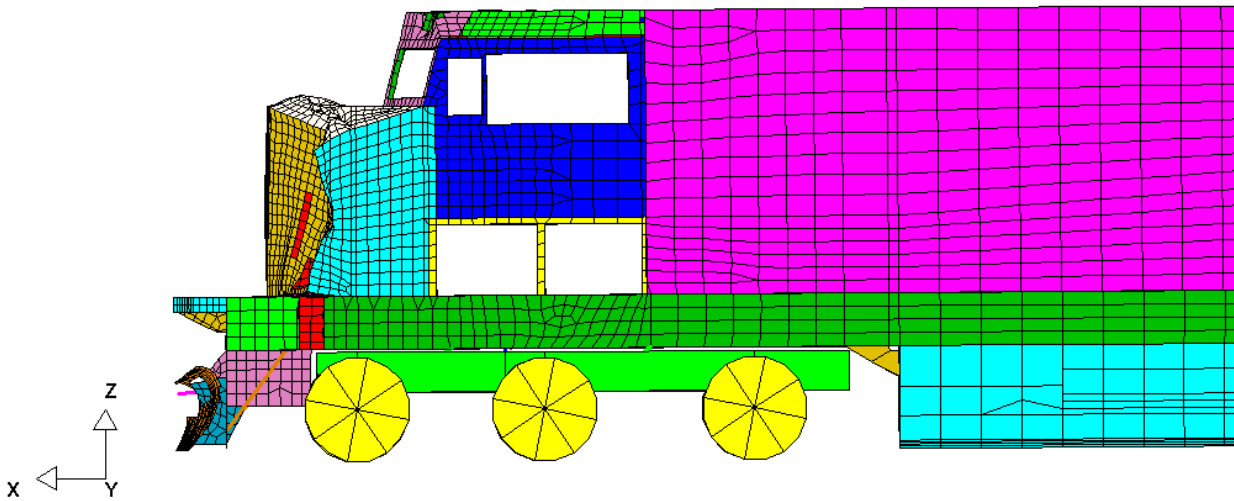


*Figure 79. Lateral view of the deformed Loco2 with strengthened windshield and corner post area at  $t = 0.5$  seconds for the 50 mph collision*

### 5.2.2 Strengthening of Short Hood

The same collision scenario between the Loco2 consist and container was used to assess the benefits of strengthening the short hood. In this case, less deformation occurred in the windshield and corner post area (Figure 80), compared to the baseline model (Figure 35). This is unlike the results of the Loco1 locomotive study in which no obvious benefit was obtained for the same strengthening. Although the positions of the container relative to the top of the locomotive platforms and collision posts were exactly the same for both cases, the difference in geometric shape of the short hood of the two locomotives is believed to have caused the different results. The short hood of the Loco2 locomotive has the same width as its platform, while the short hood of the Loco1 locomotive is tapered (in plan view) and narrower than its platform. The engagement area between the container and short hood for Loco2 locomotive was therefore larger than that for Loco1 locomotive, which resulted in more damage to and less downward pitch motion for the container than in the Loco1 collision. Also, the diagonally-outward sloping top of the hood in Loco2 could have had an effect in deflecting the container differently.

With the strengthening of this short hood, the container sustained even more damage and had even less pitch motion energy resulting in much less damage to the windshield and corner post area. In summary, the extra width and shape of this short hood reduced the damage to the cab through reduction of the pitch-down tendency of the container, and the greater damage inflicted onto the container as opposed to the locomotive.

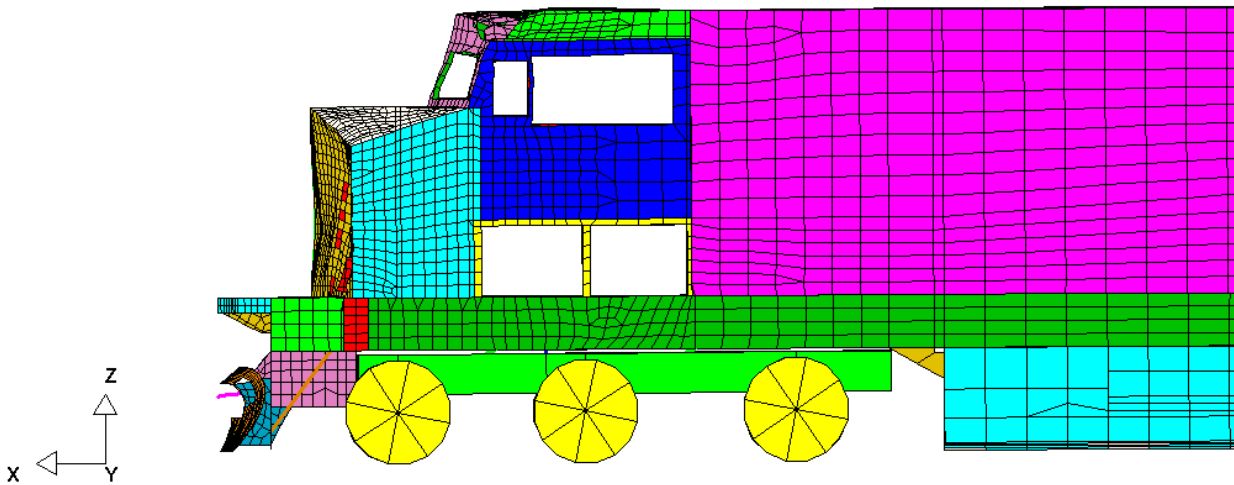


*Figure 80. Lateral view of the deformed Loco2 with strengthened short hood at  $t = 0.5$  seconds for the 50 mph collision*

### 5.2.3 Upward Extension of the Collision Posts

For the two-thirds offset collision between the moving Loco2 consist (30 mph) and stationary box car consist, little benefit was obtained as shown in Figure 81 compared to the baseline model (Figure 32). In this collision scenario, most engagement occurred between the locomotive underframe, and lower portion of the collision post and the lead box car corner. Although the left collision post was directly involved in collision, its strength is mainly determined by the shear and bending strength of its lower portion. This is due to the fact that the collision post is more or less like a cantilever beam with its base fixed. Thus increasing its height would not significantly increase its overall strength in this situation. However, this strengthening could be beneficial in cases with higher uploads, such as collisions with the loose ISO-type container off a double-stack car.

However, further work could be also be performed through addition of the strengthening flanges, as done for Loco1. These could be expected to provide similar improvements, and it was not necessary at this time to repeat them for Loco2.

### 5.3 Summary of Strengthening Studies

Several modifications in the front end and cab design of two large freight locomotives from different manufacturers were evaluated based on a selection of realistic collision scenarios, each intended to tax the structures involved. The basic objectives of demonstrating the value of the

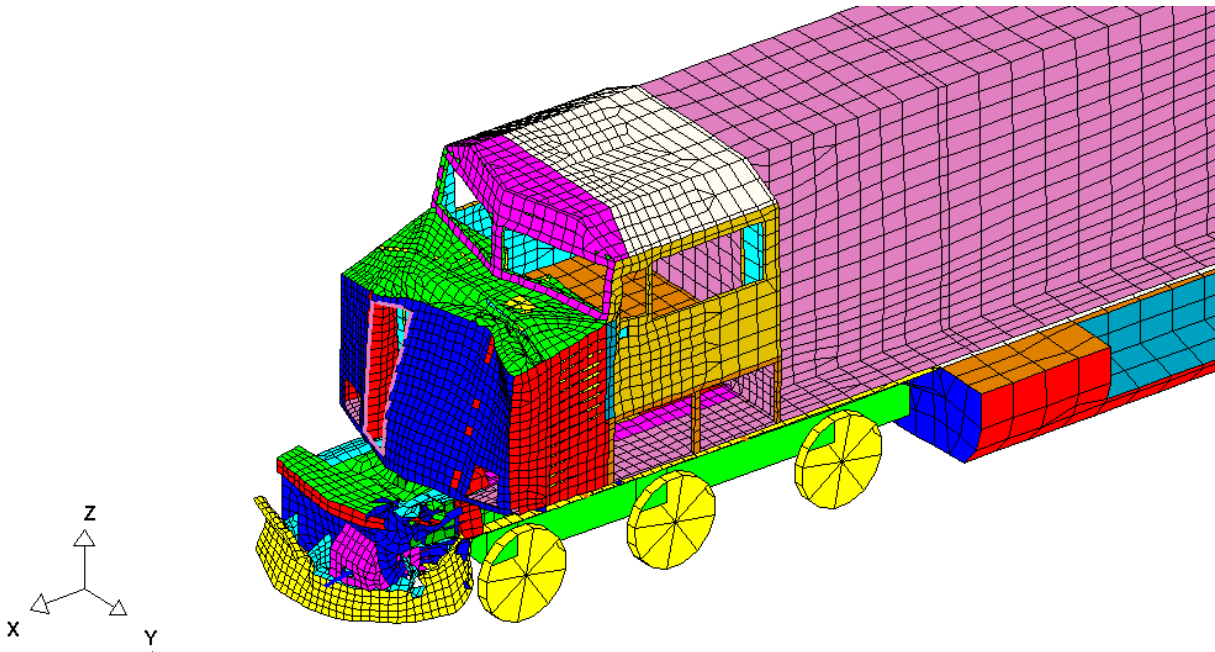


**Figure 81. Deformed Loco2 with strengthened collision posts at  $t = 1$  s for the 30 mph case**

simulation method, and of showing how design improvements could be assessed, were demonstrated.

Strengthening of the windshield posts is definitely beneficial, seen in cases in which roughly double the section modulus of the members was tried, using a high/offset collision with a loaded ISO container. These type of studies could be used by designers in conjunction with the RSAC-type strengthening anticipated to meet the new AAR S-580 in those locations.

Laterally stiffening the collision posts by adding flanges (“I-beam” type configuration) was also beneficial, but the added flanges had to be of sufficient size, and the base connection enhanced, in order to produce the benefits. Use of 10 in flanges with the same thickness as the post, plus appropriate base connection strength, reduced axial/lateral crush 40 to 50 percent in the offset collision with the box car consist used.

One other finding is that incorporating components of increased strength does not always result in a safety improvement. The objective of crashworthiness improvements is ultimately to improve the survivability of the crew and to minimize damage to equipment and property. In one case, described in subsection 5.1.2, a strengthened short hood resulted in more damage to the cab in collisions with an ISO container. Automobile designers found that providing optimal structural stiffness ahead of the passenger compartment (“crush volumes”) better protected the occupants, but this strategy can produce different results when applied to a locomotive cab.

The basic lesson is that a new design needs to be evaluated by treating all the locomotive structures together as a system and by analyzing the behavior in various possible collision or test scenarios to assess true effects. Initial design ideas will always be supported by a simple, local calculation in the design process. However, the interrelationships when the full structure and environment must always be considered, as with these simulations, for confidence in their final results.

## 6. CONCLUSIONS AND RECOMMENDATIONS

---

Based on the development of the locomotive collision simulation approach, and the analytic studies performed, the following conclusions and recommendations are drawn.

### 6.1 Conclusions

#### 1. Simulation Characteristics

- The dynamic simulation of colliding consists using the LS-DYNA code (or an equivalent) provides a valuable insight into the mechanics of the deformation and kinematics of colliding locomotives and cars. The crashworthiness of the locomotive and car structures, and the peak cab acceleration levels experienced by the crew can be determined given the speeds, structural details of vehicles, and the configuration of the consists at the time of collision.
- In the simulation method developed here, several innovations were developed which enabled the collision process to be visualized with good fidelity. These included having the overall consist and individual vehicles or objects incorporated into a single overall model, with interactions accounted for via this “model-in-model” approach. Suspensions and draft gear, including nonlinearities of stops and limits, were also incorporated.

#### 2. Simulation Benefits

These simulations can be used to provide information on:

- Design of structural modifications for improved crashworthiness: Preliminary concepts can be evaluated rapidly at low cost before final design efforts are made.
- Planning of full-scale tests and refining test plans in advance of actual testing.
- Redesign of the interior of locomotives, including seat restraints or interior modifications for reduced injuries to the crew in the event of a collision: The method can include compatible human dummies for injury evaluation.
- Simulation of actual past accidents to study the possible crash sequence and events: Two such accidents have been simulated and the predictions are in reasonable agreement with the report published by the NTSB.

### 3. Crash Mechanics Observations

The simulations showed that:

- For the majority of crash scenarios, almost all of the crash event takes place in the first one or two seconds. Crew members have to anticipate the collision prior to its occurrence for egress and other preparations to reduce their injuries.
- Increase in the speed of collision does increase the duration of peak acceleration levels. In some situations, however, there is no proportional increase in the peak acceleration levels themselves. This aspect may be important in the considerations of redesign of the locomotive structure.
- Besides the speed and structural makeup on the colliding vehicles, the presence of lateral “offset” is an important parameter that can influence the outcome of the collision event. These can occur at turnouts or similar track layouts. In the case of locomotive to locomotive collisions, simulations with 40 in and 80 in offsets were performed and the results were compared. The smaller overlap allowed the underframes to “nest” and “slide by” each other, but the outboard cab zones were destroyed. The larger overlap increased the contact loads and acceleration levels in the cab. In offset collisions with freight cars, the offset allowed the freight carbody to impact the cab corners outside the protection area of the standard collision posts.

### 4. Structural Improvements

Preliminary analysis using the simulation showed that the following structural improvements to the locomotive have merits from a crashworthiness point of view.

- Strengthening the windshield/cab corner posts: The simulations of the hopper car and container offset collisions with the locomotive showed the benefit of strengthening of the corner post, corner post-to-roof connection, and the windshield frame. Using a relatively large change of doubling the cross-sectional areas eliminated the upper windshield corner joint detachment and reduced deflections overall in the area.
- Increased lateral stiffness of collision posts: In the current design, the lateral stiffness of the locomotive collision posts is relatively small, these being vertical plates supported by welding to the short hood sheets. In some locomotives, the top of the collision posts are free. The simulations revealed that crashworthiness can be improved in offset collision conditions by increasing the lateral stiffness of the collision posts themselves. The studies showed that this could be best accomplished by adding lateral flanges to the existing posts, both to the front and rear sides, significantly increasing their lateral bending stiffness.
- Thickening of short hood: The simulation of a locomotive with the high, offset ISO-container collision shows that increased short hood thickness on the order of 50 percent will produce mixed results on crashworthiness. The container, striking high on the hood just outside the

collision posts, will penetrate the hood less in the axial direction, but the greater hood strength will have the unexpected effect of increasing the pitch-down motion of the high container onto the roof, increasing damage there. The thickening of the hood sheets would likely improve protection of the cab from objects impacting lower down. The conclusion is therefore that such strengthening could be introduced, but the simulation analysis of highly-located impact objects show a need for roof strengthening under those conditions.

## **6.2 Recommendations**

Results of this research suggest the following:

- Two historic accidents were identified for simulation, with one involving a rear-end collision with an unloaded intermodal car consist fully simulated for verification purposes. There are several other accidents reported by the NTSB and FRA which should be simulated for gaining confidence in the application of the simulation method proposed here.
- The simulation method should be extended to include interior crashworthiness analyses, using human “dummies” to evaluate the injuries sustained by the crew during collisions. Depending on the acceleration levels of the crew member, the type and direction of the collision, and his or her position at the time of impact, the member could strike a side window, front console, overhead panels, and in severe cases, the roof or windshield. The injury sustained by the crew member due to his/her impact on the interior object can be identified in the form of head, neck, limbs or organs injured, and the extent of injury can also be quantified. This will also aid in improving the design of the cab interior.
- Detailed parametric studies are required to redesign the locomotive structure for cost-effective improved crashworthiness.
- Limited full-scale instrumented tests can be conducted for validation of the simulation tool. Careful planning of the tests is critical to obtain good quality technical data at a reasonable cost. The simulation tool presented here can be used in planning cost-effective tests under meaningful scenarios to provide valuable data to both industry and Government, as well as to validate the model.





## 7. REFERENCES

---

1. *LS-DYNA User's Manual*. Livermore, CA: Livermore Software Technology Corporation, 1997. Version 940.
2. *HyperMesh User's Manual*. Troy, MI: Altair Computing, Inc., 1998. Version 2.1.
3. *The Car and Locomotive Cyclopedia*. Omaha, NB: Simmons-Boardman, (1997).